GLOSSIC HORIZON FORMATION IN COARSE-LOAMY BISEQUAL SOILS

By

Christopher James Baish

A THESIS

Submitted to
Michigan State University
in partial fulfillment of the requirements
for the degree of

Geography – Master of Science

2020

ABSTRACT

GLOSSIC HORIZON FORMATION IN COARSE-LOAMY BISEQUAL SOILS

By

Christopher James Baish

Coarse-loamy soils with glossic horizons have not been extensively studied in the upper Great Lakes region, and thus, questions remain regarding their genesis. As a first step toward resolving this problem, I examined glossic horizon development in two calcareous coarse-loamy, bisequal soils in NE Lower Michigan. Data collected from these soils were integrated with published pedogenic models to develop a unifying model that illustrates the most likely pathways of glossic horizon formation in similar soils of the region. The model involves the acidification of a calcareous parent material, followed by mechanical translocation of clay (and associated Fe-oxides) and fine silt to a preferred (illuvial) zone under oxidizing conditions. The illuvial zone, a Bt horizon, eventually functioning as an aquitard during seasonally wet periods, facilitates temporary localized saturation and change in redox status near its upper boundary. Subsequently, clay-bound Fe compounds are reduced and eluviated from the zone, resulting in the destabilization, degradation, and remobilization of illuvial cutans to form glossic features. The expression of glossic features evolve gradually as a result of micro-erosion and eluviation of clays and fine silts from preferred locations within the degrading zone, the magnitude of which follows a distinct sequence at progressive stages of the degradational process: (1) fine clay, (2) coarse clay, and finally, (3) fine silt. With time, the glossic character of the degrading zone becomes increasingly pronounced, until ultimately, little to no evidence of the former Bt horizon remains. At this point, Bt horizon morphology has progressed through glossic to an albic horizon.

ACKNOWLEDGEMENTS

I would first like to thank the Department of Geography, Environment, and Spatial Sciences as a whole for accepting me into the Spartan community and providing me the opportunity to continue to develop and pursue my passion for science and education. I am grateful for the assistantships that made my attendance at Michigan State University possible and for the Graduate Office Fellowships that I received that allowed me to complete the necessary field and laboratory work for this project.

I owe my deepest gratitude and appreciation to my committee Chairperson and graduate advisor, Dr. Randy Schaetzl. Dr. Schaetzl has been an invaluable source of knowledge and advice throughout my graduate program, and I am thankful for all of the time he has selflessly dedicated both to this project and to mentoring me. His unwavering guidance and encouragement have had an immeasurable impact on my confidence in myself and my abilities as a student, writer, and scientist. I am grateful to have the opportunity to continue working closely with him as I continue onward into the PhD program here at Michigan State University.

I am also greatly indebted to my remaining committee members, Dr. Alan Arobgast and Dr. David Rothstein, for their constructive and thoughtful suggestions during the formulation of this thesis. I would like to further extend my appreciation to Dr. Arbogast for largely serving as "second" mentor during my graduate program. I am grateful to him for consistently holding me to a very high standard and for always encouraging me to think about the "big picture" of my research.

A special word of thanks is due to my undergraduate advisor at the University of Northern Iowa, Dr. Dennis Dahms. I will forever be grateful to Dr. Dahms for inciting my love for soils and

geography, inspiring and encouraging me to attend graduate school, and continuing to remain a strong and supportive advocate for me throughout my subsequent professional and academic endeavors.

Lastly, I need to thank my family, particularly my parents, for their enthusiastic and unflagging support throughout my life and education. I am grateful for the knowledge and values that they have instilled in me, especially the importance of integrity, hard work, and always giving full effort to every presented task and opportunity. I also need to thank my girlfriend, McKenzi, for being my primary foundational support since uprooting to Michigan and for always motivating and believing in me.

A final, but certainly not diminished acknowledgement goes out to the many people not mentioned above that have influenced my personal growth and education over the last several years. I sincerely thank each of you for all of the lessons, both large and small, that you have taught me throughout this journey.

TABLE OF CONTENTS

LIST OF TABLES

LIST OF FIGURES

KEY TO ABBREVIATIONS

ρ_B – bulk density

μm – micrometers

μA – microamps

≈ – approximately equal to

≤ – less than or equal to

≥ – greater than or equal to

% – percent

AAS – atomic adsorption spectrophotometry

ac – acres

Al_{ox} – oxalate-extractable aluminum

asl – above sea level

° C – degrees Celsius

CA - Canada

cal yr B.P. – calendar years before present

CEC – cation exchange capacity

cm – centimeters

CMOS – complementary metal-oxide semiconductor

CPSD – Cumulative Particle Size Distribution (Langhor et al., 1976)

EDXRA – energy dispersive x-ray analysis

e.g. – for example

et al. – and others

Fe_{ox} – oxalate-extractable iron

FMU – Forest Management Unit

g – grams

GLO – General Land Office

GPS – Global Positioning System

hr – hours

i.e. – that is

keV – kilo-electron volts

kg – kilograms

km – kilometers

LD – lithologic discontinuity

LGM – last glacial maximum

LIS – Laurentide Ice Sheet

LOI – loss-on-ignition

m – meters

Ma – million years ago

me - milliequivalents

min – minutes

mL – milliliters

mm – millimeters

NIST – National Institute of Standards and Technology

NOAA – National Oceanic and Atmospheric Administration

NRCS – Natural Resource Conservation Service

NWS – National Weather Station

ODOE – optical density of oxalate extract

OSD – official soil series description

PAD-US – Protected Areas Database of the United States

POD - Podzolization Index (Schaetzl and Mokma, 1988).

ppm – parts per million

PSA – particle-size analysis

pXRF – portable x-ray fluorescence

QC – quality control

RO – reverse osmosis

sec – seconds

SEE – Soil Series Extent Explorer

SEM – scanning electron microscope

SOC – soil organic carbon

SOM – soil organic matter

SPNL – Soil and Plant Nutrient Laboratory (Michigan State University)

SSURGO – Soil Series Geographic Database

UK – United Kingdom

US – United States

USDA – United States Department of Agriculture

USGS – United States Geological Survey

UV – Uniformity Value (Cremeens and Mokma, 1986)

viz – videlicet or that is to say

CHAPTER 1

INTRODUCTION

Maps showing the general distribution of soils in the Lower Peninsula of Michigan often report a broad zone (or ecotone) separating two distinct *"*provinces*"* (Figure 1.1) (Veatch, 1931; Kellogg, 1936; Wilde, 1946; Veatch 1953). These provinces are defined according to the major taxonomic[1] soil types that occur there, and thus, they reflect the primary pedogenic processes that influence soil development across the province. In the southern province, which spans much of southern Lower Michigan[2], well-drained soils are forming in mostly finer-textured glacial sediments and tend to classify taxonomically as Alfisols or Inceptisols. Soil development in this region is dominated primarily by decarbonation, acidification, and subsequently, lessivage (i.e., clay translocation). Typical profile morphologies exhibit characteristics associated with the vertical translocation and accumulation of silicate clay minerals, e.g., A – E – Bt – C. Alternatively, in the northern province, which spans northern Lower Michigan and most of the Upper Peninsula, well-drained soils are forming in mostly coarser-textured glacial sediments and tend to classify as Spodosols, or contain spodic-like properties in their upper solum. Soil development in this region is dominated primarily by acidification, followed by podzolization, and typical profile morphologies exhibit characteristics associated with the vertical translocation and accumulation of sesquioxides (i.e., iron and aluminum) and organic matter, e.g., A – E – Bs – C.

Pre-settlement vegetation surveys of Lower Michigan typically describe a boundary separating two major forest types, namely the "floristic tension zone", that roughly coincides with

[1] All taxonomic terminology utilized in this thesis is reported according to the most recent version (12th ed.) of '*Soil Taxonomy'* (Soil Survey Staff, 2014).

[2] For the purpose of simplicity, the term 'Lower Michigan' is utilized throughout the remainder of this thesis to refer to the Lower Peninsula of Michigan.

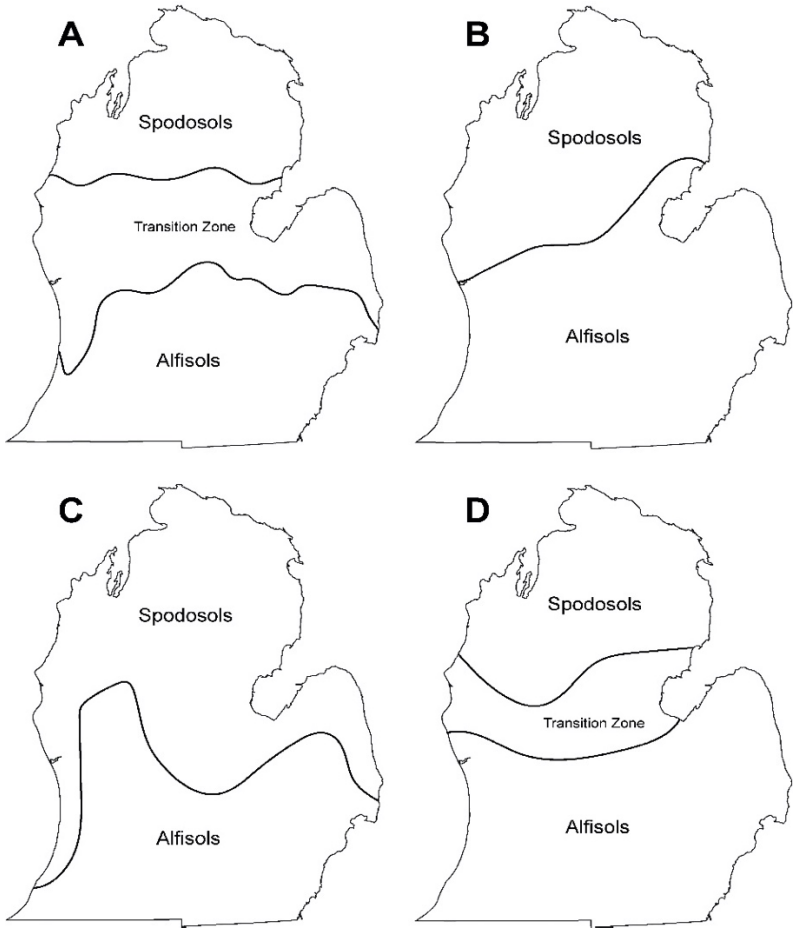

Figure 1.1. Spodosol and Alfisol provinces in Lower Michigan according to (A) Veatch (1931), (B) Kellogg (1936), (C) Wilde (1946), and (D) Veatch (1953). Figure based on Schaetzl and Isard (1991, Figure 3).

the boundary separating the major soil provinces (Schaetzl and Isard, 1991; Andersen, 2005). North of the tension zone, most forest assemblages are composed of coniferous or mixed coniferous-deciduous communities dominated by eastern hemlock (*Tsuga canadensis*), eastern white pine (*Pinus strobus*), red pine (*Pinus resinosa*), sugar maple (*Acer saccharum*), and yellow birch (*Betula allegheniensis*) (Barbour and Billings, 2000). South of the tension zone, the forest assemblages are primarily composed of broadleaf deciduous communities dominated by sugar maple, American beech (*Fagus grandifolia*), oak (*Quercus*), and hickory (*Carya*) (Barbour and

Billings, 2000). Generally, coniferous species tend to be more successful on the coarser-textured soils in the northern region, whereas the dominance of finer-textured soils south of the tension zone allow deciduous species to out-compete conifers (Veatch, 1931; Medley and Harman, 1987; Schaetzl and Isard, 1991; Hupy and Yansa, 2009). Dissolved organic (fulvic) acids produced during the decomposition of coniferous litter are capable of complexing iron (Fe) and aluminum (Al) cations in the upper soil profile, rendering them mobile. These "free" organometallic complexes are then translocated to the subsoil in percolating water (podzolization). Because decomposition of broadleaf litter does not produce the necessary types or quantities of fulvic acids, soils forming in similar parent materials in the southern region do not develop strong podzolic morphologies, but instead show only some reddening in the B horizon (i.e., rubification) with little or no actual translocation. Many of these soils classify as Entisols.

In well-drained, coarse-textured soils forming under mixed coniferous-deciduous forest in northern Lower Michigan, the degree of podzolic expression varies predictably across a generally west-east gradient (Figure 1.2). This trend is attributed primarily to annual winter snowfall distribution and has been particularly well documented in soils forming in sandy glaciofluvial outwash sediments (Schaetzl and Isard, 1991; Isard and Schaetzl, 1995; Schaetzl, 2002; Schaetzl et al., 2015; Schaetzl et al., 2018). In lake effect areas immediately adjacent to Lake Michigan, where snowpacks tend to be thickest and persist the longest (Eichenlaub, 1970; Schaetzl and Isard 1991; Henne and Hu, 2010), well-drained sandy soils typically contain a strongly developed spodic horizon and classify as Typic Haplorthods or Typic Durorthods. As snowpacks become thinner and less persistent eastward across the gradient, the degree of podzolic expression on similar sites becomes increasingly less pronounced, until in the northeastern part of the peninsula, most of the soils on sandy parent materials are Typic Udipsamments with only slightly reddened B horizons.

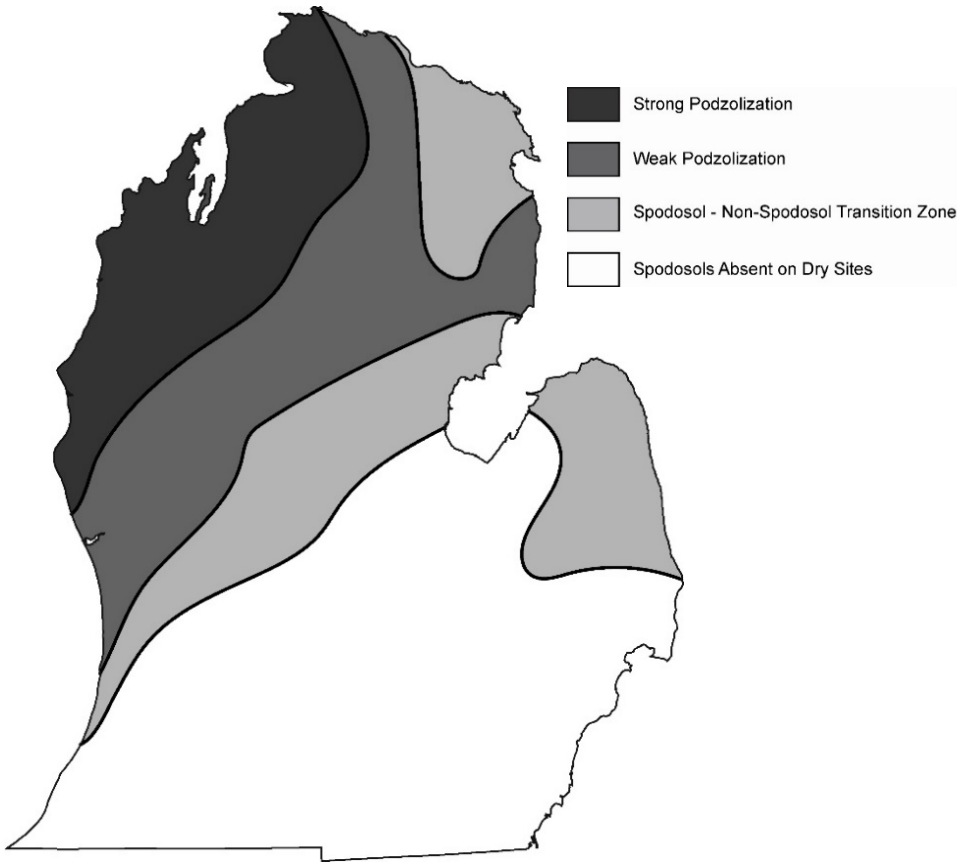

Figure 1.2. Zones of varying strength of podzolic expression for well-drained, coarse-textured soils in Lower Michigan. Figure based on Schaetzl and Isard (1991, Figure 4).

Well-drained soils forming in calcareous coarse-loamy parent materials show generally similar spatial trends in their degree of development across northern Lower Michigan. Unlike their sandier counterparts, however, these soils often also exhibit varying degrees of influence of lessivage in their morphologies. Thus, they differ from typical Spodosols and Alfisols in that they usually contain both a spodic or spodic-like (E-Bs) sequum and an alfic (E-Bt) sequum. Such soils are by definition "bisequal", and hence seem to intergrade between Spodosols and Alfisols (Veatch and Miller, 1934; Gardner and Whiteside, 1952; Nygard et al., 1952; Allen and Whiteside, 1954; Schaetzl, 1996). Soils exhibiting similar bisequal morphology have been reported across the upper

Great Lakes region, including New York (Cline, 1949; Bullock et al., 197), Minnesota (Harpstead and Rust, 1964), Wisconsin (Beaver, 1966; Hole, 1975), and Ontario [CA] (Stobbe, 1952). Often found marking the interface between the upper and lower sequa is a glossic horizon (Cline, 1949; Ranney and Beatty, 1969; Bullock et al., 1974; Hole, 1975; Schaetzl, 1996; Weisenborn and Schaetzl, 2005), defined as a diagnostic subsurface horizon that is ≥ 5 cm in thickness and consists of an eluvial part (i.e., albic materials), which constitute 15 to 85% (by volume) of the horizon, and an illuvial part (i.e., remnant pieces) of an argillic or other clay-enriched horizon (Soil Survey Staff, 2014; Figure 1.3). In locations where the upper sequum is relatively poorly developed (i.e., in the eastern portion of northern Lower Michigan), such soils classify as Typic or Haplic Glossudalfs. Where the upper sequum contains a spodic horizon, soils with a glossic horizon often classify as Alfic Haplorthods.

Figure 1.3. Close-up view of a glossic (E/B) horizon of the Millersburg series, a Haplic Glossudalf, in northeastern Lower Michigan (Montmorency County). Photograph by R. Schaetzl.

According to *Soil Taxonomy*, the glossic horizon forms as a result of degradation of an argillic or other clay-enriched horizon (Soil Survey Staff, 2014). The process of degradation occurs as soil materials, namely clay minerals and associated "free" iron oxides, are removed and vertically redistributed lower in the soil profile along preferred water flowpaths, such as between peds. As a result, a distinct boundary typically develops between the E and the Bt horizon, where eluvial material appears to extend downward as irregular "bodies" and/or "tongues" into the upper portion of the underlying illuvial horizon. In essence, the glossic horizon is a discontinuous and sometimes broken eluvial-illuvial transition zone. In order to represent the transitional nature of the glossic horizon in taxonomic description, it is distinguished with an E/B or B/E designation. In Lower Michigan, 79 soil series have been identified and mapped that contain a diagnostic or "taxonomically evident" glossic horizon (Soil Survey Division, Accessed 2019).

1.1 Problem Statement

Despite the abundance of calcareous coarse-loamy soils containing glossic horizons in northeastern Lower Michigan, they remain relatively poorly documented, and thus, uncertainty remains as to the applicability of current pedogenic theory to explain their genesis. Although such soils have been previously reported on in this region, e.g., Schaetzl (1996) and Weisenborn and Schaetzl (2005), relatively little emphasis has been placed on how these horizons actually form. Soils containing glossic horizons and forming under conditions similar to those in northeastern Lower Michigan have been reported on in a few instances in nearby areas of the upper Great Lakes region [e.g., Bullock et al. (1974) and Cline (1949) in New York; Harpstead and Rust (1964) in Minnesota; Ranney and Beatty (1969) and Hole (1975) in Wisconsin]. However, only two of these studies, i.e., Ranney and Beatty (1969) and Bullock et al. (1974), were focused specifically on

glossic horizon genesis, and both date to the mid-20th century, with little work accomplished in the past 50 years. Furthermore, both of these studies were focused on soils forming in parent materials that are of loam texture or finer. Since these early papers, many new procedures have been developed that allow this type of soil to be investigated more thoroughly and at a finer resolution. Additionally, more recent models for glossic horizon genesis have been reported in other (i.e., non-regional) locales [e.g., Jamagne et al. (1984) in France and Payton (1993b) in England]. Such procedures and models, however, have not yet been applied to further our understanding of Michigan's glossic soils.

1.2 Goal and Objectives

The primary goal of this research is to provide modern and data-informed insight into the pedogenic mechanisms driving the genesis of glossic horizons in calcareous coarse-loamy parent materials, through intensive examination of two representative pedons in northeastern Lower Michigan. The specific objectives of this thesis research are to: (1) identify and characterize two coarse-loamy textured soils, each of which contains a glossic diagnostic horizon; (2) use data collected from these soils to infer glossic horizon genesis; and (3) evaluate findings in light of applicable conceptual models of glossic horizon genesis that have been previously reported in the literature in order to develop a new model – one that integrates existing models and findings from this study.

1.3 Justification

Soils containing a glossic horizon have never been extensively studied in Michigan. Furthermore, regionally applicable models, nearly all of which date back more than five decades,

have not examined glossic horizon genesis in coarse-loamy parent materials. In essence, current theory regarding the development of glossic soils in Michigan with similar characteristics to those in this study is based largely on dated observations from soils forming under different conditions in other regional locales. Thus, this research, through detailed, pedon-scale investigation, will contribute both a more complete and modern characterization of glossic soils in Michigan and the broader upper Great Lakes region, as well as a new, unifying model that illustrates the most likely pathways of glossic horizon formation in similar soils of the region. Knowledge gained from this body of research is important to (1) advancing current theories in soil genesis and (2) enhancing the classification, mapping, and management of glossic soils in this region.

1.4 Scope and Delimitations

In order to design a study framework that would allow the goals and objectives of this research to be reached, a set of boundary conditions were necessarily established. First, it is important to note that the intent of this research is not to examine an extensive number of "glossic" soils. Although conceptually such an approach would allow for statistical treatment of data across a range of soils (*sensu* Schaetzl, 1996), it would not allow for investigation at the scale necessary to make accurate and reliable inferences regarding glossic horizon genesis. Instead, this research is focused on a detailed pedological characterization of two pedons, both of which contain a well-developed (i.e., diagnostic) glossic horizon.

Second, it is important to note that the purpose of this research is not to report on the bisequal nature of "glossic" soils in northeastern Lower Michigan, which has been well documented by previous authors (Veatch and Miller, 1934; Gardner and Whiteside, 1952; Nygard et al., 1952; Allen and Whiteside, 1954; Schaetzl, 1996). Instead, this research is focused on the

investigation of glossic horizon genesis as it occurs within the broader context of soil profile evolution, which here has resulted in the formation of bisequal morphology. Furthermore, because this study is not designed with the intention to wholly explain bisequal profile formation, soil profile evolution was assumed to follow the "dual process" development theory[3] initially proposed by Cline (1949) and Frei and Cline (1949) for soils in New York, and later endorsed for soils in Michigan (Gardner and Whiteside, 1952; Schaetzl, 1996; Weisenborn and Schaetzl, 2005).

[3] Generally, the "dual process" development theory involves a two-step process. First, a parent material is acidified and undergoes lessivage (clay translocation), which creates an E-Bt sequum. Next, as the E horizon becomes increasingly acidic and clay impoverished, podzolization is eventually initiated, forming a Bs horizon in the former E horizon of the sequum formed by lessivage. Therefore, two distinct sequua are formed in a single solum by a combination of two different suites of pedogenic (eluvial-illuvial) processes: (1) podzolization and (2) lessivage.

CHAPTER 2

STUDY AREA

In this study, I examine two bisequal soil pedons containing a glossic horizon, mapped by the NRCS as within the Millersburg series, in central Montmorency County, Michigan (≈45°04'29.8"N 84°08'00.1"W). The study site is in the southern portion of the Atlanta State Forest, ≈10 km north of the City of Atlanta, about 100 m east of Stevens Spring Road (SE 1/4, SE 1/4, Section 13, T31N, R2E, Briley Township) (Figure 2.1); pedon 1 (ATL-1) is located approximately 3 m north of pedon 2 (ATL-2). Both pedons are well-drained and are beneath a mixed coniferous-deciduous forest on a north-facing, concave, backslope position of a dissected coarse-loamy textured glacial till upland. In order to place the study site within the context of its broader regional setting, this chapter provides background information on its physiography, glacial history, vegetation history, climatic conditions, soil geography, and land use.

2.1 Physiography

The study site is located within the Atlanta Channeled Uplands landform region, as defined in Burgis's (1977) physiographic map of northeastern Lower Michigan. This region encompasses ≈1,500 km^2 in portions of Montmorency, Otsego, and Cheboygan Counties, and is characterized by heavily dissected ground moraine ridges that are interspersed by broad, flat-floored valleys (Figure 2.2). The isolated ridges, which trend in a mostly northeast-southwest direction, are composed of thick sequences of coarse-loamy textured glacial till and intercalated sandy outwash. The ridge upon which the study site is located rises ≈35 m above the surrounding valleys (Figures 2.3 and 2.4). The tills in this region are calcareous (Perkis, 1997; Purkey, 2013), owing to the influence of Paleozoic (≈542-251 Ma) carbonate bedrock that underlies much of the area and areas

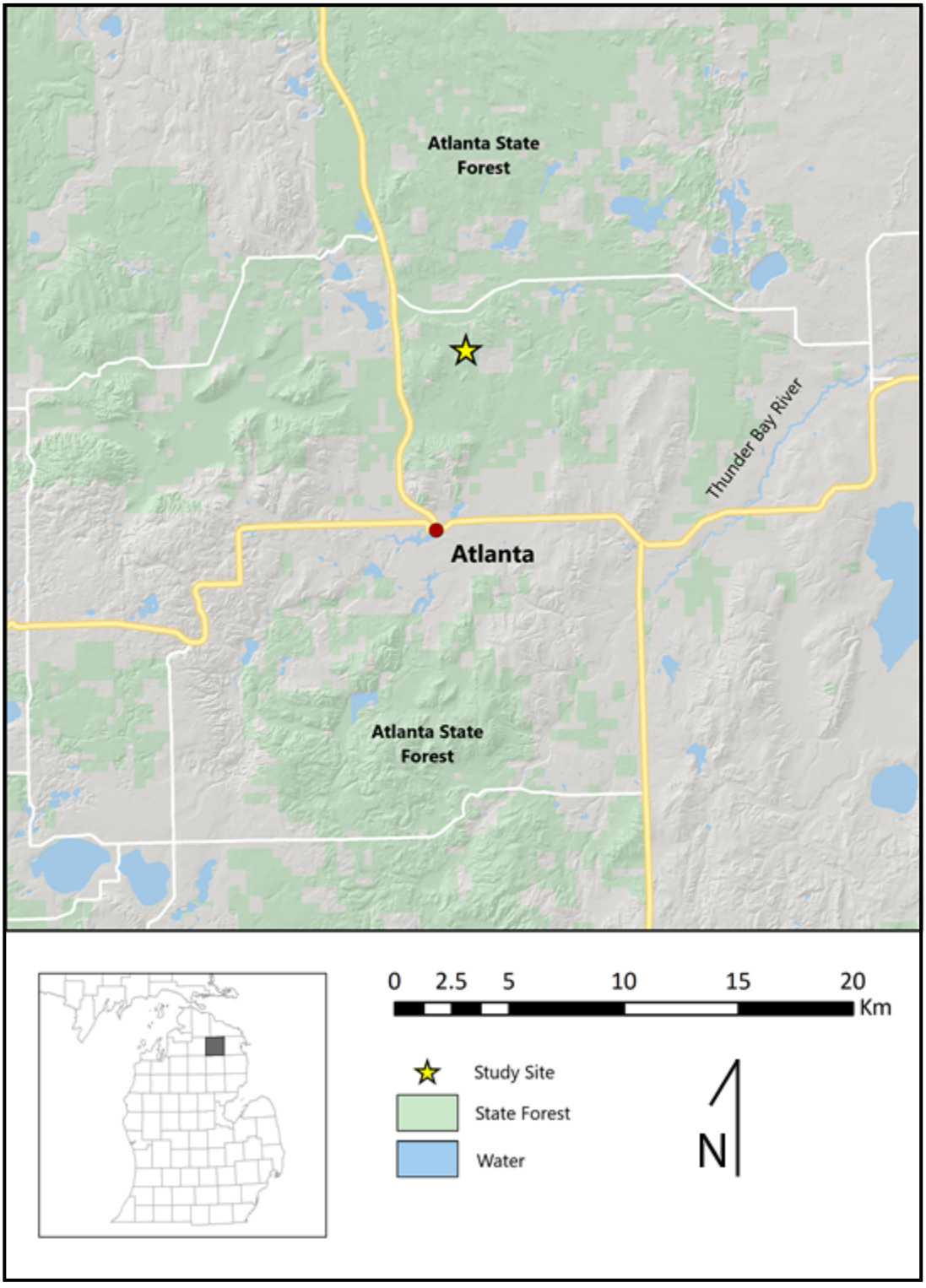

Figure 2.1. Location of the study site in Montmorency County, Michigan.

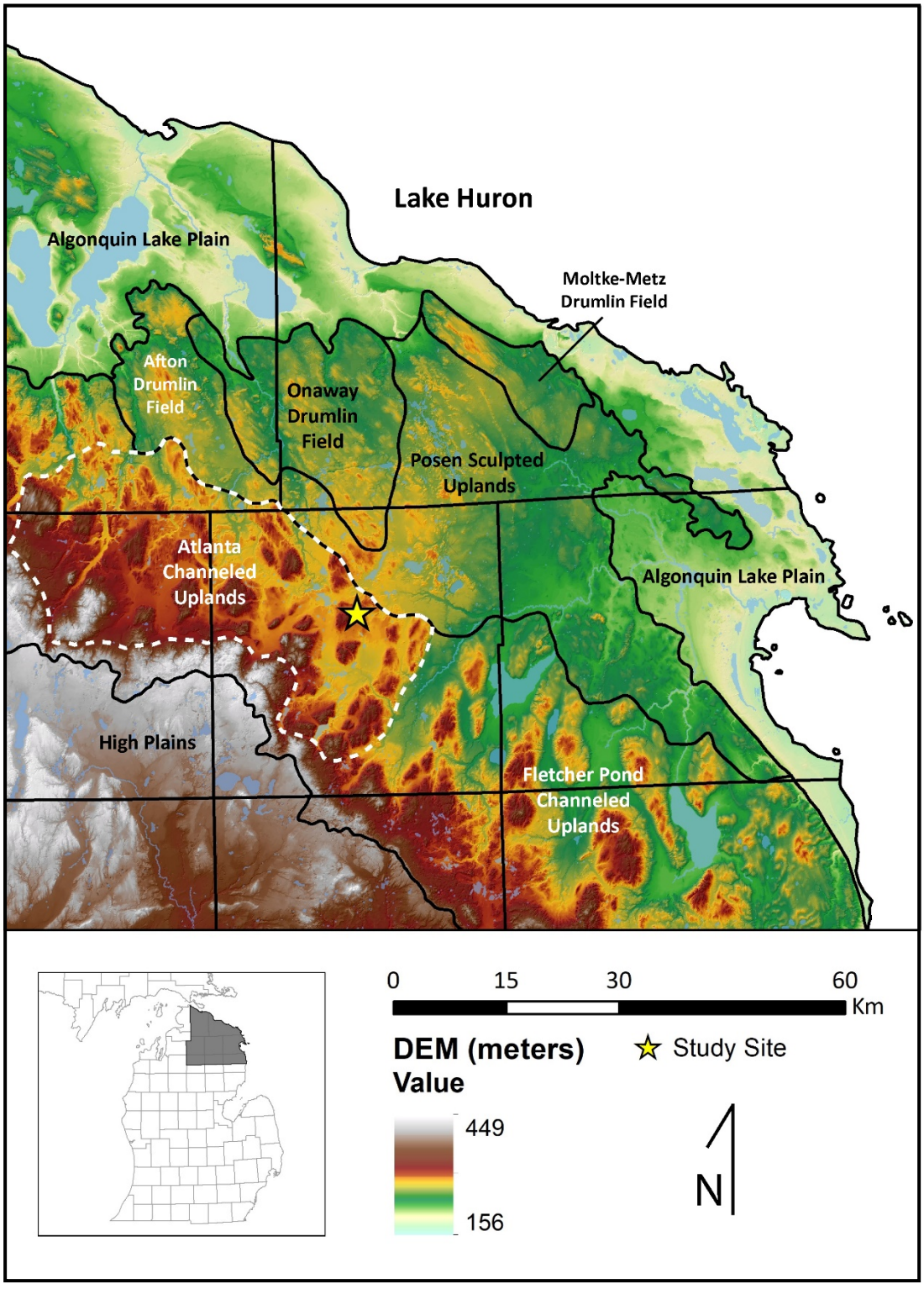

Figure 2.2. Major physiographic regions and study site location in NE Lower Michigan based on Burgis (1977) and Schaetzl et al. (2013).

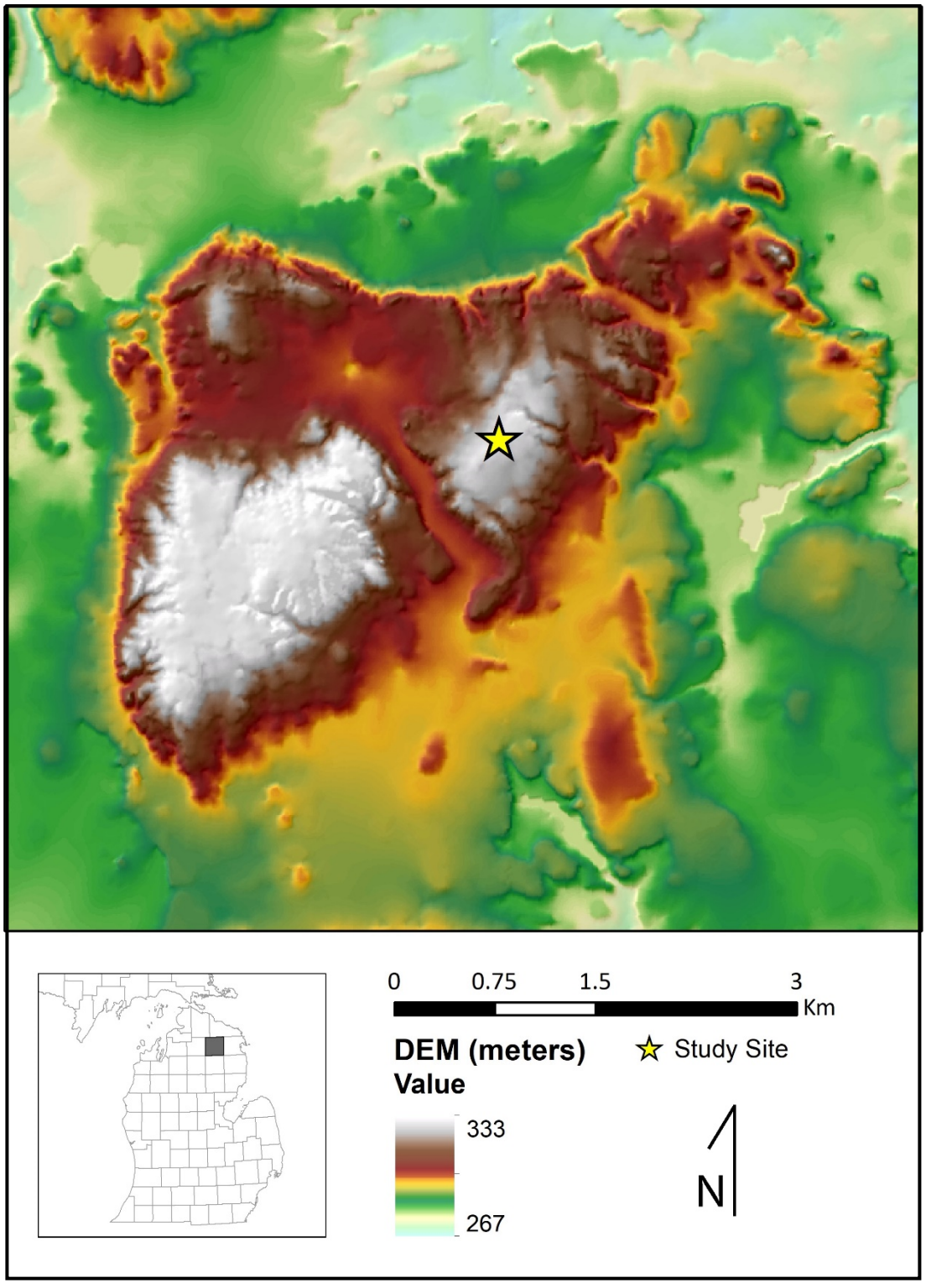

Figure 2.3. Shaded relief DEM (10 m) of study site in Montmorency County, Michigan.

immediately to the north (Schaetzl, 1996; Schaetzl, 2001). Sandy glaciofluvial outwash deposits, occasionally with large contents of gravel, tend to underlie the intervening valleys. According to Burgis's (1977) nomenclature, the Port Huron morainic system, known locally as the Johannesburg Moraine (Purkey, 2013), the Fletcher Pond Channeled Uplands, and Onaway-Afton drumlin fields bound the region on its southern, eastern, and northern margins, respectively (Figure 2.2).

Schaetzl et al. (2013) included the study area in the broader Northern Lower Peninsula Tunneled Uplands subsection of the Northern Lower Peninsula High Hills physiographic region. This subsection combines the Port Huron morainic system with the adjacent "Channeled Upland" regions of Burgis (1977), forming a contiguous band between the broad, high elevation, sandy glaciofluvial outwash dominated plains to the south (i.e., High Plains) and the lower relief, drumlinized till plain and lacustrine influenced terrains to the north (Figure 2.2).

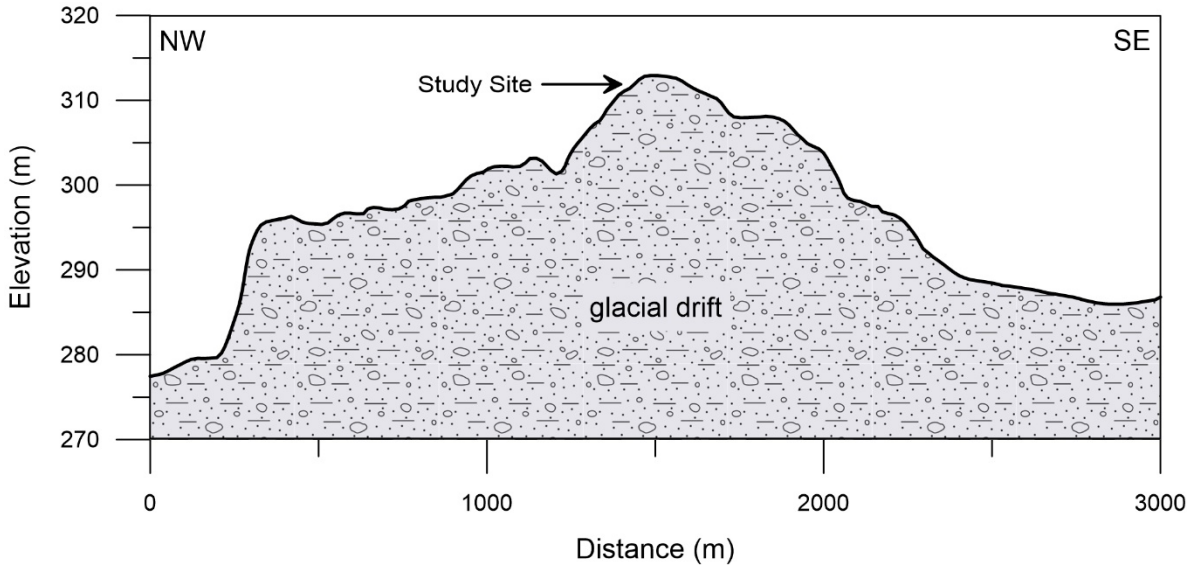

Figure 2.4. Topographic cross-section of the ground moraine ridge upon which the study site is located. The cross-section intersects the short axis of the ridge (NW-SE), through the study site location. The pedons are located at ≈312 m (asl).

2.2 Glacial History

During the Pleistocene Epoch, the Laurentide Ice Sheet (LIS) repeatedly covered northeastern Lower Michigan, although the exact number of times remains unclear (Farrrand, 1995). The Wisconsin glaciation, which began ≈75,000 cal yr B.P., was the last major glacial episode to influence this region (Larson et al., 1994; Schaetzl, 2001; Krist and Lusch, 2004). By ≈20,000 cal yr B.P., the LIS had advanced well beyond Lower Michigan, reaching its maximum southerly extent, termed the Last Glacial Maximum (LGM), in Illinois, Indiana, and Ohio (Dyke et al., 2002). After reaching its LGM position, the ice sheet began a rapid retreat northward, interrupted by a series of readvances at approximately 18,700, 15,500, and 13,800 cal yr B.P. (Larson et al., 1994; Larson and Schaetzl, 2001; Krist and Lusch, 2004). The surficial sediments and landforms of northeastern Lower Michigan are correlated to glacigenic process operative since ≈15,500 cal yr B.P. (Burgis, 1977; Blewett et al., 1993; Schaetzl, 2001; Figure 2.5).

The readvance at ≈15,500 cal yr B.P., known as the Port Huron advance, covered most of northeastern Lower Michigan and eroded and buried older glacial deposits into a thick veneer of sandy drift. Landscape and till fabric data reported by Schaetzl (2001) indicate that the Port Huron ice flowed into the region in a mostly southeasterly direction from the Lake Michigan Basin, eventually turning to the southwest near its marginal position in Otsego, Montmorency, and Oscoda Counties. Upon reaching its marginal position, the ice built a prominent end-morainic system (i.e., Port Huron Moraine) (Figure 2.5), which trends in a mostly northwest-southeast direction and rises ≈120 m above the valleys behind it (Burgis, 1977; Farrand, 1995). The morphology and sedimentology of the Atlanta Channeled Uplands, which lies immediately north (or inside) of the Port Huron Moraine, suggest that the outer margin of the ice likely stagnated and melted rapidly shortly after reaching its maximum extent (Burgis, 1977; Blewett and Winters,

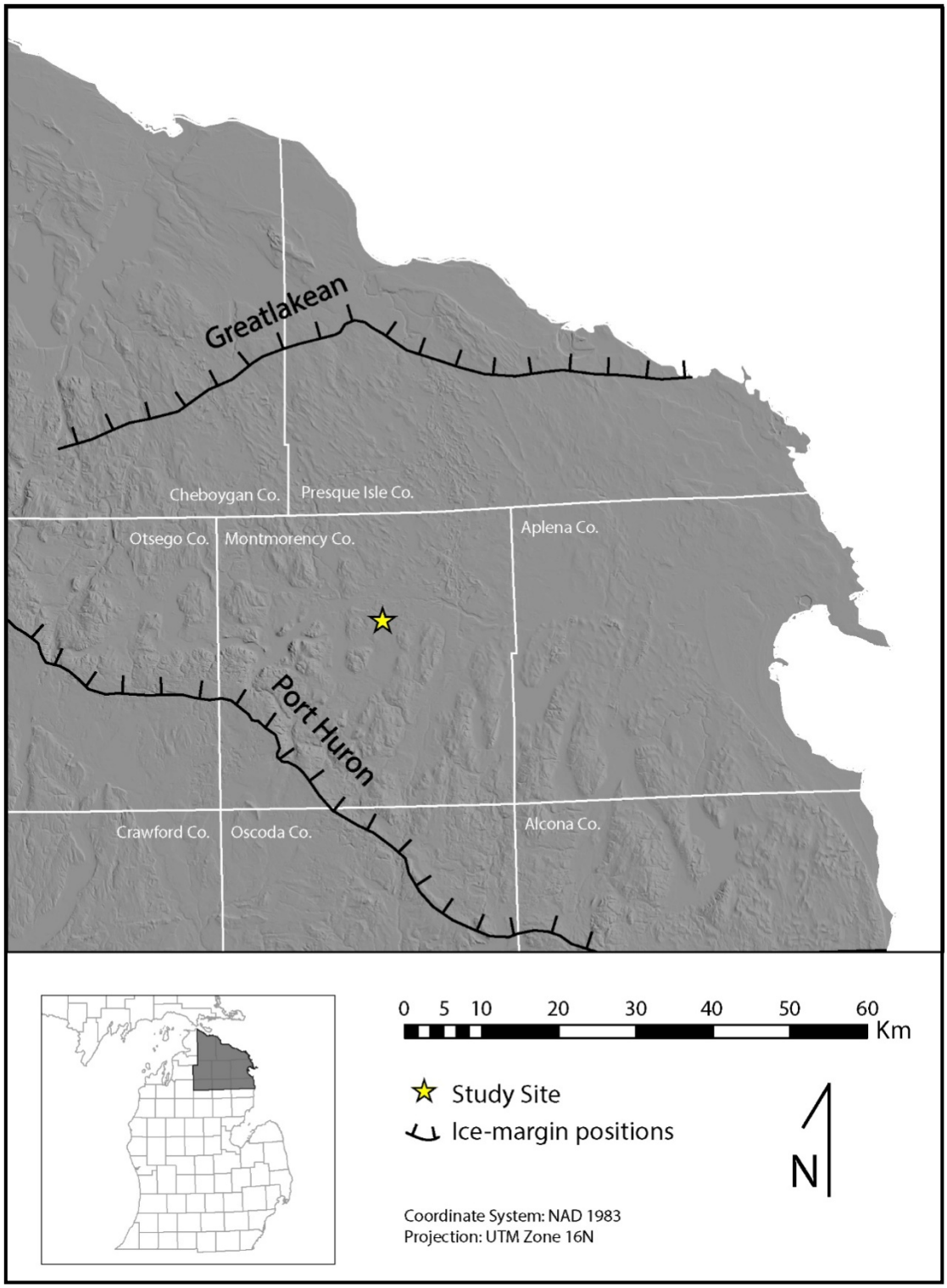

Figure 2.5. Late Wisconsin ice-margins in NE Lower Michigan. From Blewett et al. (1993) and Schaetzl (2001).

1995; Schaetzl, 2000; Schaetzl, 2001), as it is assumed that the dissection of the ground moraine ridges in the region occurred during the formation of subglacial meltwater-fed tunnel channels.

Although a subsequent readvance occurred in northeastern Lower Michigan at ≈13,800 cal yr B.P., known as the Greatlakean advance, its precise marginal position in the northeastern Lower Peninsula remains largely undefined and subject to debate, primarily due to the lack of a prominent or continuous end morainic system (Melhorn, 1954; Burgis, 1977; Schaetzl, 2001). The most recent research on the landforms and sediments associated with the Greatlakean readvance in northeastern Lower Michigan, reported by Schaetzl (2001), indicates that Greatlakean ice was likely confined only to the central and northern portions of Cheboygan and Presque Isle Counties. Therefore, it can be assumed that the study site became (and remained) subaerial and pedogenically active following the retreat of the Port Huron ice from the region, very early in the Two Creeks Interstade (Larson et al., 1994; Schaetzl, 2001).

2.3 Vegetation History

Although no full paleobotanical records currently exist for landscapes associated with the Port Huron readvance in northeastern Lower Michigan, pollen and plant macrofossil data reported by Yansa et al. (2020) from nearby Silver Lake (≈45 km northwest of the study site) provide valuable insight into potential vegetation colonization and succession in the Atlanta Channeled Uplands region following final deglaciation. According to these data, upland sites surrounding Silver Lake were dominated by mature boreal forest species, particularly white spruce (*Picea glauca*) and balsam fir (*Abies balsamea*), until ≈10,600 cal yr BP. After this time, climatic warming and associated drying led to a shift from boreal forest species to northern mixed coniferous–deciduous forest species largely dominated by pine (*Pinus strobus*, *Pinus banksiana*,

and *Pinus resinosa*), an early variant of the forests that exist in the study area today. Pollen and plant macrofossil data reported by Schaetzl et al. (2013) from the Tower Buried Forest (≈35 km north of the study site), show generally similar trends.

The General Land Office (GLO) survey for Montmorency County was undertaken between 1840 and 1858 to document vegetation at the time of initial European settlement. These data indicate that a diversity of forest communities occupied the landscape at this time (Comer et al., 1995; Comer et al., 1997; Figure 2.6). The most common communities were (1) northern mixed coniferous–deciduous forests, specifically forests of beech – sugar maple – hemlock (*Fagus grandifolia – Acer saccharum – Tsuga canadensis*) and hemlock – white pine (*Tsuga canadensis – Pinus strobus*); and (2) mixed pine forests, specifically jack pine – red pine (*Pinus banksiana – Pinus resinosa*), white pine – red pine (*Pinus strobus – Pinus resinosa*), and white pine-mixed hardwoods. Generally, on uplands, mixed coniferous-deciduous forests dominated on mesic sites, whereas mixed pine forests dominated on drier sites. In the lowlands, mixed pine forests dominated on drier sites, whereas swamp forest, specifically communities of black ash (*Fraxinus nigra*), white cedar (*Thuja occidentalis*), mixed conifer, and hardwood swamp, dominated on poorly drained sites. Although these species still exist today in the area, natural population assemblages have been largely altered by anthropogenic disturbance, e.g., logging and post-logging fires.

Much of northeastern Lower Michigan, including the study region and study site, experienced widespread logging in the late 1800s and early 1900s that modified the preexisting forest compositions (Whitney, 1987). Removal of the largest conifers and many of the hardwoods during this period led to conditions favorable for the establishment of subordinate species that had formerly played a minor role in pre-settlement forest communities. Today, the second-growth vegetative cover at the study site is dominated by early successional species, particularly quaking

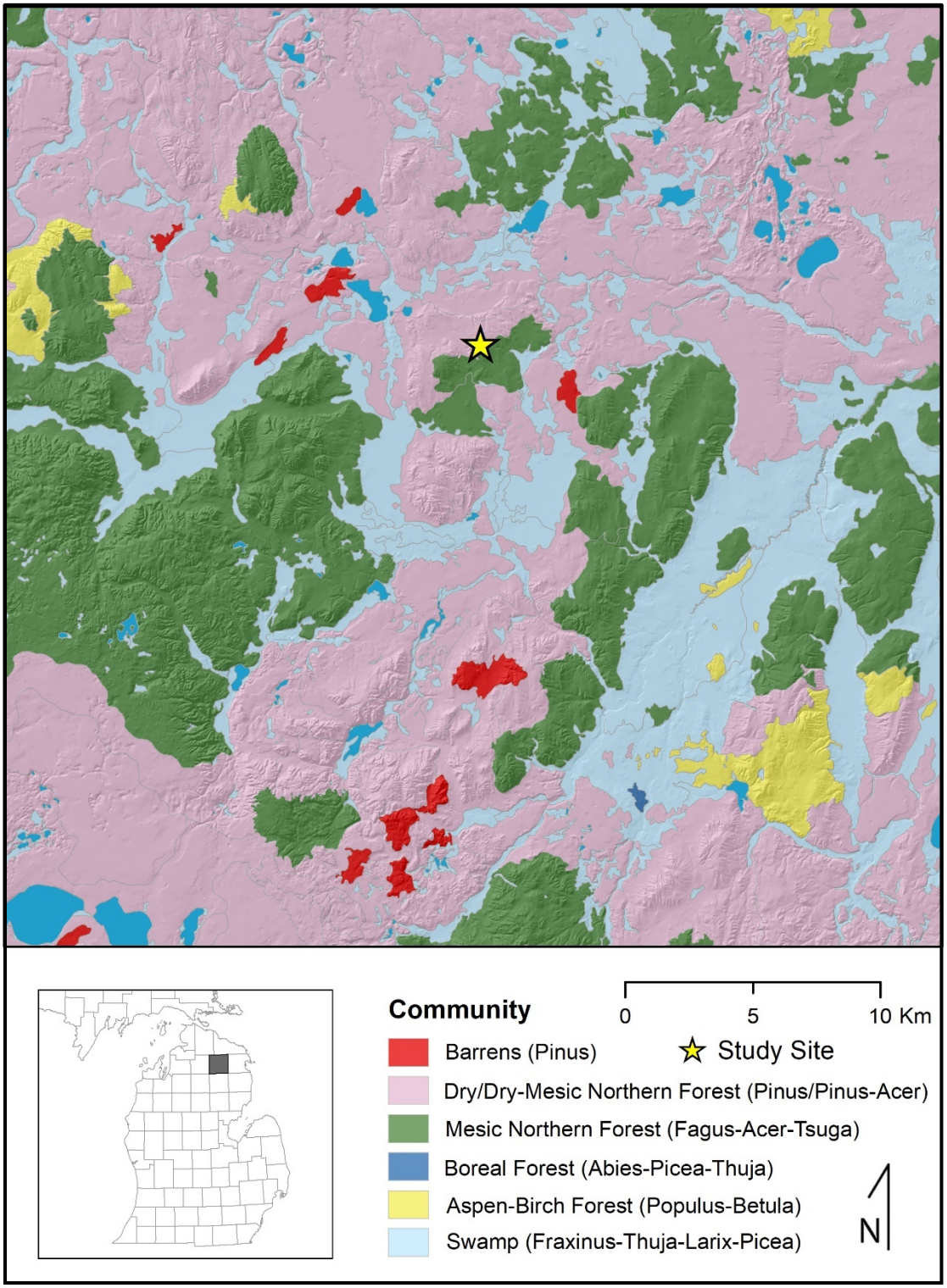

Figure 2.6. Pre-settlement vegetation cover (ca. 1800) of Montmorency County, MI (Comer et al., 1995; Comer et al., 1997).

aspen (*Populus tremuloides*), northern red oak (*Quercus rubra*), red maple (*Acer rubrum*), and black cherry (*Prunus serotina*), with only minor components of white pine (*Pinus strobus*) and paper birch (*Betula papyrifera*). Despite the lasting effects of logging, evidence of early recovery is evident in the understory composition, which is dominated by saplings of red maple, northern red oak, black cherry, white pine, and paper birch, with only minor components of quaking aspen occurring in or near large openings.

2.4 Climatic Conditions

The modern climate of northeastern Lower Michigan is classified as warm-summer, humid continental (Köppen Dfb), characterized by warm summers and long, cold winters with ample precipitation in all seasons. Due to its position along the northeastern margin of the High Plains physiographic region (Schaetzl et al., 2013), the Atlanta Channeled Uplands region experiences colder temperatures and a shorter growing season than locations of similar latitude nearer to the Great Lakes (Denton, 1985; Eichenlaub et al., 1990). As a result of the increase in elevation, coupled with prevailing westerly winds, the region also experiences some lake effect, particularly in its western portion (i.e., Otsego County), as evident by increased snowfall during late autumn and early winter (Eichenlaub, 1970; Eichenlaub et al., 1990; Schaetzl and Isard, 1991; Henne et al., 2007). National Weather Station (NWS) data obtained for the city of Atlanta are provided in Table 2.1 and represent the climatic conditions at the study site.

The mean annual temperature (1960-2018) for Atlanta is 5.8° C, with a mean January temperature of -7.9° C and mean July temperature of 19.5° C (Figure 2.7). The mean length of the growing season (i.e., frost-free period) is 121 days. The last freezing temperature (< 0° C) in spring typically occurs on ca. May 24th; the typical date for the first freezing temperature (< 0° C) during

autumn occurs on ca. September 22nd. The total mean annual precipitation in Atlanta averages 66 cm, of which 42 cm (64%) falls between April and September (Figure 2.7). Snowfall generally occurs from October through April. The mean annual snowfall for the 1960-2018 period is 171 cm, of which 98 cm (57%) falls between November and January. The mean maximum snow depth is approximately 25 cm. During the spring snowmelt period (March and April), soil infiltration totals in Atlanta generally range from 12 to 14 cm (Schaetzl and Isard, 1991).

Table 2.1. Average climate data, as recorded in Atlanta, Michigan, approximately 8 km SW of the study site.

NWS Station: Atlanta (Montmorency County)
Geographic coordinates: 45°00'17" N 84°08'26" W
Elevation (asl): 267 m
Data source: NOAA Online Weather Data (NOWData)
Date range: 1960-2018

Month	Temperature 1960-2018 (°C)	Precipitation 1960-2018 (cm)	Snowfall 1960-2018 (cm)	Snowfall Depth 1960-2018 (cm)
January	-7.9	3.0	44.9	19.6
February	-7.4	2.3	35.2	25.1
March	-2.2	3.3	26.5	16.3
April	5.2	5.2	9.5	1.4
May	12.1	7.0	0.1	0
June	16.9	7.0	0	0
July	19.5	7.4	0	0
August	18.5	8.1	0	0
September	14.5	7.6	0	0
October	7.9	6.3	1.0	0
November	1.6	4.8	16.5	1.8
December	-4.6	3.8	37.0	9.5

Annual mean (°C)	Annual mean (cm)	Annual total (cm)
5.8	65.8	170.8

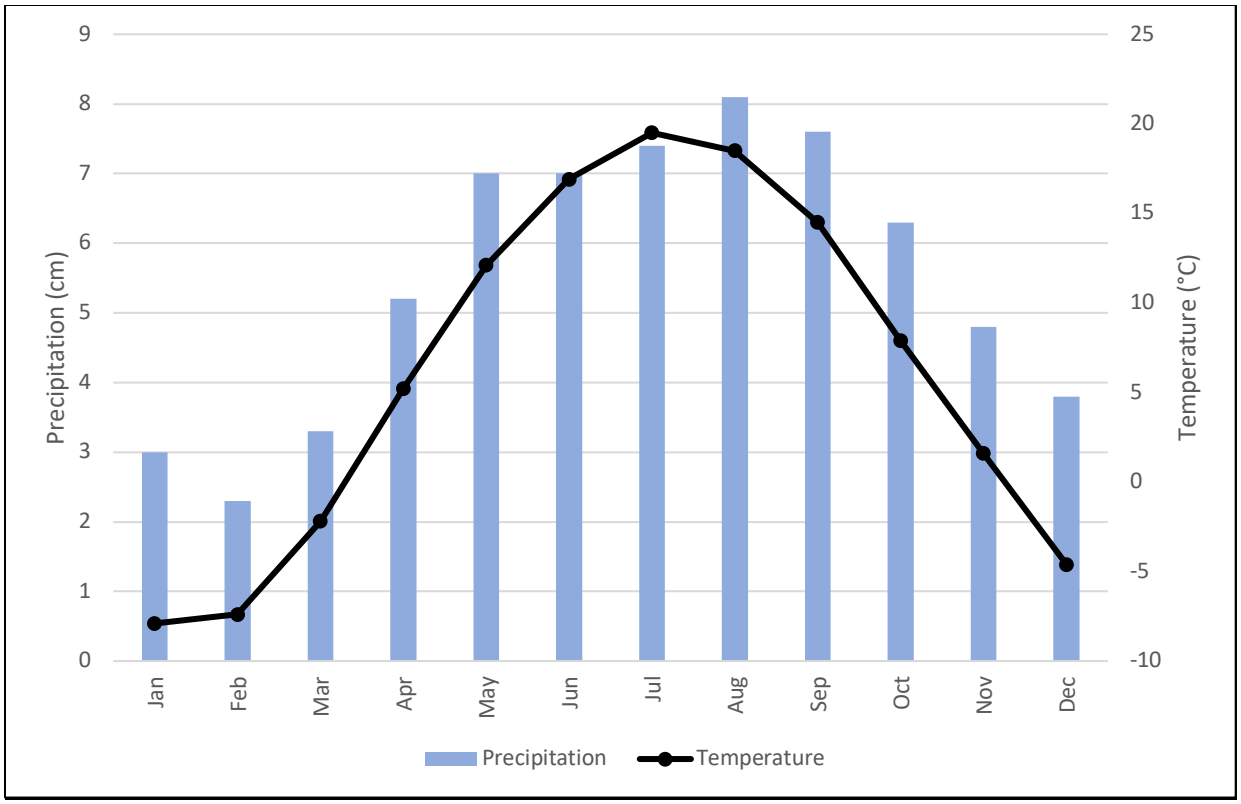

Figure 2.7. Climograph for Atlanta, Michigan, based on data from 1960-2018 (Table 2.1).

The soil temperature regime in Atlanta is frigid, characterized by a mean annual soil temperature < 8.0° C, and a difference in mean summer and mean winter soil temperatures > 5.0° C at a depth of 50 cm (Purkey, 2013; Soil Survey Staff, 2014; Soil Survey Division, Accessed 2019). According to data reported by Isard and Schaetzl (1995), the mean annual soil temperature (1951-1991) at 50 cm depth in Atlanta is 5.6° C, with a mean summer soil summer temperature of 12.8° C, and mean winter soil temperatures that are below freezing (-0.3° C). Due to cold winter temperatures and thin insulating snowpacks, particularly in the early season (December and January), soils in Atlanta are susceptible to frequent freeze-thaw cycles (Isard and Schaetzl, 1995). On the average, Atlanta experiences ≈20 freeze-thaw cycles per winter season (Isard and Schaetzl, 1995).

2.5 Soil Geography

Soils within the Atlanta Channeled Uplands are taxonomically diverse and include Alfisols, Spodosols, Entisols, Histosols, and Inceptisols; the spatial extent and distribution of these different soil types is dependent primarily upon local climatic conditions, landscape position, parent material, and depth to the water table. Upland positions on ground moraine ridges within the region mostly consist of well and moderately well drained, bisequal Alfisols and Spodosols forming in calcareous coarse-loamy textured glacial till. Spodosols on such positions are limited to the western portion of the region (i.e., Otsego County), where snowfall trends enhance podzolization process and the development of well-developed spodic horizons (Schaetzl and Isard, 1991; Schaetzl et al., 2018). Valleys surrounding upland ridges tend to be mostly occupied by excessively and somewhat excessively drained Entisols and Spodosols that have formed in outwash, and very deep, poorly and very poorly drained Histosols in depressions.

At the study site, soils forming on level to nearly level upland positions classify taxonomically as Millersburg series (coarse-loamy, mixed, active, frigid Haplic Glossudalfs). The Millersburg series has been reported only in northeastern Lower Michigan, where it is of moderate extent (≈32,955 ac). Millersburg pedons are generally irregular in shape and range in size from 0.5 to 1,200 ac (Soil Survey Division, Accessed 2019). In Montmorency County, this soil type comprises ≈20,850 ac (5.9%) and is frequently mapped in a complex with minor components of Klacking (loamy, mixed, semiactive, frigid Arenic Glossudalfs) and Graycalm (isotic, frigid Lamellic Udipsamments) soils (Figure 2.8) (Purkey, 2013). The typical Millersburg pedon has a loamy sand texture and contains a weakly developed spodic-like upper sequum overlying a glossic horizon that has formed in the upper portion of an argillic horizon. Klacking (Arenic Glossudalf) soils tend to occupy lower and steeper positions on upland ridges, while Graycalm (Lamellic

Udipsamment) soils are often found on deep, sandy outwash sediments in intervening valley bottoms. Klacking soils typically contain an argillic horizon composed of lamellae[1] overlying a thick, weakly expressed (i.e., non-diagnostic) glossic horizon, while Graycalm soils lack an argillic horizon. Table 2.2 illustrates the subtle differences and similarities between the three series. Additional taxonomic data for each series is provided in Appendix A.

Table 2.2. Comparison of major diagnostic characteristics between typical Millersburg, Klacking, and Graycalm pedons in Montmorency County (Purkey, 2013).

Diagnostic	**Millersburg-Klacking-Graycalm Complex**		
Character	**Millersburg**	Klacking	Graycalm
Drainage Class	**Well drained**	Well drained	Somewhat excessively drained
Parent material	**Loamy sand glacial till**	Sandy glacial deposits	Sandy glacial outwash
Slope	**0 to 6%**	6 to 18%	0 to 6%
Epipedon	**Ochric**	Ochric	Ochric
Subsurface diagnostic horizon	**Argillic Glossic**	Argillic	None
Solum thickness	**109 cm**	>203 cm	>203 cm
Depth to carbonates	**86 cm**	Not reported	Not reported
Lowermost horizon pH class	**Moderately alkaline**	Slightly acid	Moderately acid
Typical horizon sequence	**A-E-Bw-E/B-B/E-Bt-BC-C**	A-Bw1-Bw2-Bw3-E&Bt-B/E	A-Bw1-Bw2-Bw3-E&Bt

[1] In *Soil Taxonomy*, lamella (plural: lamellae) are defined as thin (< 7.5 cm) illuvial horizons (or bands), typically occurring in vertical series of two or more, that contain an accumulation of silicate clay relative to their overlying eluvial horizons. (Soil Survey Staff, 2014).

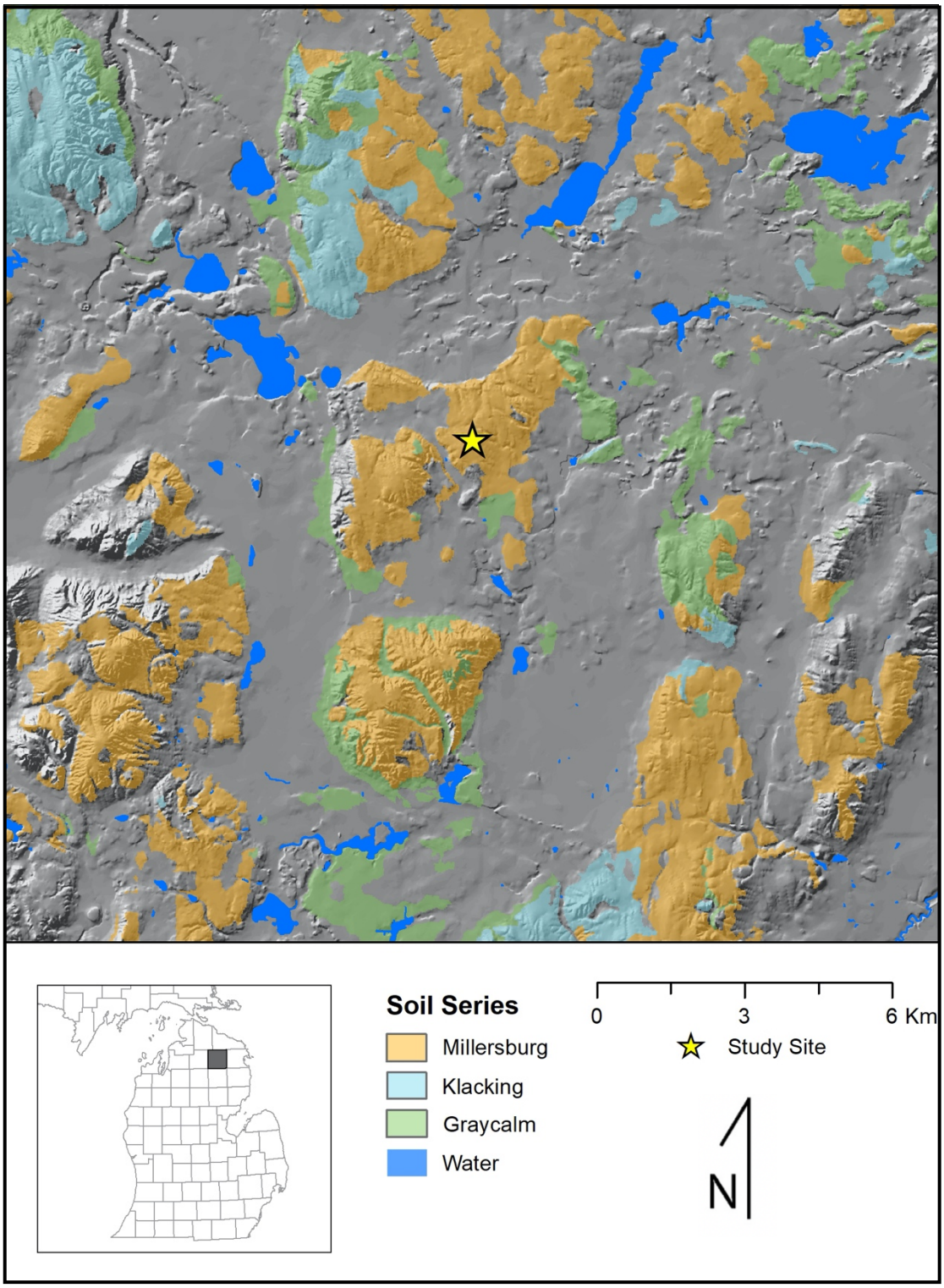

Figure 2.8. Distribution of the Millersburg-Klacking-Graycalm Complex in central Montmorency County, MI (Soil Survey Staff, 2019).

2.6 Land Use

Montmorency County has a total area of 361,371 ac, of which about 279,294 ac (≈77.3%) are currently forested (NOAA, 2016). In total, approximately 130,652 ac (≈36.2%) of the county is owned by the Federal or State government, which includes about 120,743 ac (≈43.2%) of the forested land area. Public ownership of much of the county's forestland was established following the end of the logging era in the early 1900's (Purkey, 2003). The majority (≈92.4%) of the managed forestland in the county is located within the Atlanta State Forest area, including the section where the study site is located. The Atlanta State Forest area is part of the broader Atlanta Forest Management Unit (FMU), which encompasses portions of Alpena, Cheboygan, Montmorency, and Presque Isle Counties in Northeastern Lower Michigan, and is managed primarily for timber production, recreation, and oil and natural gas development (Haxby, et al., 2013). Only about 16,548 ac (≈4.6%) of Montmorency County's land area is currently used for agricultural purposes, primarily cropland (≈3.0%) (NOAA, 2016). According to the 2017 Census of Agriculture (US Department of Commerce, 2019), cropland in the county is devoted primarily to production of forage crops (≈42.2%), namely hay, and soybeans (≈23.1%). About 27,721 ac (≈7.9%) of the remaining portion of the county is grassland, 17,079 ac (≈4.7%) is wetland, 9,781 ac (≈2.7%) is water, and 9,333 ac (≈2.6%) is used for development (NOAA, 2016).

Areas mapped as Millersburg soil series in Montmorency County are generally used for woodland (Purkey, 2013). Although the forest at the site has been harvested at least once since the late 1800s (Whitney, 1987; Purkey, 2013), the current status of the stand suggests that the soils have probably not been disturbed within the past several decades. Although Millersburg soils are not considered prime farmland, they are occasionally utilized as pasture for grazing (Purkey, 2013).

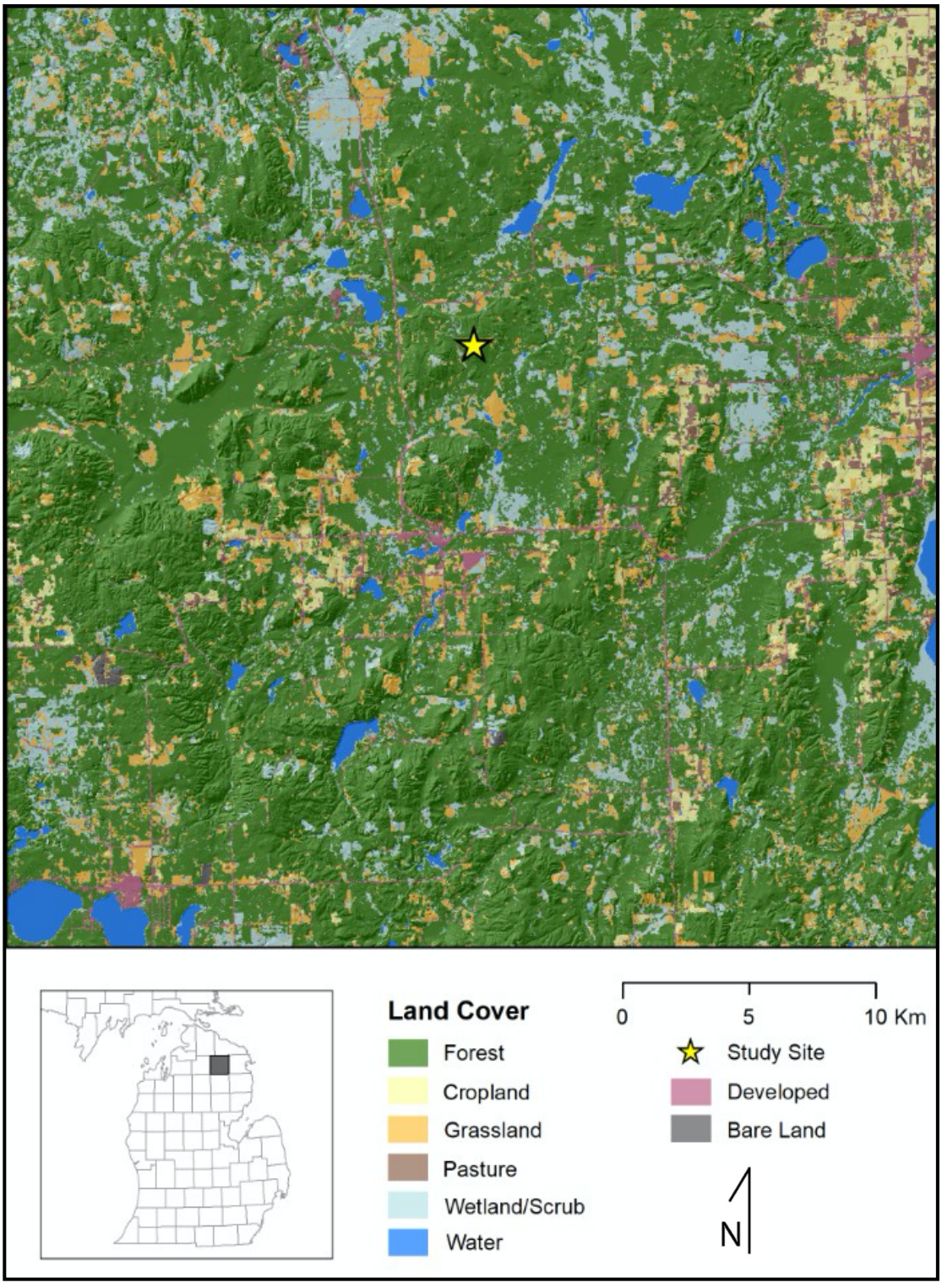

Figure 2.9. Thirty-meter landcover classification (ca. 2016) of Montmorency County, MI (NOAA, 2016).

2.7 Summary

The study site, set within northeastern Lower Michigan, has a complex geomorphic history, as evident by the variation in regional topography and surficial sediment distribution. Development of this distinct terrain was influenced primarily by glacigenic processes associated with the Port Huron readvance during the Late Pleistocene. The region is dominated by isolated high-relief ground moraine ridges that are interspersed with broad, flat-floored relict subglacial tunnel valleys. Following final deglaciation, a mature boreal forest developed in the area, before shifting to a pine–dominated, northern mixed coniferous–deciduous forest as a result of regional climatic warming and associated drying in the early Holocene. Soils forming in calcareous, coarse-loamy glacial till parent materials on upland positions in the region tend to exhibit bisequal morphologies with varying degrees of expression. Soils on such positions in the eastern portion of the region, which remain frozen for most of the winter due to thin snowpacks, contain a weakly developed spodic-like upper sequum overlying a glossic horizon that has developed in the upper portion of an argillic horizon. Most of the locations where such soils occur (including at the study site) have remained forested throughout their pedogenic history and have experienced relatively minor anthropogenic disturbance, allowing for the study of soil forming processes under seemingly natural conditions.

CHAPTER 3

METHODS

The purpose of this chapter is to describe the methodological approach to addressing the objectives of this research and the rationale for using those methods. Discussion is provided on the procedures that were employed to locate a specific site for study, as well as the field- and laboratory-characterization of the two pedons that were selected for investigation.

3.1 Site Selection

In order to identify a suitable site for study, I first queried the NRCS Official Soil Series Description (OSD) database to compile a list of all soil series mapped in Michigan that contain a diagnostic or "taxonomically evident[1]" glossic horizon (Soil Survey Staff, Accessed April 2019). For the purpose of this research, only soils series classified with well-drained soil moisture regimes (i.e., not classified as aquic) and lacking fragipan[2] characteristics were considered. Table 3.1 includes a list of all soil taxa that were initially queried, and the number of associated series. To determine which of these series occur in northeastern Lower Michigan, I examined the mapped extent of those soils that are also classified with a frigid soil temperature regime using the Soil Series Extent Explorer (SEE) web application (casoilresource.lawr.ucdavis.edu/see/, Accessed April 2019). I then examined the OSD for each glossic series identified in the region to identify

[1] A soils series containing a "taxonomically evident" glossic horizon is defined in this thesis as one which exhibits "glossic character" in an assigned E/B or B/E subsurface horizon, but that horizon is not well enough expressed that it meets the required diagnostic criteria to classify taxonomically as a glossic horizon.

[2] In *Soil Taxonomy*, a fragipan is a genetically developed layer that has a combination of firmness and brittleness and commonly a higher bulk density than the adjacent layers. Some part of the layer is physically root-restrictive (Soil Survey Staff, 2014, pg. 339).

those that met the following criteria:

(1) Has coarse-loamy, calcareous (alkaline reaction), glacial till as the parent material;

(2) Has bisequal morphology, with spodic or spodic-like (E-Bs) and alfic (E-Bt) sequa; and

(3) Has a glossic (E/B or B/E) horizon with a texturally contrasting eluvial-illuvial zone.

Soil series that met these criteria included Bamfield, Hoist, Leelanau, Millersburg, Ossineke, Perecheney, McGinn, and Omena. Next, I displayed the extent of each of these eight series in ArcGIS (Esri, California, US) using digitized USDA Soil Survey maps (SSURGO) (Soil Survey Staff, 2019) and cross-referenced their location with digitized public land maps (PAD-US) (USGS, 2018). I focused primarily on soils located in woodlots in order to maximize access to the site and to minimize the likelihood of anthropogenic disturbance. Using these criteria, I identified

Table 3.1. Well-drained non-fragic soil taxa in Michigan containing a diagnostic or taxonomically evident glossic subsurface horizon.

Order	Suborder	Great Group	Subgroup	No. of Series meeting criteria
Alfisols	Udalfs	Glossudalfs	Haplic	21
Alfisols	Udalfs	Glossudalfs	Oxyaquic	16
Alfisols	Udalfs	Glossudalfs	Arenic Oxyaquic	3
Alfisols	Udalfs	Glossudalfs	Arenic	2
Alfisols	Udalfs	Glossudalfs	Typic	2
Spodosols	Orthods	Haplorthods	Alfic	24
Spodosols	Orthods	Haplorthods	Alfic Oxyaquic	11

seven potential target areas. Within each target area, I further delimited specific locations on flat (or nearly flat) uplands near a road for field investigation.

I conducted a series of initial field investigations in May 2019 to assess the suitability of each of the seven selected target areas for more detailed study. Navigation to the target areas was made possible through use of a GPS-equipped field computer operating ArcGIS. At each target location, I examined several soil profiles using a hand-held bucket auger, and carefully inspected auger shavings to confirm whether the pedon at the site met the required diagnostic criteria listed above (pg. 29). I utilized a variety of rudimentary field tests in order to evaluate the soil, including hand texturing, color evaluation, and estimation of the proportion of the various sand size fractions. Generally, I considered a target area unsuitable for further investigation if it exhibited any of the following characteristics:

(1) Soils lacking the required diagnostic criteria listed above (pg. 29);

(2) Evidence of recent anthropogenic disturbance such as logging, grading, etc.; and/or

(3) Difficult to access due to distance from the nearest road, excessively rugged terrain, and/or dense vegetation.

Of the seven target areas that were initially assessed, three were generally suitable for further investigation. Two of the three target areas fall within the same landform region – the Atlanta Channeled Uplands (Burgis, 1977). I later revisited and reassessed both of the target areas, with the assistance of Dr. Randy Schaetzl, in order to identify a specific site location for excavation and sampling. The site so chosen was easily accessible via a former logging road, showed no signs of recent anthropogenic disturbance, as evident by the mature second-growth forest and intact surface litter horizons, and was not so dense with trees or undergrowth as to pose problems of access for a backhoe (Figure 3.1).

Figure 3.1. Study site location where soil pits were excavated and sampled. Photograph by R. Schaetzl.

3.2 Field Methods

I completed the primary field work for this research in June 2019. At the study site, I first conducted a rudimentary vegetation survey to identify the primary overstory and understory species compositions. Next, two soil pits - closely adjacent to each other - were excavated to approximately two-meter depth with a backhoe (Figure 3.2). Each pit face was cleaned to expose fresh soil and then photographed. I then described the morphology of the profile (e.g., horizonization, thickness, color, structure, consistence, texture, boundary, and coarse fragment content) according to Schoeneberger et al. (2012). Because tills in this region have been documented as calcareous (Schaetzl, 1996; Schaetzl, 2001; Purkey, 2013), the depth to unaltered parent material was determined with dilute HCl (Soil Survey Division Staff, 2017).

Figure 3.2. Excavation of the soil pits at the study site. Photograph by C. Baish.

After describing the pedon, I collected bulk samples (≈500 g) were from each genetic horizon. I began by sampling the deepest horizon and working towards the soil surface, so as to not contaminate subsequent samples. All genetic horizon samples were placed in plastic sample bags and labeled. I also collected two bulk samples (≈500 g) representing the broader eluvial and illuvial portions of the glossic horizon from the ATL-1 pedon; I carefully inspected the samples before bagging in order to ensure that the material of interest was isolated as cleanly as possible (i.e., no illuvial material in the eluvial sample; no eluvial material in the illuvial sample). Additionally, I collected samples of undisturbed peds and intact blocks of soil material (≈50 g each; hereafter "clod" samples) from select locations within various parts of the glossic horizon. I separated the clod samples into five distinct groups along a degradational sequence, based on their field appearance, during collection (Figure 3.3). Table 3.2 provides a description of the criteria

used to classify the degradational groups in the field. Clod samples were housed in foam containers (trays) and labeled according to their corresponding group. Prior to bagging, I wrapped each tray with an additional layer of both cellophane and cushioned plastic to minimize structural degradation and moisture loss during transport. Trays were stored under refrigeration (≈5° C) upon arrival to the laboratory in order to retain field-moisture conditions at the time of sampling and to prevent structural collapse upon drying. Lastly, I collected two undisturbed samples from each subsurface genetic horizon of the ATL-1 pedon for bulk density determination, by driving a standard thin-walled bulk density cylinder horizontally into the face of each horizon until flush with the soil surface.

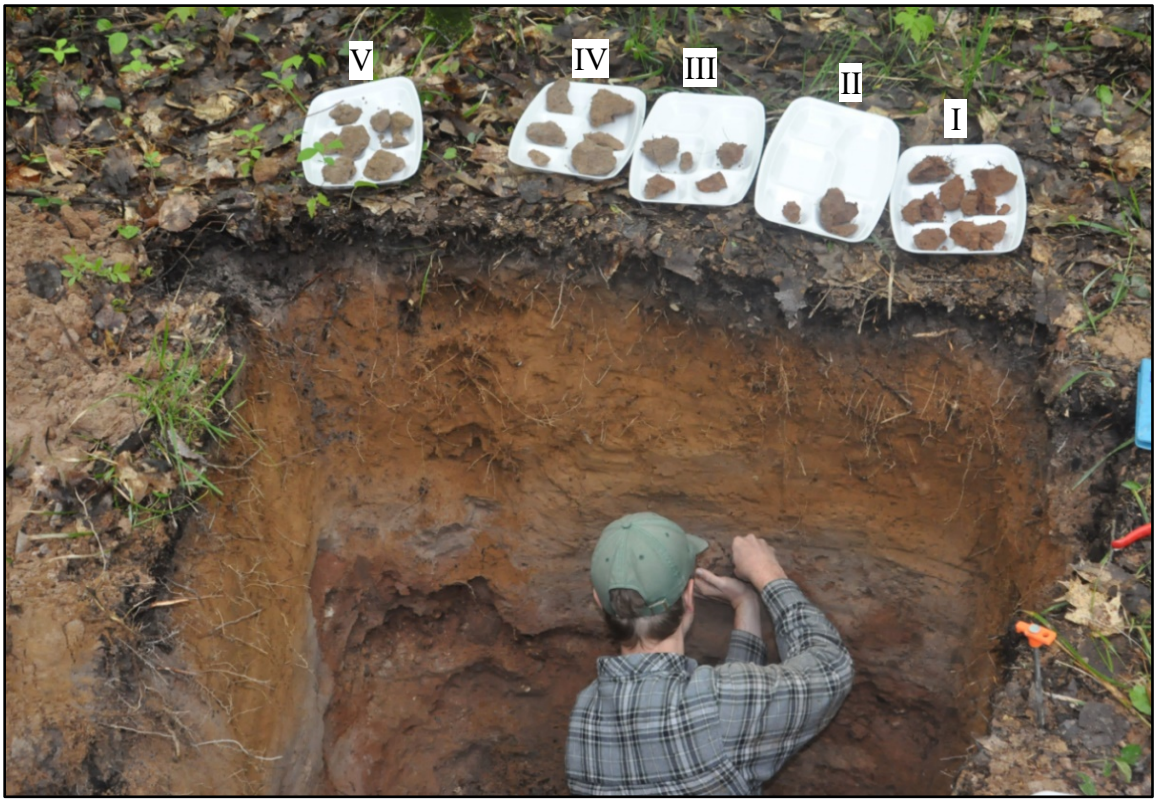

Figure 3.3. Glossic horizon (E/B) "clod" samples being collected and separated into groups in the field according to their relative degree of degradation. Roman Numerals above trays correspond to "Groups" described in Table 3.2. Photograph by R. Schaetzl.

Table 3.2. Description of the criteria used in the field to classify glossic horizon clod samples into degradational groups

Group	Name	Description
I	Non-Degraded	Peds composed entirely of illuvial material. Illuvial material has a reddish-brown color and occurs as bridges between skeletal grains and as argillans on ped faces. Little to no visible evidence of eluvial material in matrix.
II	Weakly Degraded	Peds composed primarily of illuvial material with minor components of eluvial material. Eluvial material occurs as thin coatings on ped faces and within macropores and root channels surrounding illuvial material.
III	Moderately Degraded	Peds generally composed of equal portions of eluvial and illuvial material.
IV	Strongly Degraded	Peds composed mostly of eluvial material with minor components of illuvial material. Illuvial material remains only as remnant aggregates surrounded by eluvial material.
V	Completely Degraded	Peds composed entirely of eluvial (degraded) material. Eluvial material has a whitish color and occurs as coarse-textured skeletal grains. Little to no visible evidence of illuvial material in matrix.

3.3 Laboratory Methods

Prior to performing laboratory analyses, all bulk genetic horizon samples were air-dried at 40^{o} C for 24 hr, gently disaggregated with a mortar and pestle, and passed through a 2-mm sieve to remove coarse fragments and large organics. I then homogenized the remaining fine-earth fraction (<2 mm) by passing it through a sample splitter three times in order to ensure sufficient representativeness of subsamples to be used for various laboratory analyses (Schumacher et al., 1990). Glossic horizon samples underwent similar preparation, however, prior to drying, I photographed several peds under a low-magnification binocular microscope with a DigiRetina 16MP CMOS camera (Tucsen, Ltd., Fujian, China) for documentation. Following drying, I carefully dissected peds from each group to isolate eluvial and illuvial materials to be used for subsequent analyses.

3.3.1 Glossic Horizon Ped Sampling

First, I completed dissection of the end-member groups of the degradational sequence (Groups I and V) to confirm that they contained no visible evidence of intermediate stages of degradation. I gently disaggregated several peds from each group with a porcelain pestle to examine their interior structure and composition. I included only Group V (completely degraded) peds that exhibited no evidence of remnant illuvial material in their ruptured matrix in the larger Group V sample. Conversely, I included only Group I (non-degraded) peds that exhibited no visual evidence of eluvial material in their ruptured matrix in the larger Group I sample. I also collected an additional argillan (or clay film) sample from the faces of several intact Group I peds by carefully plucking the coatings away from the underlying matrix material. Any residual sand particles that remained attached to the undersides of the cutans following plucking were removed by repeatedly passing the dried and pulverized sample through a 63 μm sieve using a sieve shaker.

Next, I completed dissection of the intermediate groups along the degradational sequence (Groups II, III, and IV) to isolate eluvial and illuvial materials, as much as possible. To isolate remnant illuvial aggregates from Group IV (strongly degraded) peds, I first sliced the peds in half along their long axis to expose the interior of the ped matrix. Next, I separated the innermost portion of exposed remnant illuvial aggregates to ensure that no residual eluvial material was included in the sample. A similar process was employed for Group III (moderately degraded) peds; however, I first scraped the exterior of the peds to remove and isolate eluvial coatings prior to slicing and sampling the interior remnant illuvial material. If any visible illuvial materials were detached during scraping, I removed them from the sample using lightweight precision tweezers. Again, a similar process was employed for Group II (weakly degraded) peds, but I scraped only ped exteriors were to remove and isolate eluvial coatings.

I completed dissection and sampling of glossic horizon peds under 3x magnification using a scalpel and steel carving tools. Table 3.3 provides a brief description of the criteria that I utilized to identify pedologic features that were sampled from peds within each group. A representative intact ped photo from each group is also provided in Figure 3.4. I dissected and sampled all peds individually; samples of similar type were ultimately combined to create one larger representative sample from which subsamples were taken for subsequent analyses. All combined samples were stored in 20 mL glass vials and labeled.

Table 3.3. Description of criteria utilized in the laboratory, to identify pedologic features to be sampled from peds within each glossic horizon group.

Group	Name	Description
I	Non-Degraded	*Illuvial (whole ped) material* – Whole peds composed of reddish-brown colored illuvial material. *Argillans* – Thin, oriented coatings of illuvial clay occurring on ped faces; smooth "waxy" surface appearance; slightly darker in color compared to underlying matrix material.
II	Weakly Degraded	*Eluvial material* – Thin (≤ 2 mm) coatings of whitish colored (bleached) sandy and silty skeletal grains, usually surrounding illuvial materials at ped margins.
III	Moderately Degraded	*Eluvial material* – Thick (≤ 5 mm) coatings of whitish colored (bleached) sandy and silty skeletal grains surrounding illuvial material. *Illuvial material* – Remnant reddish-brown illuvial aggregates ≤ 2 cm in diameter occurring in ped centers.
IV	Strongly Degraded	*Illuvial material* – Remnant reddish-brown illuvial aggregates ≤ 1 cm in diameter occurring in ped centers.
V	Completely Degraded	*Eluvial (whole ped) material* – Whole peds composed of whitish colored (bleached) sandy and silty skeletal grains.

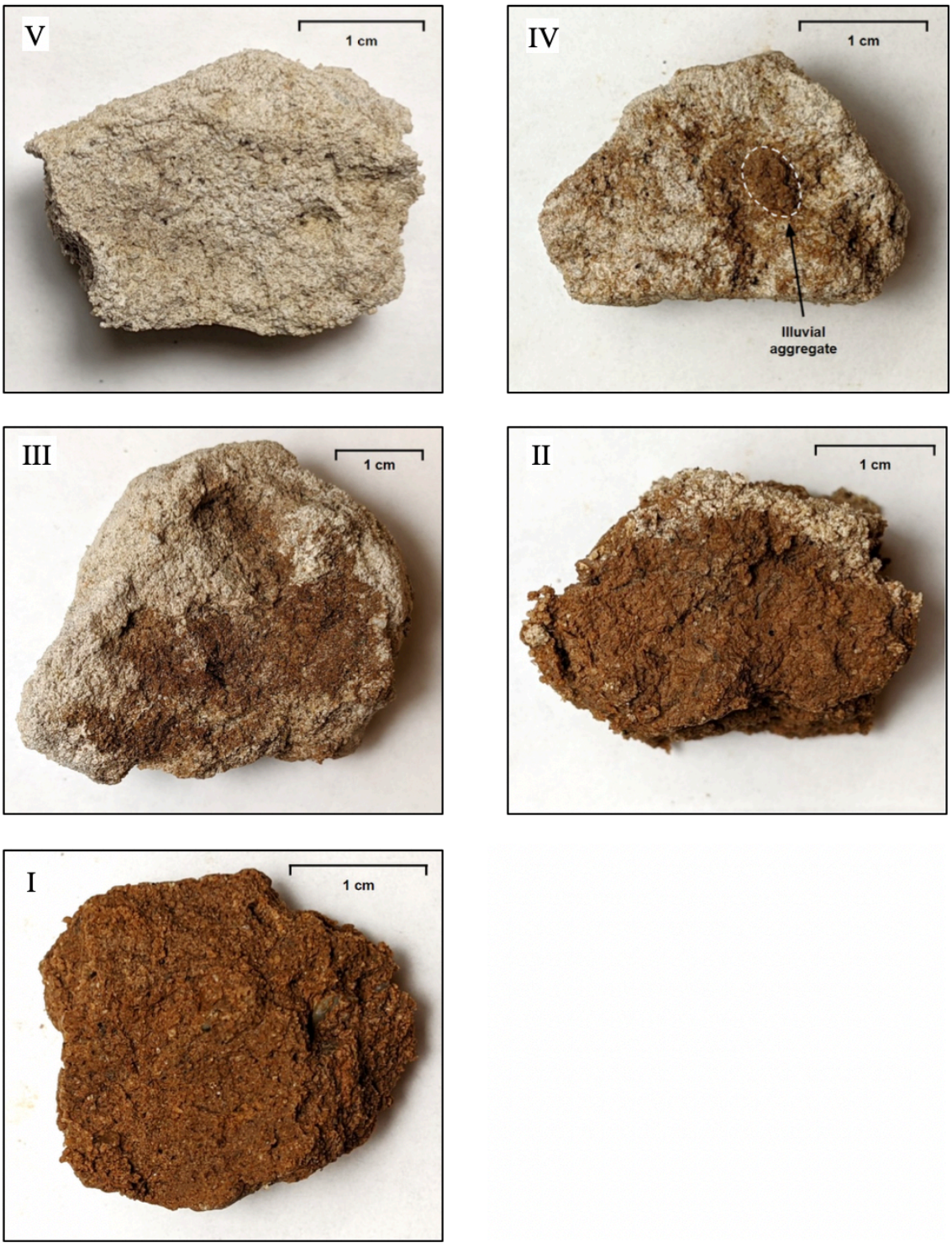

Figure 3.4 Representative examples of the interiors of intact peds from each glossic horizon group. (V) a completely degraded ped, (IV) a strongly degraded ped, (III) a moderately degraded ped, (II) a weakly degraded ped, and (I) a non-degraded ped. All peds were photographed at 1.7x magnification after air-drying for 30 minutes from field moisture condition. Photographs by C. Baish.

3.3.2 Soil Particle-size Analysis (PSA)

Soil PSA was determined according to the method previously reported by Miller and Schaetzl (2012) and used to measure grain-size distributions. Prior to PSA, I added 0.3 to 0.5 g subsamples from each genetic subsurface and glossic horizon sample to 25 mL glass vials with 5 mL of dilute dispersing solution[3] and 15 mL of distilled water. I then shook each vial for 1 hr on a rotating table to disperse any aggregates. I performed all subsequent analyses on a Malvern Mastersizer 2000E laser particle-size analyzer with a Hydro 2000MU pump accessory (Malvern Instruments Ltd., Worcestershire, UK). Initially, I analyzed each genetic horizon subsample on the laser diffraction unit two times. I then compared the two initial genetic horizon analyses in a quality control (QC) program first developed by Miller and Schaetzl (2012), and since updated (Schaetzl et al., 2020). This program determines if analyses are statistically similar enough to generate a representative textural "signature" (Figure 3.5); if a signature was not generated from the two initial analyses, I analyzed additional subsamples until the QC criteria were met. Glossic horizon subsamples were analyzed in a similar fashion; given the relatively limited quantity of some subsamples, however, the number of analyses were restricted to the amount of available material. I tabulated all PSA data in an Excel (Microsoft Corporation, Washington, US) spreadsheet in 105 size ''bins,'' ranging from 0.1 to 2000 μm, which were used to calculate particle-size distributions and assign each sample to its USDA textural class (Soil Science Division Staff, 2017). Because laser diffractometry tends to underestimate the number of particles < 2 μm (Konert and Vandenberghe, 1997), I considered the clay-silt textural break at 8 μm. The modified particle size classification system I utilized in this study is provided in Appendix C.

[3] The dispersing solution used in this study was 35.70 g $(NaPO_3)_6$ and 7.94 g Na_2CO_3 dissolved into one liter of distilled water (sensu Kilmer and Alexander, 1949).

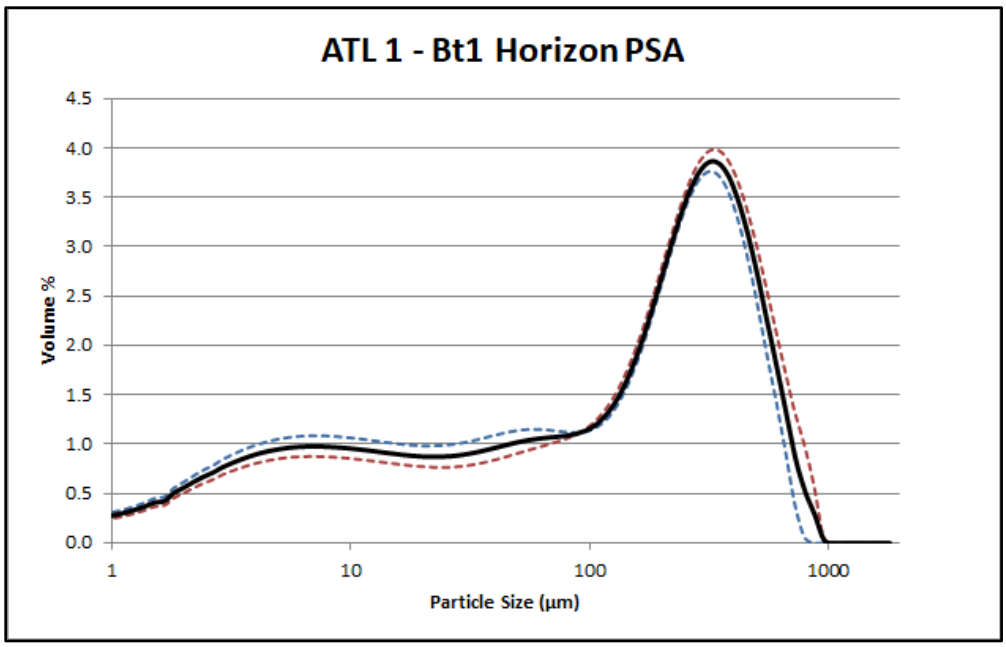

Figure 3.5. PSA QC data for the Bt1 horizon of the ATL-1 pedon. The red and blue dashed lines represent the raw particle-size distribution data from the two initial analyses on the laser diffraction unit. The black solid line represents the mean textural signature generated by the QC program.

3.3.3 Soil Bulk Density Analysis

Soil bulk density values were determined according to the methods previously reported by the Soil Survey Staff (2014). All bulk density core samples collected in the field were first air-dried at 105° C for 24 hr and then weighed to the nearest 0.01 g. Next, I gently disaggregated each sample with a mortar and pestle before passing it through a 2 mm sieve to separate coarse fragments. I measured and recorded the coarse fragment weight of each sample to the nearest 0.01 g. The bulk density of each sample was calculated according to the following formula:

$$\rho B\ (\mathrm{g/cm3}) = \frac{(\mathrm{M}_s - \mathrm{M}_\mathrm{F})}{[\,\mathrm{V}_C - (\,\mathrm{M}_F - \rho_\mathrm{F})\,]}$$

where ρ_B = bulk density of soil (g/cm^3), M_S = air-dry mass of soil (g), M_F = mass of coarse fragments (g), V_C = volume of the core (cm^3), and ρ_F = density of rock fragments (cm^3). The density of the rock fragments (ρ_F) was assumed to be 2.65 g/cm^3 (Soil Survey Staff, 2014).

3.3.4 Soil Reaction (pH) Analysis

Soil pH was determined according to the methods previously reported by the Soil Survey Staff (2014). Prior to pH analysis, I added 20 g subsamples from each genetic horizon sample to a 100 mL glass beaker with 20 mL of reverse osmosis (RO) water and stirred with a polypropylene stirring rod. I allowed the samples to stand for 1 hr, but with stirring at 15 min intervals for 30 sec. Following the final stir, I allowed each sample to stand for an additional 1 min prior to measurement. I performed all subsequent analyses on a Mettler Toledo MP220 benchtop pH meter equipped with an InLab 413 Electrode (Mettler-Toledo International Inc., Ohio, US). The electrode was calibrated according to a three-point calibration procedure using standard 10.01, 7.0, and 4.01 buffer solutions. I recorded all pH values to the nearest 0.1 unit and assigned reaction classes according to Soil Science Division Staff (2017).

3.3.5 Soil Organic Carbon Analysis

Soil organic carbon (SOC) content was estimated using loss-on-ignition (LOI), according to modified methods previously reported by Wang et al. (2012). First, I placed approximately 20 g subsamples from bulk horizon and select glossic horizon samples in pre-weighed, 30 mL porcelain crucibles and oven-dried at 105^{o} C for 4 hr to remove soil moisture. I then combusted each sample in a Thermolyne Type 1300 (Thermo Fisher Scientific, Massachusetts, US) muffle furnace at 430 ^{o} C for 8 hr to remove organic matter. This temperature was selected in order to prevent mass loss from removal of clay and carbonate minerals, both of which are present in the soils of study and may be destroyed at temperatures above 450^{o} C (Nelson and Sommers, 1996; Pribyl, 2010). I then calculated loss on ignition mass (SOM_{LOI}) as the difference between the oven-dry soil mass and the soil mass after combustion (Davies, 1974; Schulte and Hopkins 1996; Wright

et al., 2008; Wang et al., 2012):

$$\mathrm{SOM_{LOI}\ (g\ kg^{-1})} = \left(\frac{\mathrm{M_A} - \mathrm{M_O}}{\mathrm{M_A}}\right) \times 1000$$

where SOM_{LOI} = mass of soil organic matter (g kg^{-1}), M_A = air-dry mass of soil (105° C) (g), and M_O = oven-dry mass of soil (430° C). In order to estimate actual SOC content, SOM_{LOI} data were converted according to the conventional "van Bemmelen factor" of 1.724, which assumes that organic matter is composed of 58% carbon (van Bemmelen, 1890; Davies, 1974):

$$\mathrm{SOC_{LOI}\ (g\ kg^{-1})} = \mathrm{SOM_{LOI}} \,/\, 1.724$$

Considering recent literature that suggests the van Bemmelen factor may overestimate the carbon content of organic matter in many soil types, I also used a conversion factor of 2 (i.e., 50% carbon) for comparison purposes (Pribyl, 2010).

3.3.6 Soil Geochemical Analysis

Soil geochemistry was determined according to an experimental in-house method, which combines and expands upon the methods previously reported by Kalnicky and Singhvi (2001) and Stockmann et al. (2016), and used to measure elemental distributions. Prior to geochemical analysis, I first pulverized 15 g subsamples of whole-soil (i.e., unwashed of coatings) from each genetic subsurface and select glossic horizon sample with a Fritsch Vibratory Micro Mill Pulverisette 0 at ≈2 mm amplitude for 180 sec, until most of the grains were reduced to approximately silt size (< 50 µm) or less. I then added the powdered subsamples to a hollow glass tube (~40 mm volume) covered tightly on its bottom side with 4 µm Prolene thin-film, and lightly tamped the sample with a flat surfaced wooden tool in order to reduce void space between grains.

I performed all subsequent analyses on a Bruker S1 Titan handheld (i.e., portable) x-ray fluorescence (pXRF) analyzer (Bruker Corporation, Massachusetts, US) using the multi-phase 'Geo Exploration' mode with a scan time of 140 sec at 50 keV and 35 μA to evaluate the concentration of several cations or their oxides (e.g., MgO, Ca, Fe, Al_2O_3, Zr, Ti, K_2O, SiO_2, Sr, Rb and Ba). I analyzed each subsample in triplicate. I tabulated the raw geochemical data for all samples in an Excel spreadsheet and corrected the data according to in-house calibration curves generated from National Institute of Standards and Technology (NIST) standards of specific known concentration (2701, 2709, 2710, and 8704) that were analyzed with the same instrument. Because the sample size was inadequate for statistical treatment, I considered the mean of the three analyses as the representative geochemical "signature" for that particular sample. As guided by the literature, data reported in oxide form from the pXRF unit were excluded from further analysis, limiting the dataset to the following elements: Ca, Fe, Zr, Ti, Sr, Rb, and Ba (Buggle et al., 2001; Stockman, et al., 2016).

3.3.7 Soil Ion Exchange and Extractable Cations

Soil cation exchange capacity (CEC) and extractable cations for each genetic subsurface horizon in ATL-1 pedon and select glossic horizon samples were determined by the Soil and Plant Nutrient Laboratory (SPNL) at Michigan State University according to methods previously reported by Soil Survey Staff (2014). The CEC was determined with ammonium acetate (1 N NH_4 OAc) buffered at pH 7.0 (i.e., CEC-7 method). Generally, CEC-7 is determined by saturating the soil with NH_4^+ to displace cations on the exchange complex; washing the soil free of excess NH_4^+ with ethanol (C_2H_5OH); and displacing the adsorbed NH_4^+ ions on the exchange complex using sodium hydroxide (NaOH). The concentration of NH_4^+ ions in the extract solution is measured by

distillation and titration to determine the CEC (me/100g). All CEC subsamples (≈6 g) were analyzed in triplicate (≈2 g each) and the mean of the three analyses was considered as the representative CEC "signature" for that particular sample. Similar to CEC, extractable base cation content was determined with ammonium acetate buffered at pH 7.0. Following the initial saturation of the soil with NH_4^+, the concentration of the four primary displaced basic cations (Ca^{2+}, Mg^{2+}, K^+, Na^+) in the extract solution is measured by atomic adsorption spectrophotometry (AAS) to determine extractable base cation content (ppm). In order to calculate base saturation[4], I used standard base cation constant values to convert extractable cation data from ppm to me/100g (i.e., '200' for Ca^{2+}, '120' for Mg^{2+}, '390' for K^+, and '230' for Na^+). Because the parent material of the ATL pedons is calcareous, and therefore, contains "free" carbonates (Ca^{2+}), it is expected that base saturation in horizons that have not experienced significant leaching will be overestimated (i.e., exceed 100%); in such cases, I assume a base saturation of 100%, as suggested by Soil Survey Staff (2014).

[4] Base saturation is a measure of the proportion of the exchange complex that is occupied by the four primary basic cations (Ca^{2+}, Mg^{2+}, K^+, Na^+). Base saturation is calculated as a percentage of the CEC, where base saturation is equal to the sum of the extractable bases, divided by the CEC (CEC-7), and multiplied by 100 (Soil Survey Staff, 2014).

CHAPTER 4

PEDON DESCRIPTIONS

The purpose of this chapter is to present, discuss, and interpret the field and laboratory data for the two pedons sampled for this study. First, I briefly discuss site conditions to provide characterization of the external factors that influence pedogenesis at the site. Next, I discuss the two profile descriptions to provide in situ, pedon-scale characterization. I then discuss the laboratory data on the physical and chemical properties of the pedons to provide more detailed, horizon-scale characterization. Lastly, after the profiles have been characterized, I classify them according to *Soil Taxonomy* (Soil Survey Staff, 2014).

4.1 Field Characterization

The two pedons (ATL-1 and ATL-2) are located on a north-facing slope of a dissected upland near the northeastern margin of the Atlanta Channeled Uplands landform region (Burgis, 1977; Schaetzl et al., 2013). More specifically, the pedons are located on a very gentle (4%) convergent backslope position. Both pedons are well-drained, as evidenced by the absence of macroscopic pedogenic features associated with true aquic conditions (e.g., gleying). Based on field observations and previous research (Burgis, 1977; Schaetzl, 2001; Schaetzl, 2013), the ridge is composed of calcareous, coarse-loamy glacial till (> 165 cm thick) of Port Huron age (≈15,500 cal yr B.P.); the glacial till is the parent material for the pedons. The overstory vegetation at the site is dominated by quaking aspen (*Populus tremuloides*), northern red oak (*Quercus rubra*), red maple (*Acer rubrum*), and black cherry (*Prunus serotina*), with minor components of white pine (*Pinus strobus*) and paper birch (*Betula papyrifera*). The presence of mature tree cover and intact surface organic horizons (Oi and Oa horizons) suggest that erosional disturbance at the site has

been relatively minimal for at least the last several decades. The only major anthropogenic disturbances to the site would have been due to past logging operations. Additionally, no evidence of major floral or faunal bioturbation (e.g., tree uprooting or animal burrowing) was observed at the site.

4.1.1 Profile Morphology

4.1.1.1 ATL-1 Pedon

The overall profile horizonation of the ATL-1 pedon is Oi – Oa – E – Bs1 – Bs2 – E/B – Bt1 – Bt2 – BCt – C (Table 4.1; Appendix A). As suggested by its horizonation, the pedon consists of two distinct eluvial-illuvial sequa, and thus, by definition the profile is bisequal. The upper sequum (E-Bs1-Bs2 horizons), formed primarily by podzolization, characteristic of Spodosols, overlies an Alfisol-like sequum (E/B-Bt1-Bt2-BCt horizons) dominated by lessivage.

Above the spodic-like (E-Bs1-Bs2) upper sequum is a thin (<1 cm) surface layer of slightly decomposed plant material derived from a mixture of hardwood leaves, pine needles, and sticks (Oi horizon) overlying a thicker (6 cm) layer of highly decomposed leaf litter (Oa horizon) (Figure 4.1). The underlying eluvial portion (E horizon) of spodic-like upper sequum is 7 cm in thickness, has a sand texture, and is brown (7.5YR 5/2, moist) in color. The lack of an A horizon between the E and Oa horizons indicates that floral and/or faunal mixing of organic materials into the mineral soil surface has been negligible. The illuvial portion (Bs1-Bs2 horizons) of the upper sequum is 28 cm in total thickness, has a loamy sand texture, and is strong brown (7.5YR 4/6-5/6, moist) in color. Both B horizons were assigned an “s” suffix because they exhibited evidence of accumulation of sesquioxides and organic matter (i.e., podzolization), as indicated by their high color chroma values, 7.5YR hues, and greater structural development relative to the overlying E

Table 4.1 Select morphologic data for the ATL-1 and ATL-2 pedons.

HOR	Depth (cm)	Munsell color (moist)	Structure [a]	Consistence [b]	Texture [c]	Boundary [d]	Coarse Frags (vol. %)
ATL-1 Pedon							
Oi	0-1	—	—	—	—	—	—
Oa	1-7	7.5YR 2.5/1	—	—	—	a, s	—
E	7-14	7.5YR 5/2	w f sab	vfr	s	c, w	gravel: 3
Bs1	14-25	7.5YR 4/6	w fm sab	vfr	ls	c, w	gravel: 5
Bs2	25-42	7.5YR 5/6	w fm sab	vfr	ls	g, w	gravel: 5
E/B	42-58	E: 7.5YR 6/3 B: 5YR 4/4	m fm sab	fr	E: ls B: sl	c, w	gravel: 5
Bt1	58-72	5YR 4/4	m fm sab	fr	sl	c, b	gravel: 5
Bt2	72-95	5YR 4/6	m fm sab	fr	sl	g, w	gravel: 35 cobble: 20
BCt	95-123	7.5YR 5/4	m fm sab	fr	sl	g, b	gravel: 10 cobble: 5
C	123-166+	10YR 5/3	m m pl	fr	ls	—	gravel: 10 cobble: 5
ATL-2 Pedon							
Oi	0-1	—	—	—	—	—	—
Oa	1-7	7.5YR 2.5/1	—	—	—	a, s	—
E	7-14	7.5YR 5/2	w f sab	vfr	s	c, w	gravel: 3
Bs1	14-24	7.5YR 4/6	w fm sab	vfr	ls	c, w	gravel: 5
Bs2	24-56	7.5YR 5/6	w fm sab	vfr	ls	g, w	gravel: 5
E/B	56-74	E: 7.5YR 6/3 B: 5YR 4/4	m fm sab	fr	E: ls B: sl	c, w	gravel: 5
Bt1	74-81	5YR 4/4	m fm sab	fr	sl	c, b	gravel: 5
Bt2	81-98	5YR 4/4	m fm sab	fr	sl	g, w	gravel: 25 cobble: 15
BCt	98-123	7.5YR 4/4	m fm sab	fr	sl	g, i	gravel: 10 cobble: 5
C	123-140+	10YR 5/3	m m pl	fr	ls	—	gravel: 10 cobble: 5

Notes to Table 4.1:

[a] Structure grade: w = weak, m = moderate. Structure class: f = fine, m = medium. Structure shape: sab = subangular blocky, pl = platy.

[b] Consistence: vfr = very friable, fr = friable.

[c] Texture classes: s = sand, ls = loamy sand, sl = sandy loam.

[d] Boundary distinctness: a = abrupt, c = clear. g = gradual. Boundary topography: s = smooth, w = wavy, i = irregular, b = broken.

Figure 4.1. Photo of the ATL-1 pedon with approximate horizon designations.

horizon. Illuviation appears to be greater in the upper Bs1 horizon, which is slightly darker in color than the lower Bs2 horizon. Very fine and fine roots are common throughout the entire upper sequum, and a few medium and coarse roots occur in the E and Bs1 horizons.

Marking the interface between the upper and lower sequa is a well-developed, 17-cm thick glossic[1] (E/B) horizon. In vertical cross-section, approximately 70% of the horizon is composed of light brown colored (7.5YR 6/3) loamy sand eluvial material (E part). The remaining illuvial portion of the horizon (B part) has a sandy loam texture and is reddish brown (5YR 4/4, moist) in color. Evidence for translocation and accumulation of clay in the B part of the horizon occurs as clay bridges between primary grains and clay coatings lining pores. Generally, the light brown eluvial material occurs as skeletans that coat and enclose darker intact (i.e., non-degraded) illuvial material (B part). Eluvial skeletans also frequently penetrate the interior of peds as filaments along root channels and macropore pathways. Similar morphologic characteristics have been reported for glossic horizons in finer-textured soils in other Great Lakes' locales (Ranney and Beatty, 1969; Bullock et al., 1974). Unlike those previous studies, however, the degree of ped degradation in the glossic horizon of the ATL-1 pedon appears to have little relationship to depth within the horizon. In those finer-textured soils, the degradation of the Bt horizon tended to be more pronounced near the upper boundary of the glossic horizon and decreased predictably with depth along concentrated zones (i.e., tongues or interfingers) that extend downward into an underlying zone of intact illuvial material (Ranney and Beatty, 1969; Bullock et al., 1974); such morphology was not observed in the ATL-1 pedon (Figure 4.2). Rather, degradation within the glossic zone occurs largely at random, as evidenced by the frequent presence of relatively intact bodies of illuvial material in the

[1] The taxonomic classification of the E/B horizon as a glossic diagnostic subsurface horizon is discussed in section 4. 4, however, the "glossic" term is utilized to describe the horizon throughout the earlier portions of this chapter for the purpose of clarity.

upper portion of horizon that overlie zones of nearly completely degraded (albic) material. Further, the lower boundary of the horizon is generally clear and appears to be encroaching on the underlying illuvial zone relatively evenly (Figure 4.2).

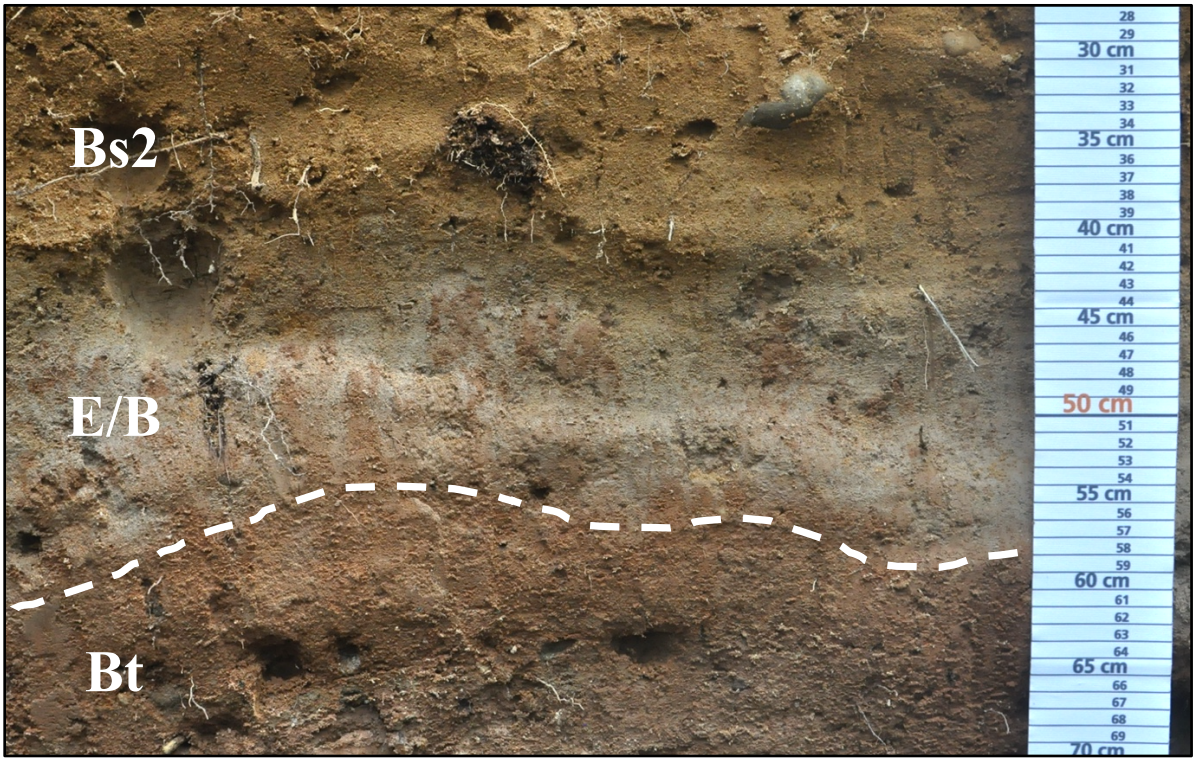

Figure 4.2. Close-up view of the glossic (E/B) horizon in the ATL-1 pedon. Photograph by R. Schaetzl.

The underlying zone of intact (i.e., mostly non-degraded) illuvial material (Bt1 horizon) is approximately 17 cm in thickness (where present), has a sandy loam texture, and is similar in color to the B part of the glossic horizon (5YR 4/4, moist). In addition to clay bridges between primary grains and clay coatings lining pores, the Bt1 horizon also shows evidence of clay translocation and accumulation in the form of argillans (or illuvial clay films) on ped faces. The argillans tend to have a slightly darker color (5YR 3/4) than the underlying soil matrix. The lower boundary of the Bt1 horizon is marked by a dense, subtly undulating "stone zone[2]" (Bt2 horizon) that is 26 cm

in thickness and dominated by gravel (35% by volume) and cobbles (20% by volume), primarily of carbonate lithology. Based on the sharp increase in coarse fragment content relative to the overlying Bt1horizon, the top of the stone zone, i.e., the upper boundary of the Bt2 horizon, was identified in the field as a lithologic discontinuity[3]. The fine-earth fraction (<2 mm in diameter) of the Bt2 horizon has a sandy loam texture and a yellowish red (5YR 4/6, moist) color. Evidence for translocation and accumulation of clay in the soil matrix of the Bt2 horizon occurs as clay bridges between primary grains and clay coatings lining pores. Additionally, thick coatings of illuvial clay occurr frequently on the surfaces of large gravels and cobbles in this horizon.

Pedogenically unaltered parent material (C horizon), as indicated by strong effervescence[4] with application of dilute HCl, underlies the stone zone. This material has a platy structure, a loamy sand texture, and is brown (10YR 5/3, moist) in color. Similar characteristics (e.g., coarse texture, brown 10YR color, platy structure, strong effervescence) have been reported for glacial tills of Port Huron age at other locations in the northeastern Lower Peninsula (Schaetzl, 1996; Schaetzl, 2001).

At some locations in the ATL-1 pit, deep tongues of illuvial material (BCt horizon) that have a sandy loam texture and are brown (7.5YR 5/4, moist) in color extend downward from the

---

[2] A stone zone, much like a stone line, is a three-dimensional (carpet-like) subsurface layer of stones in soil. They differ from stone lines, however, in that they are composed of a layer of stones that is more than approximately one stone in thickness (Johnson, 1989).

[3] A lithologic discontinuity is the point of contact (or interface) between two distinct geologic materials in a soil that has formed as a result of a change in the depositional environment, e.g., from water to wind. Each of the layers is assumed to differ substantially from the other layer in terms of particle size distribution or mineralogy, reflecting differences in inherent lithology (Schaetzl, 1998; Ahr et al., 2017).

[4] Effervescence describes the gaseous response (seen as bubbles) of the soil matrix to an applied acid-based solution (Schoeneberger et al., 2012, pg. 2-87).

bottom of stone zone and into the underlying parent material (C horizon); soil materials in the BCt tongues effervesce slightly with application of dilute HCl. The location of the tongues appears to correspond with large preferential water flow pathways that have broken through the stone zone (Figure 4.3). Generally, the glossic horizon is thicker and more strongly developed in locations above these tongues, such that a zone of intact Bt1 horizon material is often no longer present.

Figure 4.3. Illuvial tongue (BCt horizon) extending downward from the bottom of the stone zone in the ATL-1 pit. Photograph by R. Schaetzl.

4.1.1.2 ATL-2 Pedon

The ATL-2 pedon is located less than two meters from the ATL-1 pedon. Given the close proximity of the two pedons to each other, they share generally similar morphological characteristics, principally horizonation and solum thickness (Table 4.1; Appendix A). Despite these broad similarities, however, subtle differences occur in the depth, thickness, and color of some horizons between the pedons. Thus, to spare redundancy, the morphology of the ATL-2 pedon will be discussed primarily as it differs from that of the ATL-1 pedon.

The upper sequum (E-Bs1-Bs2) in the ATL-2 pedon is 14 cm thicker than in the ATL-1 pedon (49 cm vs. 35 cm). Although the lower boundary of the Bs1 horizon is slightly shallower in the ATL-2 pedon (24 cm vs. 25 cm), the lower boundary of the Bs2 horizon extends much deeper into the profile (56 cm vs. 42 cm), thus accounting for the difference in thickness of the upper sequum.

The greater thickness of the upper sequum in the ATL-2 pedon is compensated by a decrease in the thickness of the lower sequum (E/B-Bt1-Bt2-BCt) (67 cm vs. 81 cm). The total thickness of the upper E/B-Bt1 portion of the lower sequum is slightly less than in the ATL-1 pedon (25 cm vs 30 cm). Further, the glossic (E/B) horizon in the ATL-2 pedon is slightly thicker than in the ATL-1 pedon (18 cm vs. 16 cm), and more strongly degraded, as evidenced by a greater concentration of eluvial material (E part) in vertical cross-section (80% vs. 75%). Thus, the increase in thickness of the glossic horizon has largely come at the expense of the underlying Bt1 horizon, which is proportionally thinner than in the ATL-1 pedon (7 cm vs. 14 cm). The underlying Bt2 “stone zone” horizon, occurs at greater depth in the ATL-2 pedon (81 cm vs. 72 cm), is thinner than in the ATL-1 pedon (18 cm vs. 23 cm), and contains a smaller concentration (by volume) of coarse fragments, particularly gravel (25% vs 50%). Additionally, the fine-earth fraction in the

Bt2 horizon is slightly darker than in the ATL-1 pedon (7.5YR 4/4 vs. 7.5YR 4/6). Lastly, a continuous BCt horizon occurs beneath the stone zone, unlike in the ATL-1 pedon, where this horizon occurs more irregularly. Further, the occurrence of the BCt horizon in the ATL-2 pedon does not appear to be associated with any broad preferential water flow pathways through the stone zone, although such features were observed at other locations in the ATL-2 pit. It should be mentioned, however, that the BCt horizons share similar color (7.5YR 4/4-5/4) and lower boundary depth (123 cm), and thus, their occurrence has likely resulted from similar pedogenic processes, albeit at slightly different intensities.

4.1.1.3 Summary

Both pedons have typical bisequal horizonation for coarse-loamy textured soils in the area (Schaetzl, 1996), with weakly expressed spodic-like (E-Bs) horizon sequences overlying alfic (E/B-Bt) horizon sequences that show evidence of a transitional zone of degradation (i.e., a glossic (E/B) horizon) in their upper portion. Taken together, these morphologic indicators suggest that the soils are currently in an incipient stage of spodic development, as preconditioned by the formation of a coarse-textured eluvial zone in the alfic sequum below. Subsequent discussion of laboratory derived data will focus on expansion of this hypothesis.

4.2 Physical Characterization

4.2.1 Soil Texture

Particle size analysis of the fine-earth fraction (< 2 mm in diameter) of the ATL-1 and ATL-2 pedons indicate that they are dominated by sands, particularly medium and fine sands (Table 4.2). Coarse sand also makes up an appreciable component of the sand fraction, while

relatively little very fine or very coarse sand is present in either pedon. Overall, the upper sequum (E-Bs1-Bs2) in both pedons is coarser than the lower sequum (E/B-Bt1-Bt2-BCt), containing more mean total sand (≈84% vs. ≈71%). The decrease in total sand content in the lower sequum is compensated primarily by an increase in mean total clay (≈4% vs. ≈12%), although a slight increase in mean total silt also occurs (≈12% vs. ≈16-17%). Despite these generally similar trends, subtle inter-pedon differences in the vertical distribution of particle size separates occur with depth, most notably within the lower sequum horizons (Figure 4.4).

In the lower (alfic) sequum, the glossic (E/B) horizon is slightly finer in the ATL-1 pedon than in the ATL-2 pedon, containing less total sand (74% vs. 79%) and more total clay (12% vs. 10%). Overall, the total clay values are generally within the range of those found in other glossic horizons in the Great Lakes region forming in calcareous drift, which range from ≈6% to ≈27% (Harpstead and Rust, 1964; Bullock et al., 1974; Hole, 1975; Schaetzl, 1996; Weisenborn, 2001). Hole (1975) and Schaetzl (1996), however, are the only other studies to report a total sand value of > ≈50% for such soils. In the ATL-1 pedon, the E portion of the E/B horizon contains 83% sand and 7% clay, which is just slightly coarser in texture than the bulk E/B horizon value, providing an initial supporting line of evidence that the horizon is dominated primarily by degraded (eluvial) material. Furthermore, the texture of the E portion of the E/B horizon is also only slightly finer than that of the overlying Bs2 horizon (7% vs. 4%), suggesting that podzolization in these soils is likely initiated at a clay content of < 7%. Conversely, the B part of the E/B horizon in the ATL-1 pedon has a similar particle size distribution to that of the underlying Bt1 horizon, containing 62% sand and 18% clay, and indicating that the B parts of the glossic (E/B) horizon are indeed remnants of a former, intact illuvial horizon.

Table 4.2 Particle size data for the ATL pedons.

HOR	**sand** 2-0.05 mm	**silt** 50-2 µm	**clay** < 2 µm	**vcs** 2-1 mm	**cs** 1-0.5 mm	**ms** 0.5-0.25 mm	**fs** 0.25-0.1 mm	**vfs** 0.1-0.05 mm	**csi** 50-6 µm	**msi** 20-6 µm	**fsi** 6-2 µm
ATL-1 Pedon											
E	86.2	11.7	2.1	0.8	20.6	33.4	21.6	9.8	6.2	2.8	5.5
Bs1	81.2	14.1	4.7	0.6	16.1	29.9	23.3	11.3	6.5	3.1	7.6
Bs2	84.3	11.6	4.1	0.8	19.9	33.8	21.5	8.3	5.8	2.7	5.8
E/B	73.9	13.8	12.3	0.3	17.5	31.4	18.4	6.3	5.9	2.9	7.9
E part	82.6	10.0	7.4	0.5	18.4	33.4	21.0	9.3	4.5	2.1	5.5
B part	61.9	20.6	17.5	0.5	14.8	23.0	15.8	7.8	7.9	4.0	12.7
Bt1	62.1	20.0	17.9	0.5	13.0	22.0	16.1	10.5	8.1	3.9	11.9
Bt2	73.4	16.2	10.4	0.9	17.9	28.8	19.0	6.8	6.2	3.1	10.0
BCt	73.1	19.5	7.4	0.5	14.3	26.0	18.7	13.6	10.6	4.7	8.9
C	81.1	13.3	5.6	0.8	19.0	28.4	19.3	13.6	7.9	3.2	5.4

Notes to Table 4.2:

vcs - very coarse sand
cs - coarse sand
ms - medium sand
fs - fine sand
vfs - very fine sand
csi - coarse silt
msi - medium silt
fsi - fine silt

Table 4.2 (cont'd)

HOR	sand 2-0.05 mm	silt 50-2 µm	clay < 2 µm	vcs 2-1 mm	cs 1-0.5 mm	ms 0.5-0.25 mm	fs 0.25-0.1 mm	vfs 0.1-0.05 mm	csi 50-20 µm	msi 20-6 µm	fsi 6-2 µm
ATL-2 Pedon											
E	86.9	10.9	2.2	0.4	19.2	30.9	22.7	13.7	2.8	2.5	5.6
Bs1	82.1	12.9	5.0	0.4	16.4	29.2	23.6	12.5	2.8	2.7	7.4
Bs2	83.4	11.0	5.5	0.1	15.9	32.3	23.2	12.0	2.3	2.2	6.5
E/B	79.1	10.8	10.1	0.8	18.6	30.4	20.9	8.4	2.7	2.3	5.8
Bt1	64.1	19.5	16.4	0.4	11.6	23.7	17.4	11.0	4.4	4.0	11.1
Bt2	71.7	15.9	12.4	0.5	15.8	29.3	19.4	6.7	2.8	2.9	10.2
BCt	71.3	18.9	9.8	0.5	14.7	27.2	18.3	10.6	4.6	4.5	9.8
C	78.7	13.4	7.9	0.5	16.7	27.5	22.3	11.7	3.4	2.9	7.1

Notes to Table 4.2:

vcs - very coarse sand
cs - coarse sand
ms - medium sand
fs - fine sand
vfs - very fine sand
csi - coarse silt
msi - medium silt
fsi - fine silt

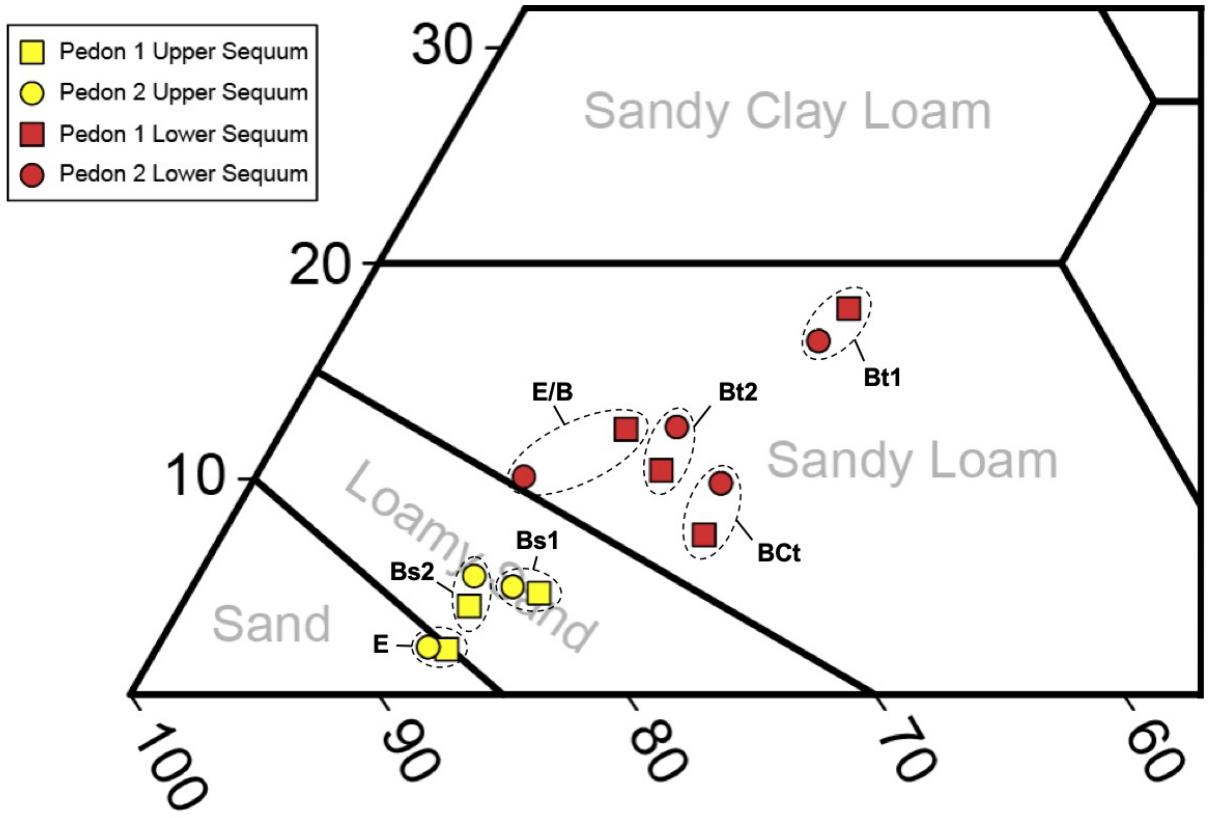

Figure 4.4. Particle-size data for the upper (spodic-like) and lower (alfic) sequum horizons of the ATL-1 and ATL-2 pedons plotted on the lower left portion of a standard NRCS textural triangle.

Clay content reaches a maximum below the glossic horizon (i.e., in the Bt1 horizon) in both pedons and decreases predictably with depth below that point. Similar to the glossic (E/B) horizon, however, the Bt1 horizon is slightly finer in the ATL-1 pedon than in the ATL-2 pedon, containing more total clay (18% vs. 16%). Unlike in the upper (E/B-Bt1) portion of the sequum, the lower Bt2 and BCt horizons of the ATL-2 pedon contain more total clay than do similar horizons in the ATL-1 pedon.

In addition to an increase in clay content, the lower sequum in both pedons also shows an increase in mean total silt contents, relative to the upper sequum (≈12% vs. ≈16-17%), the majority

of which occurs in the fine silt (8-25 μm) subfraction. In both pedons, the vertical distribution of fine silt mimics that of the clay fraction, reaching a maximum in the Bt1 horizon and decreasing predictably with depth. This trend suggests that both clay and fine silt have been mobile in these soils. Silt enriched subsurface horizons are well-documented in coarse-textured soils, and their occurrence has most commonly been attributed to translocation (Forman and Miller, 1984; Locke, 1986; Schaetzl, 1996; Schaetzl, 1998; Bockheim, 2003) and/or vertical sorting (Van Vliet-Lanoë, 1998) processes. Generally, vertical sorting is associated with frequent freeze-thaw cycles and results in the downward migration of fines and upward displacement of coarser particle fractions. Although freeze-thaw is a common phenomenon in the study area, as discussed previously (Chapter 2), it probably does not extend to the depth of the Bt horizon. Indeed, the overall vertical uniformity of the sand fraction (discussed in section 4.2.2) indicates freeze-thaw has had little influence on silt movement. Thus, I assume that the increase in fine silt in the lower sequum is likely associated with translocation processes (i.e., pervection).

Although the data from this study are inadequate for quantitative analysis, the amount of clay and fine silt observed in the lower sequum, relative to the parent material, probably cannot be entirely accounted for by translocation, thus indicating the likelihood of a secondary input source. Although an eolian contribution of silts cannot be ruled out, no potential source areas near the study site have been reported in the literature. Therefore, I conclude that the increase in clay and fine silt is, to some degree, a result of in-situ weathering and disintegration of coarser materials. Previous research has shown that frost-shattering and/or chemical dissolution of easily weatherable sands and primary clasts (such as those of carbonate lithology) can produce a significant amount of both clay and fine silt, which can later be translocated in vertically percolating water (Arnaud and Whiteside, 1963; Forman and Miller, 1984; Teveldal et al., 1990; Van Vliet-Lanoë, 1998;

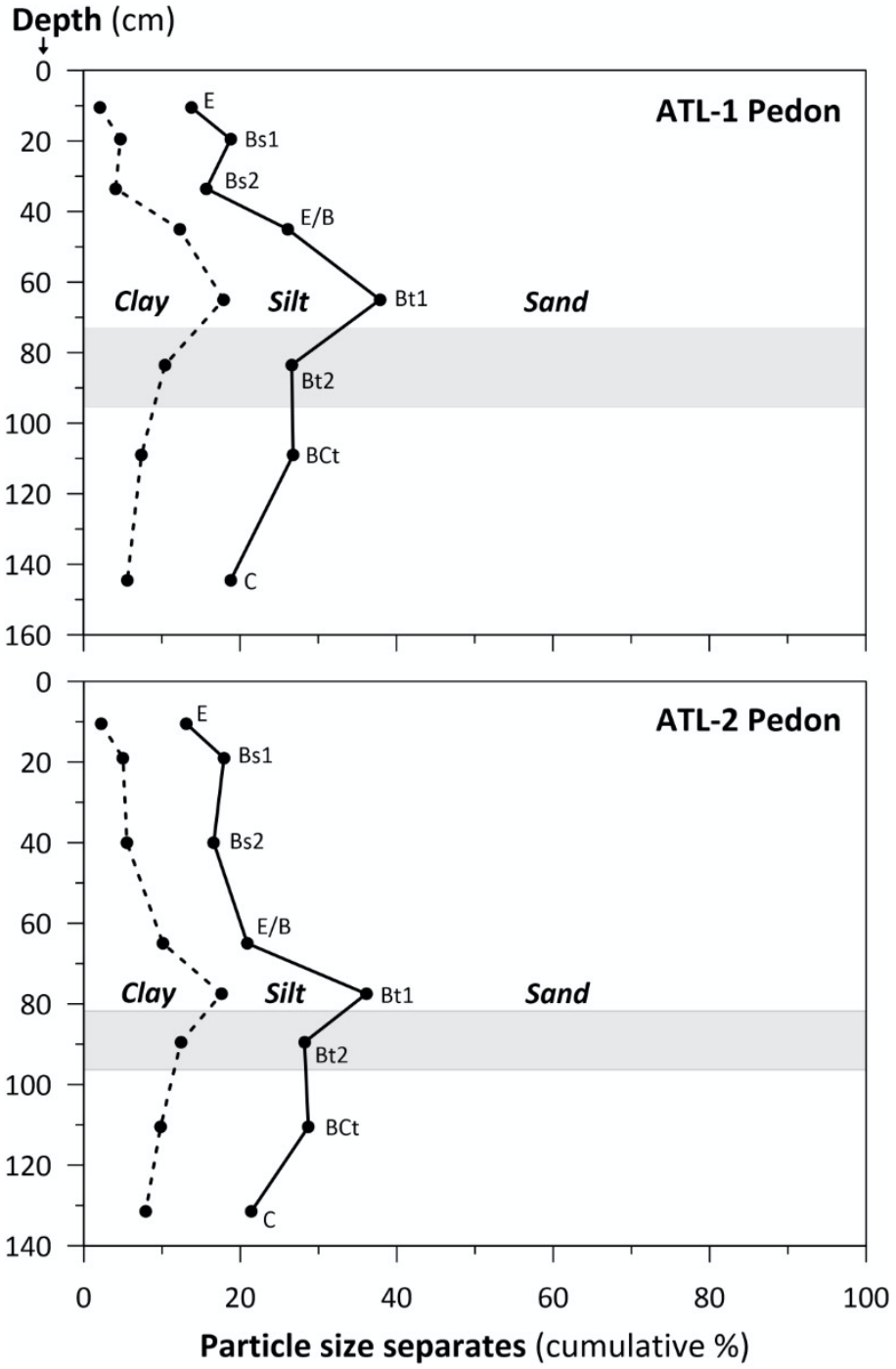

Figure 4.5. Depth trends of particle size in for the ATL-1 and ATL-2 pedons. The "stone zone" (Bt2 horizon), as identified in the field, is highlighted by the shaded band.

Birkeland, 1999). Weathering byproducts released during chemical dissolution of such materials may also result in the neoformation of clay minerals at greater depths (Eberl, 1984; Birkeland, 1999; Chesworth et al., 2008). It is generally assumed that no one process alone is responsible for the formation of clay-enriched subsurface horizons (Birkeland, 1999; Phillips, 2004; Bockheim and Hartemink, 2013; Soil Survey Staff, 2014).

Depth functions further illustrate trends in the vertical distribution of particle size separates in the two pedons (Figure 4.5). Although both pedons have generally similar horizonation, the apparent compression of the profile above the Bt2 "stone zone" horizon in the ATL-1 pedon is highlighted by broader spikes in the clay and silt curves.

4.2.2 Clay- and Fine Silt-Free Particle Size Analysis

In addition to providing textural characterization, particle size data were also utilized to supplement and reinforce (or alter and refute) the initial field call regarding a lithologic discontinuity (LD) in the field (i.e., the Bt2 horizon), and to identify any that might have gone unnoticed. Because LDs often form as a result of changes in depositional environments (Schaetzl, 1998; Ahr et al., 2017), abrupt dissimilarities in the vertical distribution of immobile particle separates, particularly sand, is considered an excellent indicator of parent material nonuniformity (Soil Survey Staff, 2014). In order to remove the effects of pedogenically mobile soil separates, i.e., clay and fine silt, in the soils, which can obscure inherent lithologic characteristics (Ahr et al., 2017), the sand subfractions were evaluated on a clay- and fine silt-free basis (Table 4.3), e.g., % clay-free sand = [(% sand) / ((% sand) + (% coarse silt))] * 100. Clay- and silt-free particle size data were (a) plotted as depth functions and (b) used to calculate two indices, both of which were developed to test for parent material uniformity in soils.

Table 4.3. Clay- and fine-silt free sand data for the ATL-1 and ATL-2 pedons.

HOR	**sand** 2-0.05 mm	**vcs** 2-1 mm	**cs** 1-0.5 mm	**ms** 0.5-0.25 mm	**fs** 0.25-0.1 mm	**vfs** 0.1-0.05 mm
ATL-1 Pedon						
E	93.3	0.9	22.3	36.1	23.4	10.6
Bs1	92.6	0.7	18.4	34.1	26.6	12.9
Bs2	93.6	0.9	22.1	37.5	23.9	9.2
E/B	92.6	0.4	21.9	39.3	23.1	7.9
Bt1	88.5	0.7	18.5	31.3	22.9	15.0
2Bt2	92.2	1.1	22.5	36.2	23.9	8.5
3BCt	87.3	0.6	17.1	31.1	22.3	16.2
3C	91.1	0.9	21.3	31.9	21.7	15.3
ATL-2 Pedon						
E	94.3	0.4	20.8	33.5	24.6	14.9
Bs1	93.7	0.5	18.7	33.3	26.9	14.3
Bs2	94.9	0.1	18.1	36.7	26.4	13.7
E/B	94.1	0.8	22.1	36.1	24.9	10.0
Bt1	88.4	0.4	16.0	32.7	24.0	15.2
2Bt2	92.6	0.5	20.4	37.9	25.1	8.7
3BCt	88.7	0.5	18.3	33.8	22.8	13.2
3C	92.6	0.5	19.6	32.4	26.2	13.8

Notes to Table 4.3:
vcs - very coarse sand
cs - coarse sand
ms - medium sand
fs - fine sand
vfs - very fine sand

The first index, the Uniformity Value (UV) index of Cremeens and Mokma (1986), is calculated as the difference in the ratio of silt plus very fine sand to total sand minus very fine sand between two adjacent horizons, minus one:

$$\mathrm{UV} = \frac{[(\%\ \text{silt} + \%\ \text{very fine sand})/\ (\%\ \text{sand} - \%\ \text{very fine sand})]_{\ \text{in upper horizon}}}{[(\%\ \text{silt} + \%\ \text{very fine sand})/\ (\%\ \text{sand} - \%\ \text{very fine sand})]_{\ \text{in lower horizon}}} - 1.0$$

It seems likely that Cremeens and Mokma (1986) chose to use very fine sand as the primary type of data in the UV index because their soils were particularly rich in fine sands. I chose to develop and use a modified UV index that instead considers the medium sand subfraction because of its greater abundance throughout the pedons. I also chose to use a sum of the coarser silt subfractions to account for the effects of fine silt translocation. A UV index value of zero indicates that the two materials (horizons) are identical in terms of relative amounts of particle size separates; the greater the deviation of the value from zero, the greater the possibility of nonuniformity in parent materials between the two horizons. I used a threshold value of ± 0.6 to identify LDs, as originally proposed by Cremeens and Mokma (1986) and later supported by Schaetzl (1998) and Tsai and Chen (2000). The other index used, the Cumulative Particle Size Distribution (CPSD) index of Langhor et al. (1976), was also calculated for the soils. It is derived as the sum of the lesser values of silt and sand subfractions between two adjacent horizons, for example:

Upper horizon					
Very coarse sand	Coarse sand	Medium sand	Fine sand	Very fine sand	Total silt
1%	21%	34%	**22%**	**10%**	**12%**

Lower horizon					
Very coarse sand	Coarse sand	Medium sand	Fine sand	Very fine sand	Total silt
1%	**17%**	**31%**	24%	12%	15%

Values in bold indicate the lower of the two quantities for that particular particle size fraction in the horizons of comparison. The lower values are summed to arrive at the CPSD index value:

$$\mathbf{1\%} + \mathbf{17\%} + \mathbf{31\%} + \mathbf{22\%} + \mathbf{10\%} + \mathbf{12\%} = 93$$

Similar to the UV index, I chose to instead use a sum of the coarser silt subfractions to account for the effects of fine silt translocation. A CPSD index value of 100 indicates that the two materials are identical in terms of relative amounts of particle size separates; the greater the deviation of the value from 100, the greater the possibility of nonuniformity in parent materials. The minimum possible CPSD index value is zero, which occurs when the materials are completely different and do not share any of the same particle size separates (e.g., one horizon is composed of only sand, while the other is composed of only silt). Unlike the UV index of Creemens and Mokma (1986), the CPSD index does not have an established threshold value beyond which LDs are identified. Rather, the CPSD index is a relative measure of how similar the two horizons, with higher values indicating greater similarity.

Clay- and fine silt-free depth functions show relatively little variability in the overall vertical distribution of the dominant sand subfractions (i.e., fine, medium, and coarse sands) in the two pedons (Figure 4.6). Generally, no more than an 8% change in the dominant sand subfractions occurs between any two immediately adjacent horizons in either pedon, including through the Bt2 "stone zone" horizon (Table 4.3). It is worth mentioning that the largest difference in the total sand content between any two immediately adjacent horizons occurs between the glossic (E/B) and Bt1 horizons in both pedons. Morphological indicators, however, strongly suggest that these horizons are genetically related, and therefore, the slight differences in total sand content was not taken as evidence for a change in inherent lithological characteristics.

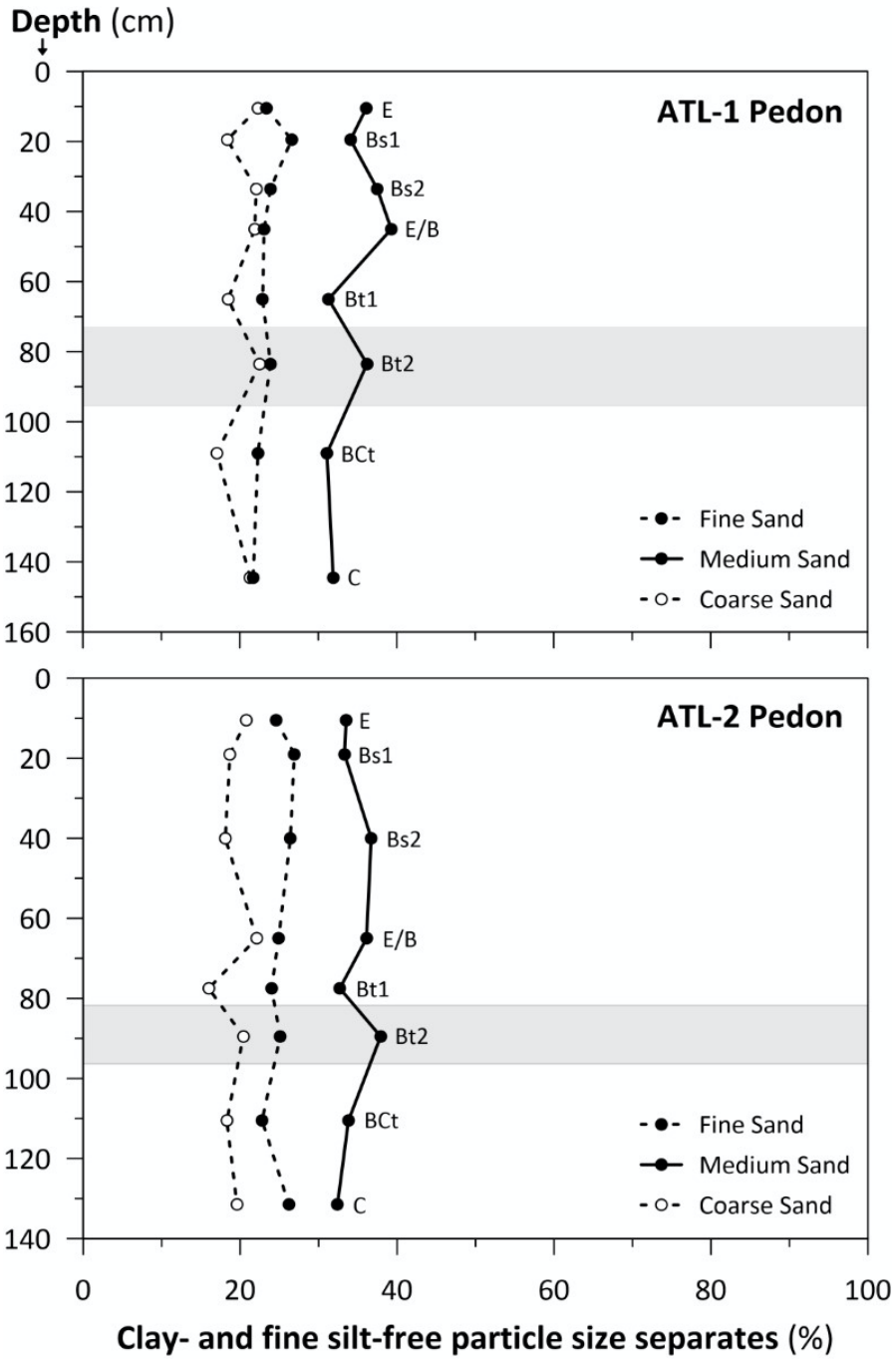

Figure 4.6. Depth trends of dominant clay- and fine silt-free sand subfractions in the ATL-1 and ATL-2 pedons. The "stone zone" (Bt2 horizon), as identified in the field, is highlighted by the shaded band.

The modified Uniformity Value (UV) index shows relatively little deviation from zero throughout either pedon (Figure 4.7; Table B.2). Generally, no UV index values > ± 0.25 occur in either pedon, with little to no variation (± 0.04) through the Bt2 "stone zone" horizon. Although not reported, similar UV index values calculated using the fine and coarse sand subfractions, both of which also occur in greater abundance than very fine sand, showed generally similar trends. Similarly, the modified Cumulative Particle Size Distribution (CPSD) index showed relatively little deviation from 100 throughout either pedon (Figure 4.8; Table B.2). Generally, no CPSD index values < 88 occur in either pedon, including through the Bt2 "stone horizon" horizon. Thus, neither of the indices identified a lithological discontinuity in either of the two pedons.

Taken together, data derived from these evaluations of the immobile particle-size separates point to the likelihood of a uniform parent material in the ATL pedons. Although it is not the intention of this research to address the origin of the stone zone in these soils, particle size data indicate that it likely does not represent a zone of contact between two materials of distinctly different geologic origin. Thus, I suggest that any subsequent physical or chemical differences in the soils, down-profile, have resulted from pedogenesis. Stone zones have been widely documented in soils (Johnson, 1989), including in the upper Great Lakes region (Schaetzl, 1996; Rindfleisch and Schaetzl, 2001; Bockheim, 2003), and many hypotheses have been presented regarding their formation. Further research examining a greater number of soils is required to speculate on the geomorphic processes responsible for the formation of the stone zone in these soils.

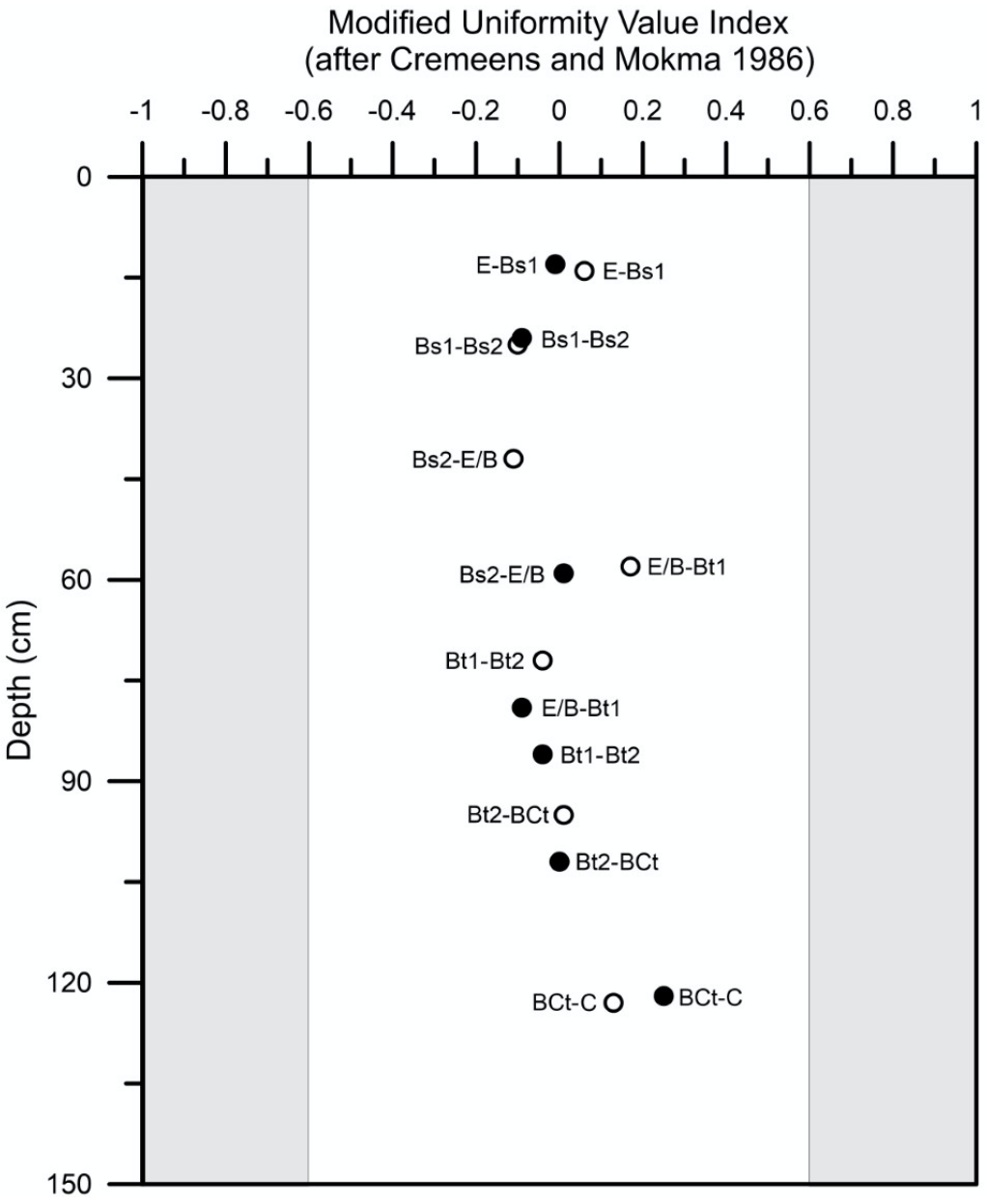

Figure 4.7. Modified Uniformity Value (UV) index data for the ATL-1 and AT-2 pedons considering the medium sand subfraction. Open circles represent UV values for the ATL-1 pedon; closed circles represent UV values for the ATL-2 pedon. Values are plotted according to the depth of contact between the two horizons of comparison. The grey boxes represent the UV index value (0.6) above which lithologic discontinuities are identified, as originally suggested by Cremeens and Mokma (1986).

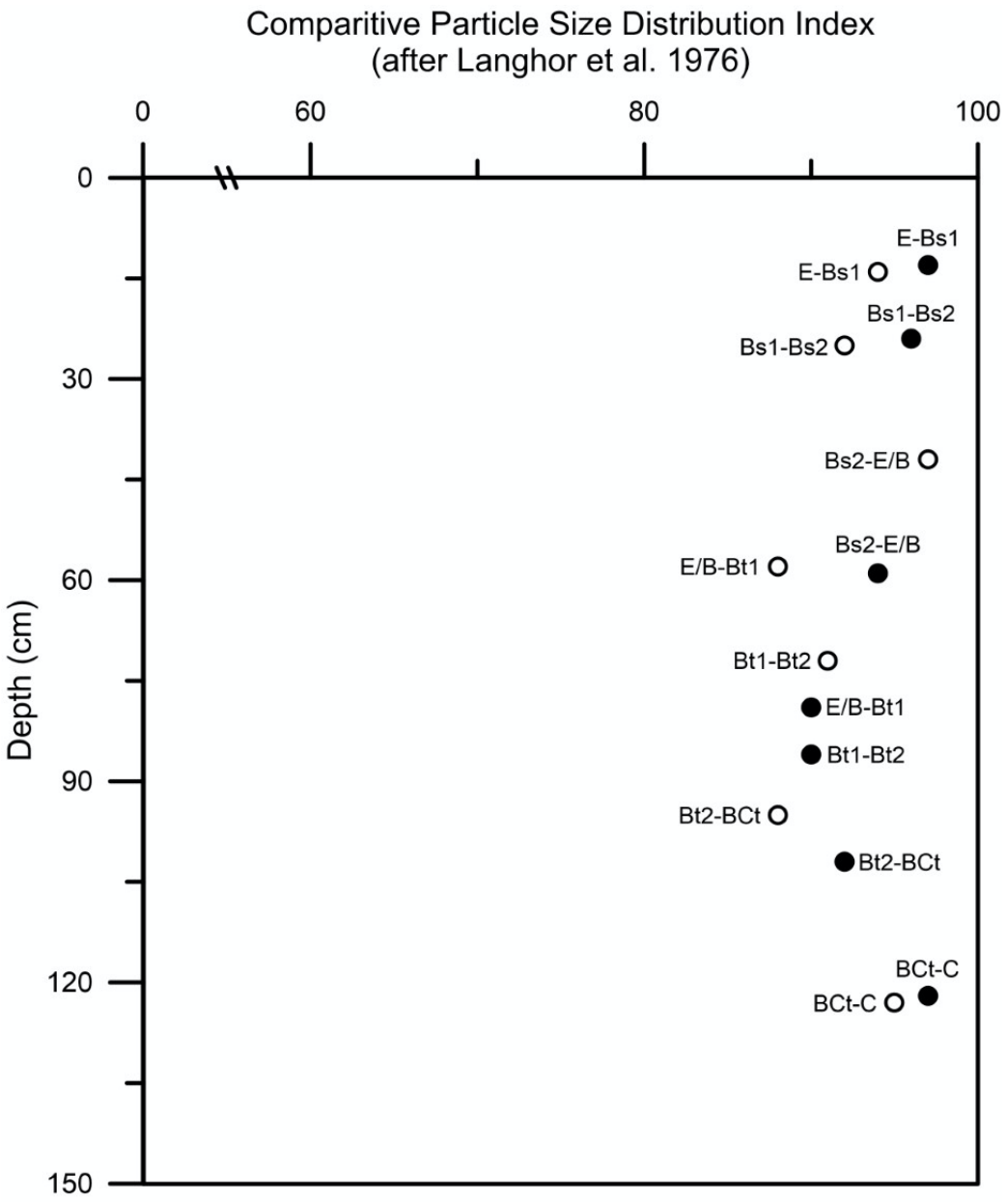

Figure 4.8. Modified Cumulative Particle Size Distribution (CPSD) index data for the ATL-1 and AT-2 pedons. Open circles represent CPSD values for the ATL-1 pedon; closed circles represent CPSD values for the ATL-2 pedon. Values are plotted according to the depth of contact between the two horizons of comparison.

4.2.3 Soil Bulk Density

Bulk density values for the ATL-1 pedon range from 1.29 g/cm3 to 1.55 g/cm^3 (with the exception of the Bt2 "stone zone" horizon) (Figure 4.9; Table B.3). Bulk density values are lowest near the soil surface and increase with depth in both pedons, as is commonly observed in most soils (Schaetzl and Thompson, 2015). Lower bulk density values (≤ 1.40 g/cm^3) in the upper sequum (E-Bs1-Bs2) horizons, despite their slightly coarser texture, are likely due to greater organic matter content, particularly in the Bs horizons (discussed in section 4.3.2), and/or bioturbation by root growth, and pore formation as roots decay. Bulk density values increase slightly in the underlying glossic (E/B) horizon (1.47 gm/cm^3), reflective of the accumulation of illuvial clay and fine silt, and concomitant loss of pore space. Schaetzl (1996) and Weisenborn (2001) both reported a value of 1.60 g/cm^3 for other non-fragic glossic (E/B) horizons in northeastern Lower Michigan. It should be noted, however, that no discussion regarding the relationship between bulk density and glossic horizon genesis in non-fragic soils has been previously reported in the literature. Interestingly, the E/B horizon has a similar bulk density to that of the associated Bt1 horizon (1.47 g/cm^3), suggesting that the soil fabric has retained its packing character despite clay loss and associated textural coarsening. Soil bulk density reaches a maximum in the C horizon (1.55 g/cm^3), providing further evidence that the material was likely deposited as a dense glacial till.

The extremely low bulk density value reported for the Bt2 horizon (0.68 g/cm^3) is anomalous. This value is likely associated with the high concentration of coarse fragments (>2 mm in diameter) that characterizes the "stone zone". The gravel content of the Bt2 horizon is approximately 50% by mass (which corresponds to ≈35% by volume). Previous data reported by Posen and Lavee (1994) and Vincent and Chadwick (1994) suggested that bulk density decreases

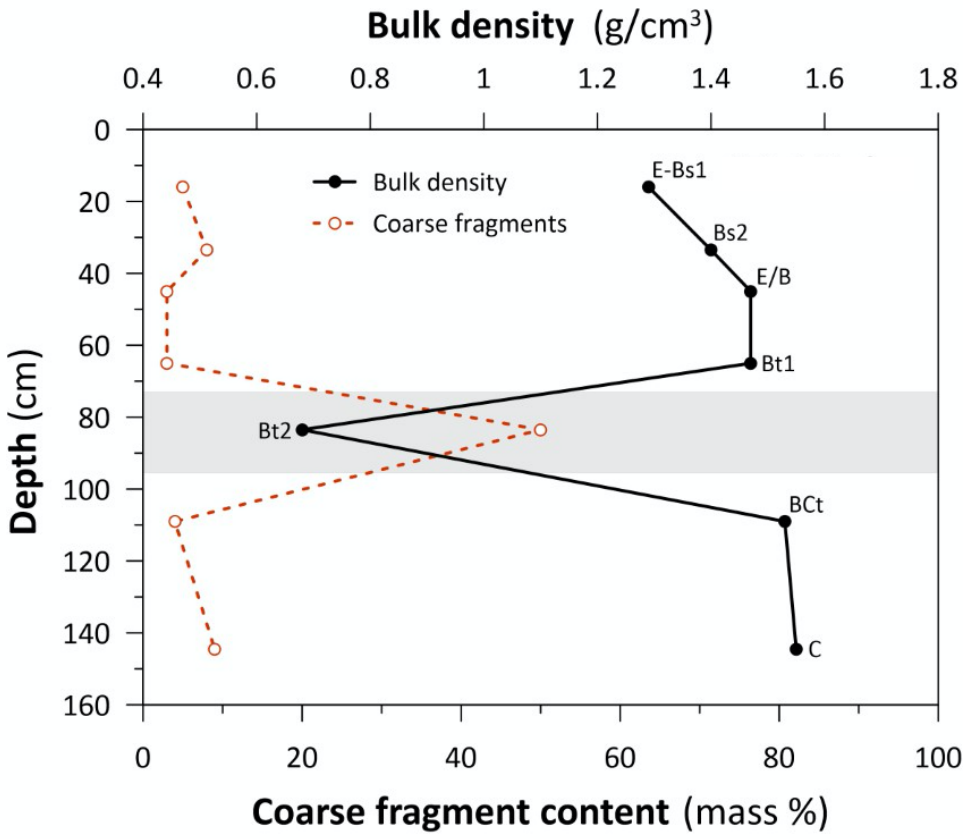

Figure 4.9. Depth trends in bulk density and coarse fragment content in the ATL-1 pedon. Reported values represent the mean of the two samples collected. The "stone zone" (Bt2 horizon), as identified in the field, is highlighted by the shaded band.

when gravel content exceeds 30% by mass (or ≈20% by volume). This relationship occurs assumedly due to the insufficient availability of fine earth faction of the soil to occupy the void spaces formed between rock fragments at high concentration (i.e., greater than 30% by mass) (Posen and Lavee, 1994). Further, because the coarser fragments tend to carry most of the external load, relatively little stress is exerted on the soil that is present (Rucknagel et al., 2007). Under these conditions, soil particles tend to not pack as closely, resulting in lower bulk density values. Such soils and sediments are described as having a *clast-supported* or *skeletal* structure (Soil Survey Staff, 2014).

4.3 Chemical Characterization

4.3.1 Soil Reaction (pH)

Soil reaction (pH) values in the ATL-1 and ATL-2 pedons ranges from very strongly acidic to strongly alkaline (Figure 4.10; Table C.1). Generally, pH values are lowest near the soil surface and increase with depth in both pedons. In the upper sequum (E-Bs1-Bs2), pH values range between 4.5 (very strongly acid) and 5.8 (strongly acid). The upper sequum, however, is slightly more acidic in the ATL-2 pedon than in the ATL-1 pedon, particularly in the E horizon (4.5 vs. 5.2). The Bs horizons, show similar trends in both pedons, with pH values between 5.3 (strongly acid) and 5.8 (moderately acid). Schaetzl (1996) reported pH values ranging from 6.0 (moderately acid) to 7.3 (neutral) for Bs horizons in other bisequal soils forming in similar parent materials in northeastern Lower Michigan. One possible explanation for the slightly lower Bs horizon pH values in the soils of study is that they are located in an area that receives slightly more winter snowfall, and in turn, experience greater infiltration and leaching during the spring snowmelt period (Schaetzl and Isard, 1991).

The bulk glossic (E/B) horizon has a pH value of 6.3 (slightly acid) and 5.9 (moderately acid) in the ATL-1 and ATL-2 pedons, respectively. These values are similar to those found in other glossic horizons in the Great Lakes region forming in calcareous drift, which range from 5.8 (moderately acid) to 6.7 (neutral) (Harpstead and Rust, 1964; Bullock et al., 1974; Hole, 1975; Schaetzl, 1996; Weisenborn, 2001). In the ATL-1 pedon, the E portion of the E/B horizon has a pH value of 6.0 (moderately acid), which aligns closely with the bulk E/B horizon pH value (6.3), providing an additional supporting line of evidence that the horizon is dominated primarily by degraded material. Furthermore, the pH of the E portion of the E/B horizon is also only slightly higher than that of the overlying Bs2 horizon (6.0 vs. 5.8), suggesting that podzolization in these

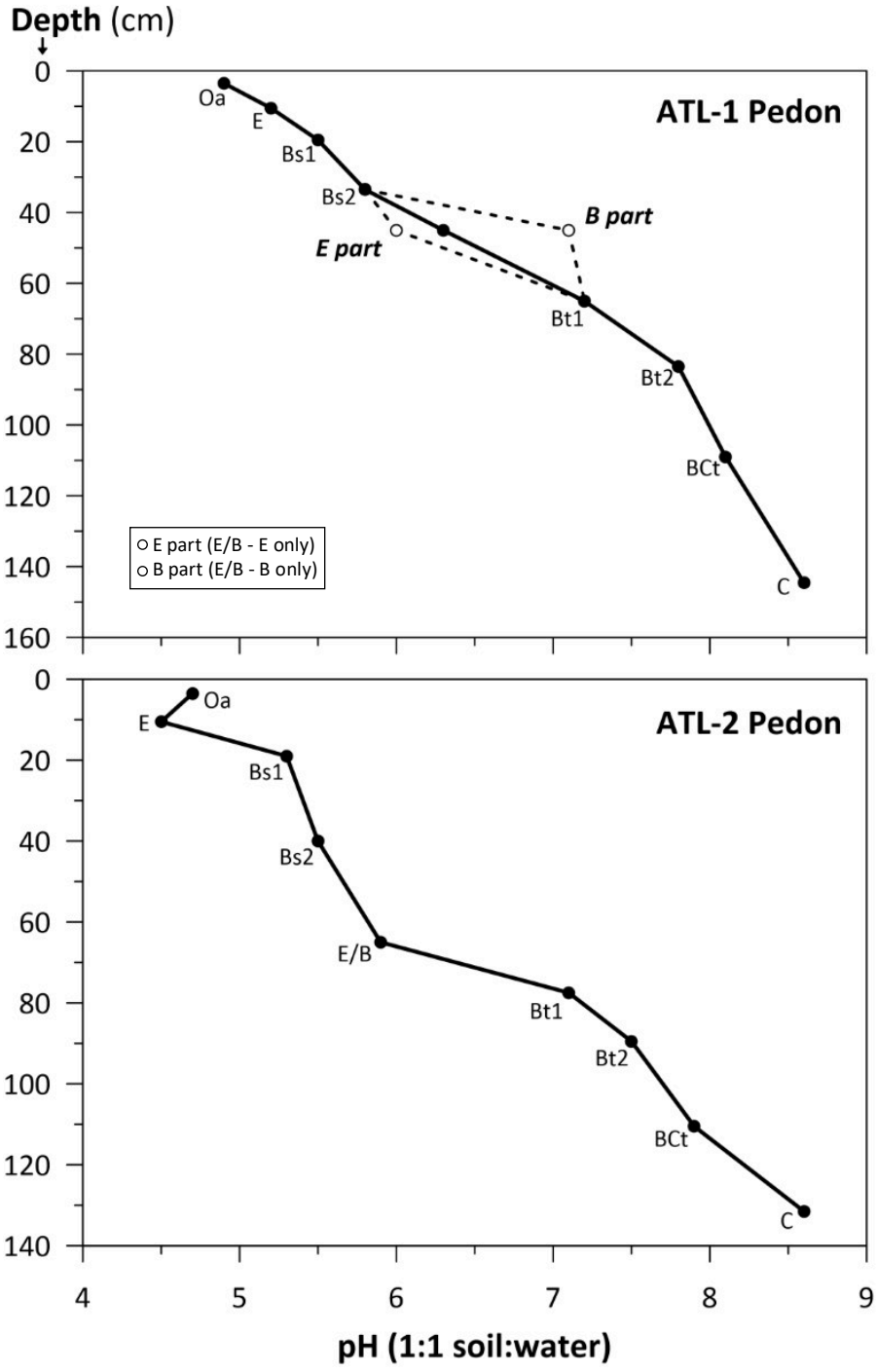

Figure 4.10. Depth trends of soil pH in the ATL-1 and ATL-2 pedons.

soils is likely initiated at a pH of < 6.0 (moderately acid). Cline (1949) also suggested a pH value of < 6.0 for the onset of podzolization in bisequal soils forming in calcareous drift in New York. The B portion of the E/B horizon in the ATL-1 pedon has a similar pH value to that of the underlying Bt1 horizon (7.1 vs. 7.2). In both pedons, pH values below the Bt1 horizon transition and continue to increase into the C horizon (8.6), reflecting the highly calcareous nature of the glacial till parent material. Schaetzl (1996) also reported a value of 8.6 (strongly alkaline) for glacial till parent materials assumed to be of Port Huron age at other locations in the northeastern Lower Peninsula.

4.3.2 Soil Organic Carbon

Organic carbon (SOC) contents in the ATL-1 and ATL-2 pedons range from 1.8 g kg^{-1} (0.2%) to 13.3 g kg^{-1} (1.3%) (Figure 4.11; Table C.2). Generally, SOC contents are higher near the soil surface and decrease with depth in both pedons. In the upper sequum (E-Bs1-Bs2) horizons, SOC contents range between 5.8 g kg^{-1} (0.6%) and 13.3 g kg^{-1} (1.3%). The Bs horizons have higher SOC contents than the overlying E horizon in both pedons, with values between 6.7 g kg^{-1} (0.7%) and 13.3 g kg^{-1} (1.3%). This trend, which is particularly evident in the ATL-2 pedon, provides an additional supporting line of evidence for the occurrence of podzolization in the upper portion of the profile. Padley et al. (1985) and Schaetzl (1996) reported SOC contents ranging from 3.2 g kg^{-1} (0.3%) to 11.4 g kg^{-1} (1.1%) for Bs horizons in other bisequal soils forming in similar parent materials in northeastern Lower Michigan.

The bulk glossic (E/B) horizon has a SOC content of 5.5 g kg^{-1} (0.6%) and 3.0 g kg^{-1} (0.3%) in the ATL-1 and ATL-2 pedons, respectively. These values are generally within the range of those found in other glossic horizons in the Great Lakes region forming in calcareous drift, which range

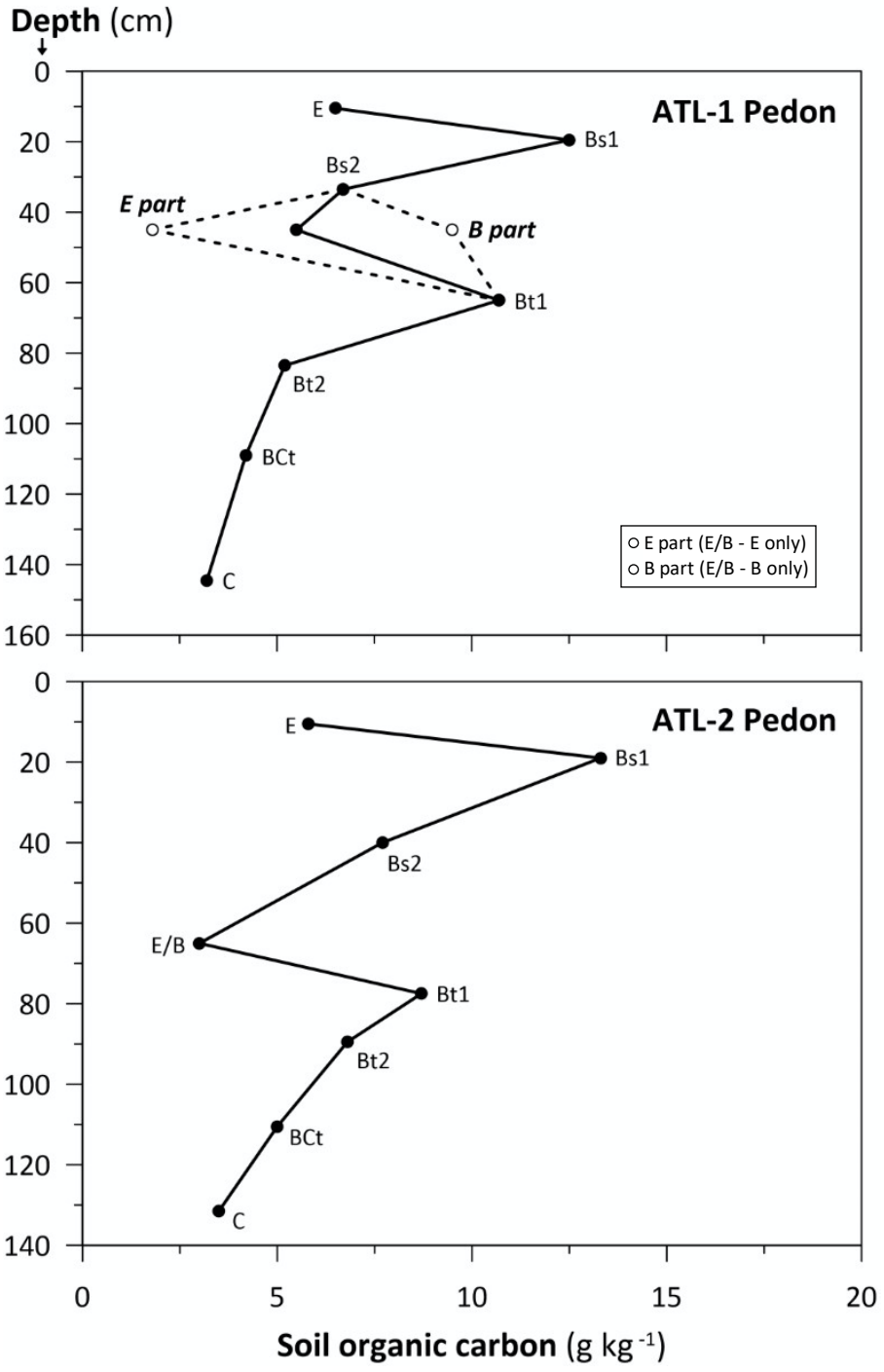

Figure 4.11. Depth trends of soil organic carbon (g kg^{-1}) in the ATL-1 and ATL-2 pedons.

from 1.0 g kg^{-1} (0.1%) to 6.4 g kg^{-1} (0.6%) (Harpstead and Rust, 1964; Hole, 1975; Schaetzl, 1996; Weisenborn, 2001). In the ATL-1 pedon, the E portion of the E/B horizon has a SOC content of 1.8 g kg^{-1} (0.2%), which is the lowest observed value in the pedon, pointing to the intensity of translocation here. Conversely, the B part of the E/B horizon has a SOC content of 9.5 g kg^{-1} (1.0%). This trend suggests that the majority of the SOC in the lower sequum is likely associated with organic matter that has formed complexes with clay. Sorption of decomposing organic residues to charged clay mineral surfaces is a common phenomenon in soils and has been observed in both Alfisols and Spodosols (Mortland, 1970; Schulten, 1998; Manjaiah et al., 2010). Thus, I conclude that the clay-organic complexes formed higher in the soil profile, which tends to be the primary location for organic matter additions (Simonson, 1978), and have since been translocated to the lower sequum. This observation is supported by the vertical distribution of SOC in the underlying Bt horizons, which generally mimics that of clay in both pedons. It should also be noted that organic coatings associated with active roots systems were occasionally observed on the surfaces of peds in the Bt1 horizon, indicating that some of these complexes have also formed in-situ.

4.3.3 Soil Geochemistry

Depth trends of immobile (resistant) elements, namely the group IV transition metals zirconium (Zr^{4+}) and titanium (Ti^{4+}), were also utilized to assess parent material uniformity (Figure 4.12; Table C.3). Generally, uniform values (and ratios) of these elements – taken from immobile soil constituents - with depth is taken to reflect parent material uniformity, i.e., lack of a lithologic discontinuity (Buggle et al., 2011; Stockmann et al., 2016; Ahr et al., 2017). It is important to reiterate that geochemical analysis in this study was conducted on the whole-soil material (i.e.,

including mobile soil constituents (clay and fine silt) and coatings), as discussed previously (Chapter 3).

Despite the influence of mobile soil constituents and coatings, Zr^{4+} depth distributions are generally linear in both pedons, especially through the "stone zone", strongly suggesting that the soils have formed in a uniform parent material (Figure 4.12). Zr^{4+} values are slightly elevated in the upper profile, however, particularly in the E horizon (658-724 ppm), and decrease with depth to the C horizon (388-404 ppm). Because Zr^{4+} is considered to be geochemically stable, its content tends to increase proportionally during weathering (Schaetzl and Thompson, 2015; Stockman, 2016); therefore, the slightly higher Zr^{4+} values in the upper profile is likely due to acidification and associated eluviation of mobile (weatherable) elements, such as Ca^{2+}. In other words, lower Zr^{4+} values in the lower profile is probably due to dilution by carbonates. The ratio of Ca^{2+} to Zr^{4+}, which generally increases with depth in both pedons, particularly below the Bt1 horizon, supports this assumption (Figure 4.12). Unlike Zr^{4+}, Ti^{4+} values vary more sporadically with depth in both pedons (Figure 4.12). A number of previous studies have shown that Ti-bearing minerals are not completely inert in soil, but in fact are susceptible to both physical and chemical weathering processes (Sudom and Arnaud, 1971; Berrow et al., 1978; Dąbkowska-Naskręt and Jaworska, 2001; Taboada et al., 2006; Anda et al., 2009; Ahr et al., 2012). Therefore, the variability in Ti^{4+} with depth may reflect weathering and subsequent translocation. Dilution by carbonates is also likely the cause of noticeably lower Ti^{4+} values in the BC and C horizons. Examination of the sand fraction (free of coatings) may result it lesser variability of Ti^{4+} with depth; however, additional analysis would be required to support this hypothesis. Thus, considering the method that was employed, Ti^{4+} does not appear to be a reliable index element for distinguishing lithologic discontinuities from pedogenic processes in the ATL pedons.

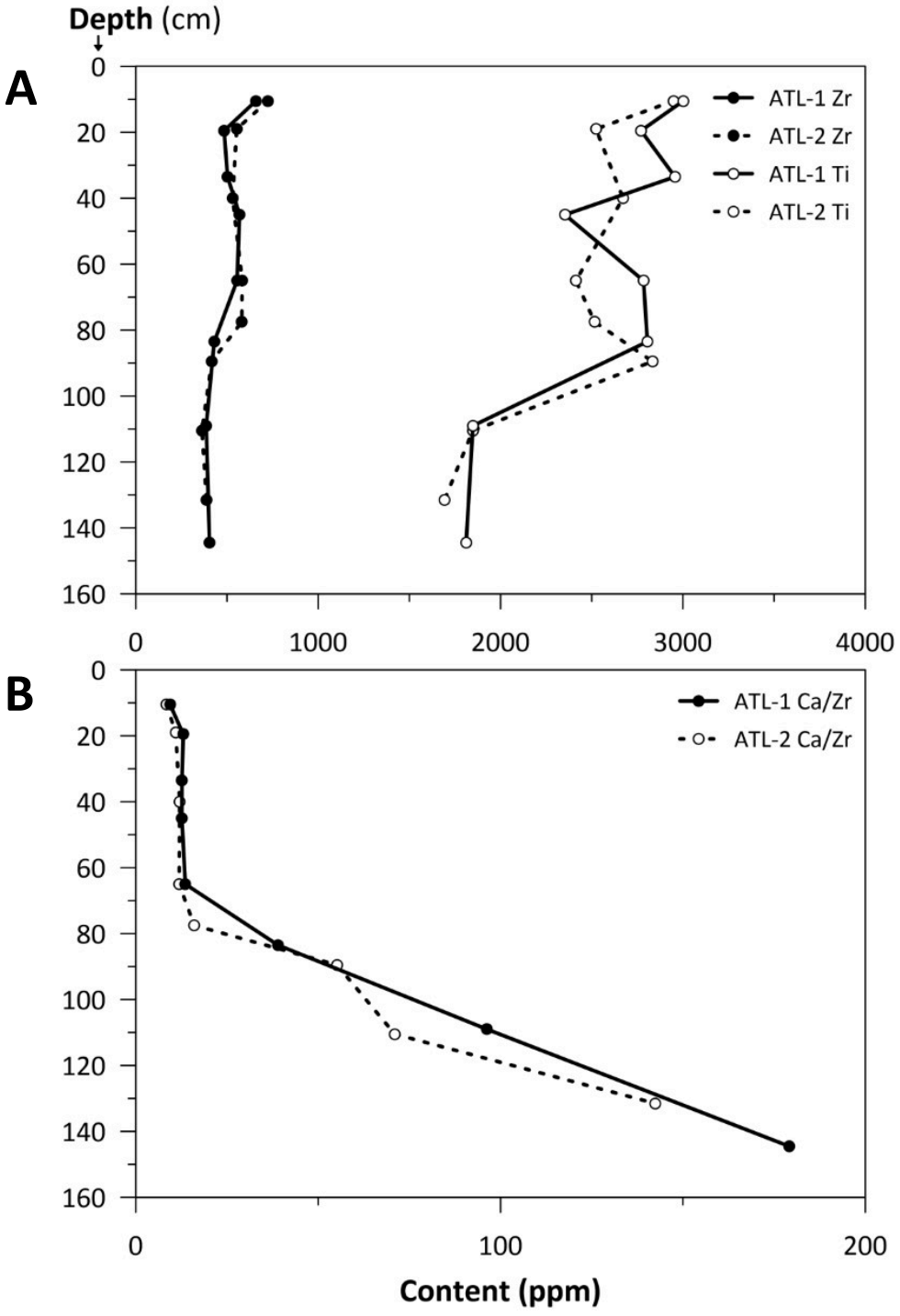

Figure 4.12. Depth trends of (A) zirconium (Zr^{4+}) and titanium (Ti^{4+}) contents (ppm) and (B) Ca/Zr in the ATL-1 and ATL-2 pedons.

Depth trends of mobile (weatherable) trace elements, particularly group II alkaline earth metals strontium (Sr^{2+}) and barium (Ba^{2+}), provide potential insight into the behavior of the clay mineral fraction. In both pedons, the vertical distribution of Sr^{2+} remains nearly uniform with depth (249-281 ppm), whereas Ba^{2+} mimics that of the clay fraction, reaching a maximum in the Bt1 horizon (854-886 ppm) and decreasing predictably to the C horizon (550-557 ppm) (Figure 4.13). It is generally assumed that Ba^{2+} is more selectively sorbed to negatively charged clay mineral exchange sites than Sr^{2+} due to its larger ionic radius[5] (Nesbitt et al., 1980; Smith, 1999; Buggle et al., 2011; Sposito, 2016). Additionally, Ba^{2+} has been found to exchange more easily with Ca^{2+} (Eylem et al. 1990), which is the dominant cation satisfying the exchange complex in the lower sequum (discussed in section 4.3.4). Therefore, considering the overall greater abundance (and availability) of Ba^{2+}in these soils, it is likely that Sr^{2+} has not been required to satisfy available exchange sites on clay minerals. This trend, however, could also reflect a dominance of illite minerals in the clay fraction, which have been shown to favor the adsorption of Ba^{2+}over Sr^{2+} on their exchange sites more strongly than other common clay mineral types, e.g., kaolinite and smectite (Eylem et al., 1990; Hatipoglu et al., 1990). Additional mineralogic data on the clay fraction, however, would be necessary to confirm this hypothesis. Nevertheless, it is worth mentioning that the Antrim Shale, the surficial bedrock that crops out immediately north (i.e., up-ice) of the study site, contains significant concentrations of illite (20-35%), with lesser concentrations of kaolinite (5-10%) and chlorite (0-5%) (Ruotsala, 1980). It seems plausible that some of this bedrock (or associated glaciogenic sediments) would have been incorporated into the parent materials deposited at the study site during the Port Huron glacial readvance.

[5] The sorption selectivity of metal ions to negatively charged clay minerals surfaces tends to increase with the ionic radius of the ion (Sposito, 2016). Thus, group I and II cations are assumed to follow the selectivity sequence: $Ba^{2+} > Sr^{2+} > Ca^{2+} > Mg^{2+} > Cs^{+} > Rb^{+} > K^{+} > Na^{+} > Li^{+}$.

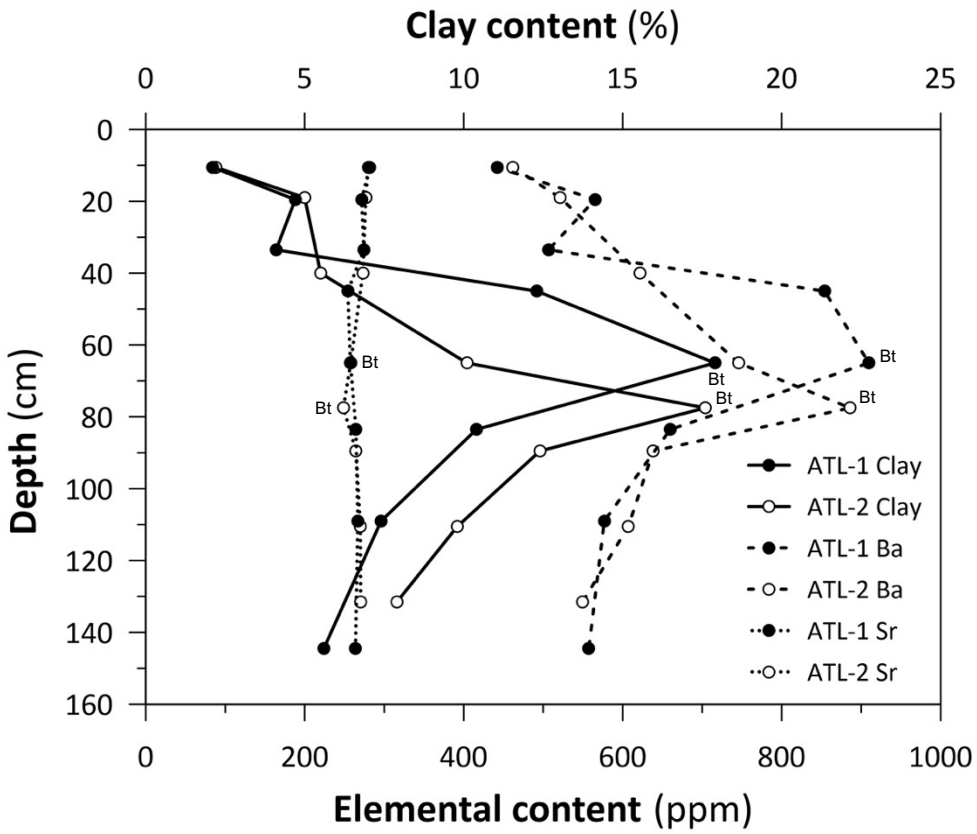

Figure 4.13. Depth trends of barium (Ba^{2+}) and strontium (Sr^{2+}) contents (ppm) in the ATL-1 and ATL-2 pedons.

Depth trends for the mobile group VIII transition metal iron (Fe) also provide potential insight into the behavior of the clay mineral fraction. Similar to what was observed for the alkaline earth metals, the vertical distribution of Fe largely mimics that of the clay fraction in both pedons, reaching a maximum in the Bt1 horizon (31625-35417 ppm) and decreasing predictably to the C horizon (13998-14302 ppm) (Figure 4.14). This trend suggests that an appreciable portion of the Fe in the lower sequum is likely sorbed (probably as Fe^{3+} in "free" iron oxides) to negatively charged clay mineral surfaces, hence the reddish (5YR hue) colors observed in the Bt horizons (Table 4.1). Surface complexation of Fe oxides to charged clay mineral edge sites is a common phenomenon in soils where adequate quantities of both substances are present in the parent

material (Duchafour and Souchier, 1978; Schaetzl and Thompson, 2015; Sparks et al., 2020). Considering the accompanying high content of SOC (discussed in section 4.3.2), it is probable that organic matter is also associated with some of the clay-iron complexes in the Bt horizons.

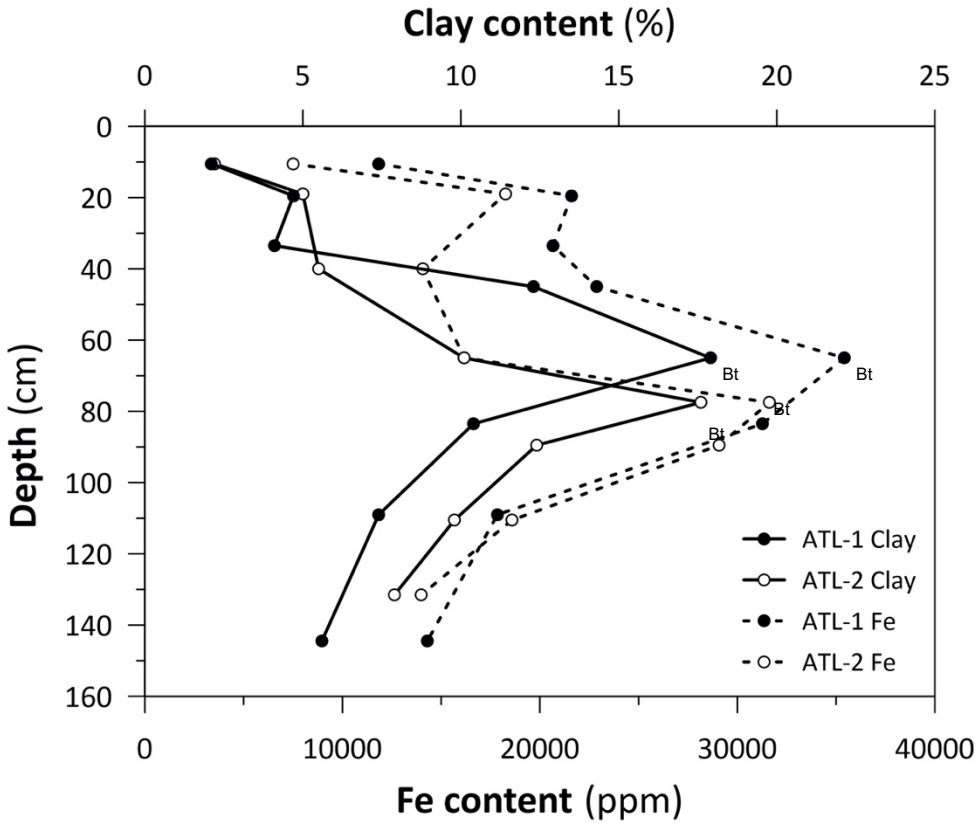

Figure 4.14. Depth trends of iron (Fe) content (ppm), relative to clay content (%), in the ATL-1 and ATL-2 pedons.

Although the particular mechanism by which Fe oxides have accumulated in the Bt horizons is unclear, based on the data collected, some potential hypotheses can be envisioned. It seems most probable that clay-iron complexes were formed during the early stages of pedogenesis and were later mobilized to the illuvial zone following the onset of lessivage. The "free" Fe oxides complexed with clay during this process were likely inherited directly from the parent material

and/or released from complexes with organic matter during turnover. It is also possible that following the onset of lessivage, oxygenated "free" Fe released during the weathering of Fe-bearing minerals in the upper, more acidic portion of the solum were translocated and precipitated in the Bt horizon, thereby forming complexes with previously deposited clays. Indeed, it is also possible that all of the aforementioned mechanisms have been active to some degree throughout pedogenesis. Although additional mineralogical data on the clay fraction would be required to identify the predominant Fe oxide species present, it is worth mentioning that "active" (or amorphous) Fe oxides (i.e., ferrihydrites), which tend to be most reactive (Sparks et al., 2020), have been shown to preferentially adsorb to fine clay (< 2 μm) mineral surfaces (Duchafour and Souchier, 1978).

4.3.4 Soil Ion Exchange and Extractable Cations

Cation exchange capacity (CEC) values in the ATL-1 pedon range from 2.0 me/100g to 9.4 me/100g (Table C.4). Generally, CEC values mimic the vertical distribution of clay and organic matter with depth, as is commonly observed in most soils (Schaetzl and Thompson, 2015). In the acidic, upper sequum (E-Bs1-Bs2), CEC values range between 2.0 me/100g and 5.3 me/100g, and base saturation values are ≤ 45%. The Bs1 horizon has a noticeably higher CEC than the overlying E horizon, with a value of 5.3 me/100g. Considering the Bs1 horizon has a low clay content (Table 4.2), its CEC value is assumed to be associated primarily with organic matter, which reaches a maximum in this horizon (Table C.2). The low base saturation value (30%) of the horizon also suggests that the exchange complex is satisfied mostly by hydrogen (H^+), iron (Fe^{2+}), and aluminum (Al^{3+}) cations, providing an additional supporting line of evidence for the occurrence of podzolization in the upper sequum. Considering the pH of the E-Bs1 horizons (5.2-5.5) (Table

C.1), however, the content of Al^{3+} satisfying the exchange complex in Bs1 horizon is assumed to be relatively low. I draw this conclusion because Al^{3+} tends to solubilize, and therefore, become available for adsorption, most effectively at pH < 5.0 (Wright, 1989; Singh et al., 2017; Rahman et al., 2018). It is worth mentioning that geochemical analyses on the ATL-1 pedon revealed an appreciable increase in Fe content in the Bs1 horizon relative to the overlying E horizon (Table C.3). Certainly, some of this increase is pedogenic; however, additional chemical extractions would be necessary to accurately speculate as to the portion that is associated with organic matter complexion. Padley et al. (1985) reported CEC values ranging from 2.5 me/100g to 7.4 me/100g for spodic-like B horizons in other bisequal soils forming in similar parent materials in northern Lower Michigan.

The glossic (E/B) horizon has a CEC value of 4.5 me/100g and a base saturation of 87%, suggesting that despite degradation, the horizon still retains an appreciable concentration of basic cations, particularly Ca^{2+}, on clay exchanges sites. This CEC value is similar to one reported by Hole (1975) for a glossic horizon forming in coarse-textured calcareous till in Wisconsin (5.0 me/100g). It is important to note, however, that few CEC values for glossic horizons forming in calcareous sediments in the upper Great Lakes region have been reported in the literature, particularly for coarse-textured soils. Significantly higher CEC values were reported by Harpstead and Rust (1964) for glossic horizons forming in finer-textured calcareous sediments in Minnesota (13.5 me/100g to 30.4 me/100g). These soils contained not only a greater overall concentration of clay, but the fraction was also dominated by montmorillonite, which has a high CEC relative to most other clay mineral types (Shainberg and Levy, 2005). CEC reaches a maximum in the underlying Bt1 horizon (9.4 me/100g), reflective of the zone of maximum clay accumulation (Table 4.2), and decreases with depth below that point. Base saturation in the Bt1 horizon (and

below) is 100% due to the presence of "free" calcium (Ca^{2+}). The presence of "free" Ca^{2+} in the lower sequum illuvial horizons indicates an adequate capacity to facilitate coagulation and/or neoformation and deposition of illuvial clays.

4.4 Taxonomic Classification

In this section, profile descriptions based on field observations, as well as physical and chemical laboratory data, are used to describe and classify the ATL-1 and ATL-2 pedons according to the 12th edition of *Soil Taxonomy* (Soil Survey Staff, 2014). Discussion is focused on the identification of diagnostic soil characteristics and horizons, classification to the family level, and comparisons of these two pedons to OSD data for the Millersburg series, under which the pedons are currently mapped.

4.4.1 Diagnostic Soil Characteristics and Horizons

4.4.1.1 Albic Materials

Albic materials are soil materials that are comprised of primary skeletal particles (i.e., sand and silt) that are largely devoid of cutans. The presence of albic soil materials in a soil is generally taken to reflect an appreciable eluvial loss of weathering products, namely clay minerals and/or "free" iron oxides, from a horizon. In *Soil Taxonomy*, albic materials have specifically defined morphological characteristics, particularly light colors (Soil Survey Staff, 2014). Briefly summarized, albic soil materials must meet one of the following criteria:

1) have a chroma of ≤ 2; and either

   (a) a value of 3 (moist) and ≥ 6 (dry); or

   (b) a value of ≥ 4 (moist) and ≥ 5 (dry); OR

2) have a chroma ≤ 3; and either

(a) a value of ≥ 6 (moist); or

(b) a value of ≥ 7 (dry); OR

3) have a chroma that is controlled by the color of uncoated grains of silt or sand, hue of 5YR or redder, and a value listed in (a) or (b) of item 1.

By virtue of their light color, the E horizon (7.5YR 5/2, moist; 7.5YR 7/2, dry) and E portion of the E/B horizon (7.5YR 6/3, moist), in both pedons, classify as albic materials (Table 4.1; Table A.2). Although it is not a required criterion in *Soil Taxonomy*, either no structure or a weak structural grade is sometimes taken as an additional indicator of the presence of albic materials (Bockheim, 2016). Peds in the E and E/B horizon of the two pedons, where they are composed of mostly albic materials, tend to have a weak structural grade (Table 4.1).

4.4.1.2 Spodic Materials

By definition, spodic materials are comprised of amorphous complexes of organic matter and aluminum, with or without the presence of iron; they occur as cutans on skeletal particles (Soil Series Staff, 2014). The presence of spodic materials in a soil is generally taken to reflect an appreciable illuvial accumulation of organometallic complexes from an overlying eluvial horizon, and thereby indicate ongoing podzolization. Soils must have spodic materials in a B horizon to classify within the Spodosol order. In *Soil Taxonomy*, spodic materials have specifically delimited chemical and morphological characteristics, including low pH, high organic carbon contents, and dark and/or red colors (Soil Survey Staff, 2014). Briefly summarized, soil materials must meet the following criteria to be considered spodic materials:

1) have a pH value in water of 5.9 or less, AND

2) have an organic carbon content of 0.6% or more, AND

3) (a) have an overlying albic horizon and meet one of the following color criteria: 5YR or redder, 7.5YR 5/4 or darker, 10YR 2/2 or darker, or 10YR 3/1, OR

(b) with or without an overlying albic horizon, meet one of the color criteria in (a) or 7.5YR hue, value ≤ 5, and chroma of 5 or 6, AND have ortstein in ≥ 10% of the pedon, OR have ≥ 10% cracked coatings on sand grains, OR have ≥ 0.50% Al_{ox} + 0.5Fe_{ox} and ≥ two times the Al_{ox} + 0.5Fe_{ox} of an overlying eluvial horizon, OR an ODOE of ≥ 0.25 and ≥ two times the ODOE[6] of an overlying eluvial horizon.

Although the Bs horizons in both pedons have pH values < 5.9 and organic carbon contents > 0.6%, their relatively light color (7.5YR 4/6-5/6) requires the presence of additional morphologic (i.e., ortstein or cracked coatings) or chemical (i.e., Al_{ox} + 0.5Fe_{ox} or ODOE) indicators in order to meet the criteria for spodic materials. Neither ortstein nor cracked coatings on sand grains were observed in any of the Bs horizons. Therefore, in order for the horizons to meet the criteria for spodic materials, they must be identified by supplemental chemical analysis.

Because this type of supplemental chemical analyses could not be conducted in our lab, two alternative approaches, based on morphological criteria, were utilized to serve as proxies for spodic development, and therefore, the presence of spodic materials. My goal/approach was to classify the two ATL pedons based on a comparison of soils with similar morphologies, all of which had already been classified by the NRCS.

[6] The optical density of the ammonium oxalate extract (ODOE) is a measure of the absorbance of extracted fulvic acids (i.e., water soluble organic matter) associated with mobile organometallic complexes (Daly, 1982). An increase in ODOE relative to an overlying eluvial horizon is used as

an indicator of the accumulation of translocated organic carbon materials in an illuvial horizon (Soil Survey Staff, 2014).

First, the strength of podzolization in each of the two ATL profiles was estimated using the POD Index of Schaetzl and Mokma (1988). The POD Index uses soil color, specifically hue and value, of the E and B horizons to assess the degree to which podzolization is expressed in a soil's morphology. Generally, larger POD Index values occur when soils have increasing contrast in B horizon color (i.e., redder hues and/or darker values) and thickness, relative to the E horizon, as well as more B subhorizons. This index has been applied successfully to soils in Michigan which either are, or are developing toward, Spodosols (Arbogast and Jameson, 1988; Barrett and Schaetzl, 1993; Schaetzl et al., 2015; Rothstein et al., 2018). The POD Index value for both ATL pedons is 2 (Table D.4), which is typical for most non-Spodosols, including those with weakly expressed podzolic development (Schaetzl and Mokma, 1988). Most Spodosols have a POD Index of 2 or higher (Schaetzl and Mokma, 1988). Thus, based on this analysis, the ATL pedons are likely to classify as non-Spodosols.

Next, the OSDs for 114 Haplorthod soil series in Michigan were examined, I compared the colors of their uppermost spodic (B) horizon to that of the Bs1 horizon in the ATL pedons (7.5YR 4/6). The rationale behind such an assessment is that podzolic expression is typically greatest in the B horizon immediately subjacent to an E horizon; therefore, if the Bs1 horizon in the ATL pedons does meet the criteria for spodic materials, assumedly at least a few other Spodosols in the state should have a similar color in their uppermost spodic (B) horizon. Virtually all (111 of 114) of the Haplorthods in Michigan, however, contain an uppermost spodic (B) horizon color that does not require the presence of additional morphological or chemical indicators in order to be identified as containing spodic materials (i.e., they are darker and/or redder than 7.5YR 4/6) (Figure 4.15) (Soil Survey Staff, Accessed April 2020). The only Haplorthod with a 7.5YR 4/6 color its

uppermost spodic (B) horizon is the Epworth series, an Entic Haplorthod, Epworth soils tend to occur in acidic, sand textured sediments located immediately adjacent to Lake Michigan. Thus, it is likely that Epworth soils have stronger spodic development than do the soils of study, as the podzolization process tend to be enhanced in soils with coarser-textured parent materials that experience greater infiltration flux during the spring snowmelt period, as discussed previously (Chapter 1). This assumption is further supported by the comparatively less red E horizon in Epworth soils (10YR 5/2 vs. 7.5YR 5/2), suggestive of stronger leaching and eluviation. It is important to note that the two Haplorthods classified with a 10YR color in their uppermost spodic (B) horizon (Isabella and Twining) (Figure 4.15) were established prior to the implementation of chemical criteria in *Soil Taxonomy*. According to current taxonomic criteria, these series would fail to classify as Haplorthods. Interestingly, recent (08/2012) revisions to the Isabella OSD state that the typical pedon "fails the chemical criteria for a spodic horizon" and is being classified simply "based on morphology", which raises concerns as to the accuracy of the series classification.

In summary, the low POD Index values (2), coupled with the fact that nearly all Spodosols in Michigan contain colors in their spodic horizon that do not require additional morphological or chemical indicators in order to be identified as spodic materials, leads me to conclude that podzolization in the ATL pedons, although active, has not been ongoing long enough, or lacks sufficient strength, for illuvial materials observed in the upper sequum to be meet the criteria for spodic materials. Therefore, I conclude that the soils do not meet the criteria necessary to classify as Spodosols.

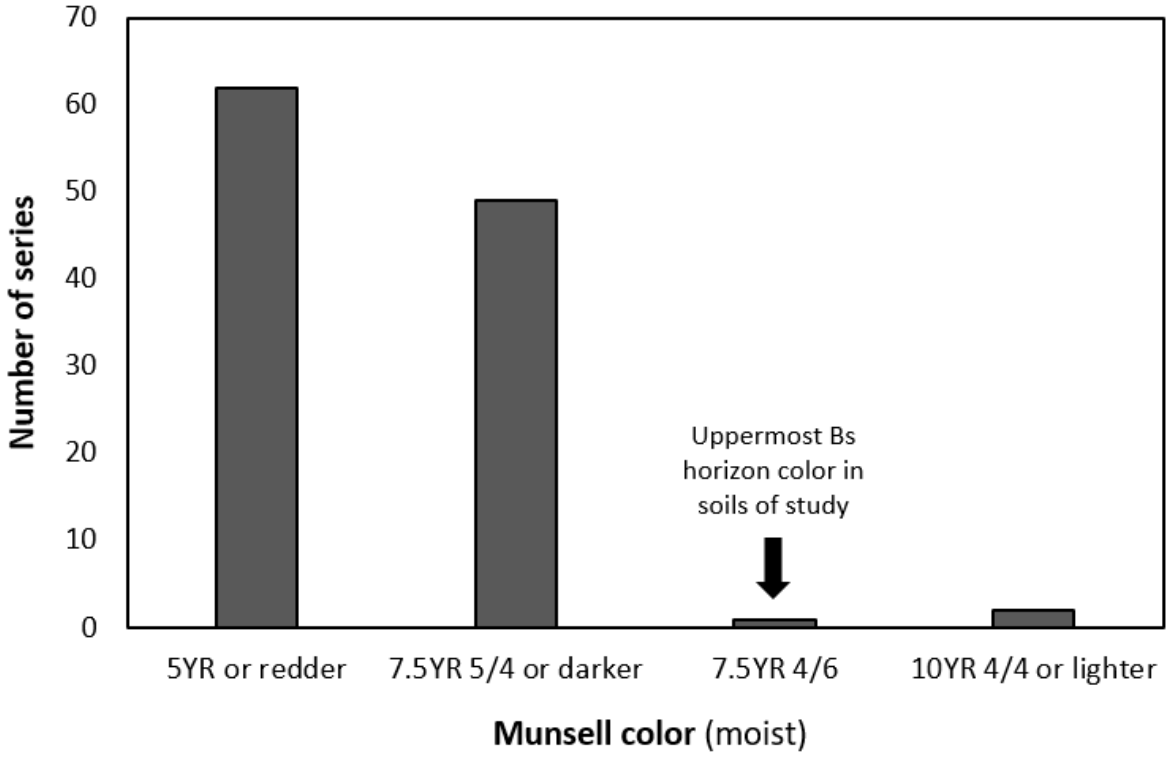

Figure 4.15. Uppermost (darkest) B horizon color in the spodic diagnostic subsurface horizon of the 114 Haplorthods who have their official series description location in Michigan (Soil Survey Staff, Accessed April 2020).

Following the initial completion of this section, an opportunity arose for supplemental chemical analysis to be completed by the USDA-NRCS Kellogg Soil Survey Laboratory (KSSL). The amounts of organically bound aluminum (Al_{ox}) and iron (Fe_{ox}) and optical density of the oxalate extract (ODOE) were determined for the upper sequum (E-Bs1-Bs2) horizons in the ATL-1 pedon according to ammonium oxalate extraction methods previously reported by the Soil Survey Staff (2014). Generally, the amounts of organically bound Al and Fe are negligible in the E horizon and increase in the underlying Bs horizons (Table 4.4). Both Al_{ox} and Fe_{ox} values are noticeably higher in the Bs1 horizon than in the Bs2 horizon, although both horizons contain more Al_{ox} than Fe_{ox}. Values for ODOE show a generally similar trend with depth (Table 4.4). Despite

the overall increase in Al_{ox}, Fe_{ox}, and ODOE in the Bs horizons, however, the observed values do not meet the minimum threshold required for taxonomic classification as spodic materials (3-b, listed above). Thus, the oxalate extraction data provide quantitative support to previously discussed conclusions, thereby confirming that podzolization in the ATL pedons, although active and ongoing, lacks sufficient strength for the soils to be considered Spodosols.

Table 4.4 Ammonium oxalate extraction data for the upper sequum horizons of the ATL-1 pedon.

	% of < 2 mm			
HOR	**Al_{ox}**	**Fe_{ox}**	**Al_{ox} + 0.5Fe_{ox}**	**ODOE**
E	-	tr	tr	0.01
Bs1	0.28	0.27	0.41	0.17
Bs2	0.19	0.12	0.25	0.06

Notes to Table 4.4:
tr = trace

4.4.1.3 Ochric Epipedon

Both pedons contain an ochric epipedon that extends from the soil surface to a depth of 14 cm and includes the Oi, Oa, and E horizons (Table 4.6; Table A.2). In *Soil Taxonomy*, the ochric epipedon is used to describe an epipedon (i.e., diagnostic surface horizon) that fails to meet the criteria of other epipedon types that have not been purposefully human-altered, primarily because it is too thin, has too light of color, or contains too little organic carbon (Soil Survey Staff, 2014). The ochric epipedon has no defined diagnostic features or qualities and may extend through an eluvial (E) horizon or to the upper surface of a diagnostic subsurface illuvial horizon (if present). In the soils of study, the surface organic (Oi and Oa) horizons are too thin (7 cm) to be recognized

as a histic or folistic epipedon (Table 4.1). Further, the light color (7.5YR 5/2, moist) and low SOC value of the underlying eluvial (E) horizon indicates a lack of organic carbon accumulation in the mineral soil surface, and thus, does not meet the requirements for a mollic or umbric epipedon (Table 4.1; Table C.2).

4.4.1.4 Albic Horizon

Both pedons contain an albic horizon from a depth of 7 to 14 cm that is the E horizon (Table 4.1; Table A.2). In *Soil Taxonomy*, the albic horizon is used to describe a subsurface horizon that is greater than 1 cm in thickness and is composed of > 85% percent (by volume) albic materials (defined above) (Soil Survey Staff, 2014). The presence of an albic horizon in a soil is generally taken to reflect a particularly appreciable eluvial loss of clay minerals and/or "free" iron oxides. In essence, the albic horizon is a well-developed eluvial (E) horizon with a particularly light color. In both the ATL-1 and ATL-2 pedons, the E horizon is 7 cm thick and contains no visibly noticeable cutans on skeletal particles in any part of the horizon.

4.4.1.5 Glossic Horizon

Both pedons contain a glossic horizon that includes the E/B horizon (Table A.2); the glossic horizon occurs from a depth of approximately 42 to 58 cm and approximately 56 to 74 in the ATL-1 and ATL-2 horizons, respectively (Table 4.1). In *Soil Taxonomy*, the glossic horizon is used to describe a subsurface horizon that is ≥ 5 cm in thickness and consists of an eluvial part (i.e., albic materials), which constitute 15 to 85% (by volume) of the glossic horizon, and an illuvial part (i.e., remnant pieces) of an argillic or other clay-enriched horizon (Soil Survey Staff, 2014). As discussed previously (Chapter 1), the presence of a glossic horizon in a soil is generally taken to

reflect the degradation of a clay-enriched horizon whereby soil materials, namely clay minerals and associated "free" iron oxides, are removed and redistributed lower in the soil profile. In the ATL-1 pedon, the glossic horizon is 16 cm thick and the eluvial portion, which meets the criteria for albic materials (as discussed previously), comprises approximately 70% (by volume) of the horizon. In the ATL-2 pedon, the glossic horizon is slightly thicker (18 cm) and composed of a greater volume of albic materials (80%).

4.1.1.6 Argillic Horizon

Both pedons contain an argillic horizon that includes the E/B, Bt1, Bt2, and BCt horizons (Table A.2); the argillic horizon occurs from a depth of approximately 42 to 123 cm and approximately 56 to 123 in the ATL-1 and ATL-2 pedons, respectively (Table 4.1). The presence of an argillic horizon in a soil is generally taken to reflect a subsurface enrichment of clay, primarily via physical translocation from an overlying eluvial horizon (i.e., lessivage). In *Soil Taxonomy*, the argillic horizon has specifically defined morphological and physical characteristics, including appreciable thickness, presence of illuvial clay features (e.g., clay bridging primary grains or clay coatings lining pores and/or ped faces) and a significant increase in clay relative to an associated overlying eluvial horizon (Soil Survey Staff, 2014). Briefly summarized, a subsurface soil horizon must meet the following criteria to be considered an argillic horizon:

1) have one of the following thicknesses, based on particle-size class:
   (a) ≥ 7.5 cm thick if of a particle-size class finer than sand; or
   (b) ≥ 15 cm thick if of sand particle-size class; AND
2) have evidence of clay illuviation in the form of oriented clay bridging sand grains, OR clay films lining pores, OR clay films on both vertical and horizontal surfaces of peds,

OR thin sections with oriented clay bodies that comprise > 1% of the section; AND

3) have a greater amount of total clay than an overlying eluvial horizon, as follows:

(a) ≥ 3% (absolute) for eluvial horizons with < 15% total clay, or

(b) 1.2 times for eluvial horizons with 15 to 40% total clay, or

(c) ≥ 8% (absolute) for eluvial horizons with ≥ 40% total clay.

According to *Soil Taxonomy*, in soils where the argillic horizon is degrading, such as those that contain a glossic horizon, the top of the argillic horizon is identified as the point where the increase in clay content is met after mixing (Soil Survey Staff, 2014). By this definition, a glossic horizon that is composed of mostly degraded (albic) material (i.e., an E/B horizon) may be considered part of the argillic horizon if its clay content, after mixing, exceeds the clay content of the overlying horizon by the required amount. In the soils of study, the Bs2 horizon, which immediately overlies the glossic (E/B) horizon, contains 4.1% and 5.5% total clay in the ATL-1 and ATL-2 pedons, respectively (Table 4.2). In both pedons, the E/B horizon contains > 3% clay (after mixing) relative to the Bs2 horizon. It is important to note, however, that the E part of the E/B horizon alone, at least in the ATL-1 pedon, exceeds the required minimum clay increase requirement. Therefore, the top of the argillic horizon is marked by the upper boundary of the E/B horizon. This classification highlights the transitional nature of the glossic (E/B) horizon in these soils; although the E part of the horizon shows evidence of significant eluviation, it still retains an appreciable amount of clay relative to the overlying horizons that are experiencing a different set of pedogenic processes (i.e., podzolization). The remaining lower sequum illuvial (Bt1-Bt2-BCt) horizons also meet the increase in clay requirement relative to the Bs2 horizon, indicating that the base of the argillic horizon extends to the maximum depth of leaching and clay illuviation (i.e., the top of the C horizon).

4.4.2 Taxonomic Classification

Using the field- and laboratory-characterization data along with diagnostic characteristics and horizons, the ATL-1 and ATL-2 pedons were classified to the family level according to *Soil Taxonomy* (Soil Survey Staff, 2014) (Table 4.5). Individual pedon data was considered for classification to the subgroup level, while only data from the ATL-1 pedon (because it is more complete) was considered for further classification to the family level. Because the pedons have generally similar characteristics, however, the family level classification is assumed to also apply to the ATL-2 pedon. Family descriptors identified in the ATL-1 pedon include the particle-size, cation-exchange activity, and soil temperature classes; other descriptors were not used because of insufficient data. The descriptors are identified for the soil control section of the pedon, which by definition, consists of the upper 50 cm of the argillic horizon (Soil Survey Staff, 2014). Because the control section is composed of multiple horizons (i.e., the E/B, Bt1, and part of the Bt2), a weighted average is used (Table D.1).

At the order level, the pedons classify as Alfisols, reflective of the presence of the argillic horizon. Given their general regional location and lack of pedogenic features typically associated with true aquic conditions (e.g., gleying) the pedons are considered to have a udic[7] soil moisture regime, and therefore, classify as Udalfs. At the great group level, the pedons classify as Glossudalfs, reflective of the presence of the glossic horizon. Because the glossic horizon does not meet any special criteria, with the exception of being less than 50 cm in total thickness, the pedons classify as Haplic Glossudalfs at the subgroup level.

At the family level, the soil control section contains two contrasting particle-size components ("elements") that are > 12.5 cm in thickness (Table D.2). The upper (E/B-Bt) element, containing > 15% sand coarser than fine sand and < 18% total clay, classifies in the coarse-loamy particle-

Table 4.5. Taxonomic classification of the ATL-1 and ATL-2 pedons according to Soil Survey Staff (2014).

Order [a]	Suborder [b]	Great Group [c]	Subgroup [d]	Family [e]
Alfisols	Udalfs	Glossudalfs	Haplic Glossudalfs	Coarse-loamy, active, frigid

Notes to Table 4.5:
[a] order formative elements: “alf”: Alfisol
[b] suborder formative elements: "ud": udic moisture regime
[c] great group formative elements: "gloss": presence of a glossic horizon
[d] subgroup adjectives: "haplic": glossic horizon < 50 cm in thickness
[e] family adjectives: “coarse-loamy”: particle-size class; “active”: cation-exchange activity class; “frigid”: soil temperature class

size class. Conversely, the lower (Bt2 “stone zone”) element, containing > 35% (by volume) coarse fragments, classifies in the sandy-skeletal particle-size class. Because the coarse-loamy (upper) element of the control section contains > 50% sand coarser than fine sand, however, the soil is not considered to have strongly contrasting particle-size classes (i.e., coarse-loamy over sandy-skeletal). Therefore, because the upper (E/B-Bt) element of the control section is the dominant element (60% by volume), the pedons classify with coarse-loamy particle-size family. The soil control section also has CEC/clay ratio of 0.45 (Table D.3), and thus, the pedons classify as having an active cation-exchange activity class. Because the pedons have a mean annual temperature of < 8° C and a difference between mean summer and mean winter temperatures of > 6° C at a depth of 50 cm (as discussed in Chapter 2) they classify as having a frigid soil temperature.

[7] Generally, a udic soil moisture regime is one in which the soil is neither dry for as long as 90 cumulative days nor for as long as 60 consecutive days in the 90 days following the summer solstice at periods when the soil temperature at 50 cm below the surface is above >5 °C (Soil Survey Staff, 2014, pg. 30).

4.4.3 Comparison to Millersburg OSD

The typical pedon for the Millersburg series (ID# 91MI119002) is located in the Atlanta State Forest area of Montmorency County, Michigan, approximately 16 km north of the study site. As discussed previously (Chapter 2), Millersburg soils are classified as coarse-loamy, mixed, active, frigid Haplic Glossudalfs and contain an ochric epipedon and albic, glossic, and argillic diagnostic subsurface horizons. Although the ATL pedons share generally similar taxonomic characteristics to the series level, notable morphological and chemical differences were observed that warrant further discussion.

According to the Millersburg OSD, associated soils tend to lack an organic (O) horizon and contain an A horizon at the mineral soil surface. The ATL pedons, however, contain both Oi and Oa horizons with an immediately underlying E horizon (i.e., no A horizon). Interestingly, the only other available laboratory data on the Millersburg series (ID# S1999MI135001; hereafter "MB-2" pedon) is reported for a pedon (≈30 km north of study site) that contains both an O and A horizon but lacks an underlying E horizon. Furthermore, the upper sequum B horizon(s) in both the typical Millersburg and MB-2 pedons are designated with a "w" suffix, suggesting only weak pedogenic development. Although the B horizons in the ATL pedons do not meet spodic requirements and fall within the range of Bw horizon colors reported for Millersburg soils (7.5YR 4/6-5/6), I nevertheless interpret their presence, in context of the broader upper sequum morphology (Oi-Oa-E-Bs1-Bs2), to indicate active podzolization. Therefore, I assigned the B horizons with an "s" suffix (as discussed in section 4.1.1). Relative chemical difference between the Bs and overlying E horizons, particularly greater concentrations of organically bound Al and Fe (as discussed in section 4.4.1), support this designation.

The upper sequum morphological differences observed in these pedons suggests that the

degree of spodic expression in Millersburg-type soils likely varies according to site specific conditions. One possible explanation for the apparently stronger spodic development in the upper portion of the ATL pedons is the relative landscape position of the study site; unlike the typical Millersburg and MB-2 pedons, the ATL pedons are located on a north-facing slope. According to Hunckler and Schaetzl (1997), cooler and moister microclimatic conditions on north facing slope positions in northern Michigan facilitate development of thicker O horizons and greater infiltration rates, and therefore, podzolization processes tend to be accelerated in soils found at such locations. Additionally, the slope position on which the ATL pedons are located has concave (convergent) planform, whereas the typical Millersburg and MB-2 pedons are located on slope positions with convex (divergent) planform. Generally, soils on landscape positions with convergent planform tend to be more strongly developed due to the preferential accumulation of water (Pennock et al., 1987).

Greater development in the upper portion of the ATL pedons is further reflected in deeper depth to the glossic (E/B) horizon (42 cm and 56 cm) than in the typical Millersburg and MB-2pedons (25 and 36 cm) (Table 4.6). The E/B horizon in the ATL pedons, however, is notably thinner (16 and 18 cm) than in the typical Millersburg and MB-2 pedons (33 cm and 41 cm). This trend continues into the underlying Bt1 horizon, which is also thinner in the ATL pedons (14 cm and 9 cm) than in the typical Millersburg and MB-2 pedons (20 cm and 17 cm). Therefore, the lower boundary of the Bt1 horizon occurs at a shallower depth in the ATL pedons (72 cm and 81 cm) than in the typical Millersburg and MB-2 pedons (both 86 cm). In sum, the E/B-Bt1 zone in the ATL pedons, despite occurring at a greater depth in the solum, has a shallower lower boundary, and as a result, is of significantly lesser thickness (30 cm and 25 cm) than reported in the typical Millersburg and MB-2 pedons (61 cm and 50 cm). It is important to note that no subsurface stone

zone or significant concentration of coarse fragments, as observed immediately below the Bt1 horizon in the ATL pedons, is reported in either the typical Millersburg or MB-2 pedons, suggesting that it may be a relatively localized phenomenon.

Table 4.6. Select E/B-Bt1 horizon morphological data for Millersburg-type soils.

Pedon	**Upper Depth** (cm)	**Lower Depth** (cm)	**Thickness** (cm)
E/B horizon			
OSD	25	66	41
MB-2	36	69	33
ATL-1	42	58	16
ATL-2	56	74	18
Bt1 horizon			
OSD	66	86	20
MB-2	69	86	17
ATL-1	58	72	14
ATL-2	74	81	7

CHAPTER 5

GLOSSIC HORIZON CHARACTERIZATION AND INFERRED GENESIS

The purpose of this chapter is to identify and describe the primary pedogenic pathways and processes responsible for the formation of the glossic (E/B) horizon in the ATL pedons. First, I discuss select field, laboratory, and microscopic data for the five glossic horizon degradational groups (defined in Chapter 3) in the context of current pedogenic theory to infer the sequence by which the glossic horizon forms and evolves. I then evaluate the associated findings in light of previous applicable conceptual models of glossic horizon genesis in order to develop a new model – one that integrates existing models and findings from this study. The model illustrates a more likely scenario for glossic horizon genesis in calcareous coarse-loamy, upland soils in Michigan and across the broader upper Great Lakes region than explained by previous regional models. I present the model as a sequence of stages in order to capture processes that occur sequentially over time – each predicated on the occurrence of the previous.

5.1 Condition 1: Formation of the Illuvial Zone

The occurrence of a glossic horizon in soil is, by definition, preconditioned by the formation of a well-developed subsurface zone of clay accumulation, i.e., an argillic (or other clay-enriched) subsurface diagnostic horizon (Soil Survey Staff, 2014). Therefore, in order to adequately evaluate the pedogenic evolution of the glossic (E/B) horizon in the ATL pedons, an initial examination of the processes by which the argillic horizon has formed is necessarily required. Discussion in this section will focus primarily on the zone of maximum illuvial accumulation, i.e., Bt1 horizon (Group I) - the intact zone immediately subjacent to the encroaching processes of its degradation.

5.1.1 Acidification

Oftentimes, a necessary precursor to the eluvial-illuvial transfer (translocation) of pedogenic materials is soil acidification (Muhs, 1984; Schaetzl, 1996; Chadwick and Chorover, 2001; Lavkulich and Arocena, 2011; Bockheim and Hartemink, 2013). This is especially true for clay translocation processes, i.e., lessivage. Generally, acidification in calcareous materials occurs as the exchange complex of the soil becomes increasingly occupied by acidic hydrogen (H^+) cations, as soluble basic cations, particularly calcium (Ca^{2+}), are removed as a result of decarbonation. Hydrogen ions are introduced into the soil system primarily through natural disassociation of weak acids in the soil solution (De Vries and Breeuwsma, 1987), e.g., carbonic acid associated with rainfall and root respiration, and organic acids associated with the decomposition of organic matter. Hydrolysis of aluminum-bearing minerals also releases both Al^{3+} and H^+ ions into the soil system. However, as discussed previously (Chapter 5), this process tends to be notable only at sufficiently low pH (< 5.0) levels – a level observed only in the E horizon of the ATL 2 pedon (Table C.1).

Under acidifying conditions, basic cations are preferentially replaced by free H^+ ions on the exchange complex, in order to satisfy the charge of the soil solution. These base cations are then easily solubilized and removed from the soil by leaching and/or incorporated into plant biomass via biological uptake (De Vries and Breeuwsma, 1987; Chadwick and Chorover, 2001).

The process of acidification tends to be magnified in coarse-textured soils due to their inherently smaller negatively charged surface area (i.e., clay contents) on which to retain basic cations, and because the large void spaces formed between the particles facilitate rapid and deep percolation of water. Acidification is further enhanced in coarse-textured soils forming under weak and/or non-base-cycling vegetation (e.g., oak, pine, hemlock, and other conifers), because leaching

rates tend to outpace base cation return to the soil via decomposition and/or mineralization of leaf litter (Cline, 1949; De Vries and Breeuwsma, 1987; Bockheim, 1997; Fujinuma et al., 2005).

Multiple lines of evidence indicate that acidification has been an active process in the ATL pedons. Generally, the mineral horizons in both pedons have lower pH values and lower total base cation contents, particularly Ca^{2+}, relative to the parent material (Table C.1; Table C.3). These trends suggest that the depth of carbonate leaching in the soils is equal to the depth of the solum, as in most soils that have developed in calcareous parent materials. As would be expected, however, the intensity of acidification is greatest nearer to the soil surface, assumedly due to the greater influence from external acid inputs (i.e., leaf litter and rainfall), more frequent leaching/wetting events, and an overall longer exposure time to acidification processes, relative to underlying horizons. This observation is supported by pH values of < 6.0 and base saturation values of < 45% in the upper sequum (E-Bs1-Bs2) horizons (Table C.1; Table C.4). Conversely, in the lower sequum illuvial horizons (i.e., Bt1 and below), abundant "free" Ca^{2+} is still available to effectively neutralize added acidity, as indicated by pH values of > 7.0 and base saturation values of 100% (Table C.1; Table C.4).

It seems probable, as hypothesized by many previous workers in the region (discussed in Chapter 1), that acidification in these soils has been driven primarily by the long-standing presence of vegetation that produces primarily acidic litter at the study site. Assuming that the study site has experienced similar vegetation colonization and successional history as observed at nearby locations in northeastern Lower Michigan (i.e., Silver Lake and Tower Buried Forest site, as discussed in Chapter 2), the soils have been forming under conifer-dominated forest since the region became ice-free and pedogenically active (≈15,500 cal yr B.P.). Although there has assumedly been an increase in deciduous (i.e., base-cycling) species at the site over the last

century, as suggested by the presence of mature aspen and sugar maple trees (as discussed in Chapter 2), it remains unclear, based on the data collected, as to what extent (if any) this change has affected the natural acidification rate of the soils. Nevertheless, I conclude that long-term acid additions, coupled with the rapid and deep percolation capacity of the parent material, has resulted in the gradual removal of soluble reaction products in the solum, and therefore, a decrease in the overall acid neutralizing capacity of the soil.

5.1.2 Translocation

During the acidification process, a pedogenic threshold is eventually reached in which the translocation of clay minerals is activated (Muhs, 1984; Schaetzl, 1996; Chadwick and Chorover, 2001; Lavkulich and Arocena, 2011; Bockheim and Hartemink, 2013). The presence of free, exchangeable, divalent basic cations, particularly Ca^{2+}, tends to favor coagulation/flocculation of discrete clay particles in the clay-soil solution system, thereby rendering them immobile (Muhs, 1984; Chorom and Rengasamy, 1995; Schaetzl and Thompson, 2015). Generally, coagulation occurs under such conditions due to the high ionic strength (or molality) of the clay-soil solution system, which allows for close enough particle spacing that van der Waals forces (i.e., the natural attraction between uncharged particles) dominate. However, as basic cations are leached over time as a result of decarbonation, the clay-soil solution system becomes increasingly saturated with monovalent H^+ cations, thus requiring a greater total number of ions to satisfy the soil exchange complex (Chorom and Rengasamy, 1995; Schaetzl and Thompson, 2015). The large assemblage of positively charged ions lowers the ionic strength of the clay-soil solution system, causing discrete clay particles to become more distantly spaced, thereby increasing the potential for their dispersion and subsequent mobilization. Dispersion typically occurs at base saturation values <

40% (Soil Survey Staff, 2014; Schaetzl and Thompson, 2015). Although of assumedly lesser importance in calcareous soils, physical detachment (or slaking) of discrete clay particles from the soil matrix may also occur due to shear stress from rapidly percolating water (Chesworth, 2008; Schaetzl and Thompson, 2015).

Once adequately dispersed in the soil solution, discrete clay particles are capable of being translocated in percolating water. Generally, the more frequent and rapid percolating water, the more efficient it is of translocating pedogenic materials (Schaetzl and Thompson, 2015). The effect of rapid and continuous percolation events on the movement of pedogenic materials in sandy Spodosols during the spring snowmelt period (March and April) has been well-documented in northern Lower Michigan, particularly in lake-effect locales (e.g., Schaetzl et al., 2015; Schaetzl and Rothstein, 2016; Schaetzl et al., 2018). It seems probable that the same phenomenon is largely responsible for the transport of clay in the ATL pedons. During the spring snowmelt period, soil infiltration totals at the site are ≈12-14 cm (as discussed in Chapter 2), values 20-30% percent greater than reported for similar inland locales in southern Lower Michigan (Schaetzl and Isard, 1991).

In calcareous soils, the primary reason that translocated clays are deposited and accumulate in a preferred zone in the subsoil is due to an increase in basic cation content. Generally, the lower boundary of clay deposition coincides with the top of an unleached (or more base-rich) zone (Schaetzl, 1996; Applegrath and Dahms, 2001). In the soils at the study site, this boundary is the C horizon. Here, the higher availability of "free" divalent cations, particularly Ca^{2+}, causes dispersed clay particles to coagulate, thereby rendering them immobile. As discussed previously, the lower sequum illuvial horizons (i.e., Bt1 and below) contain sufficient "free" Ca^{2+} to effectively facilitate coagulation and deposition of translocated clays, as indicated by pH values of

> 7.0 and base saturation values of 100% (Table C.1; Table C.4).

Translocated clay has also been shown to preferentially accumulate at the interface between two materials of contrasting particle size, such as loamy sediments over gravel, assumedly due to differences in hydraulic tensions in the two materials (Bartelli and Odell, 1960; Khakural et al., 1993; Schaetzl, 1996; Schaetzl, 1998). In essence, percolating water cannot enter a lower, coarser-textured material until the finer-textured material above is nearly saturated, and as a result, wetting fronts may occasionally stop at or near the point of lithologic contrast. Thus, clay deposition in the Bt1 horizon of the ATL pedons has likely been further facilitated by the presence of the underlying stone zone (Bt2 horizon), which contains a significantly higher concentration of coarse fragments (Table 4.1). Additionally, the coarse fragments in the Bt2 horizon, being of predominantly carbonate-lithology, release additional Ca^{2+} to the soil solution as they weather, thereby further facilitating coagulation of discrete clay particles. Greater clay contents in Bt1 horizon of the ATL-1 pedon may be due the overall shallower occurrence of the stone zone (Table 4.1), leading to vertical compression of the overlying illuvial zone (*sensu* Schaetzl, 1998).

Lastly, translocated clay particles may also be deposited by filtration due to progressive textural-fining of the soil matrix within the developing clay-enriched zone (Chesworth, 2008; Schaetzl and Thompson, 2015). Generally, deposition of translocated clay leads to gradual shrinking of the conduits through which the percolating clay-water suspension flows, thereby increasing the capacity to retain smaller particle agglomerates. It seems plausible that the filtration effect would be magnified in soils where the zone of maximum clay accumulation occurs at or near the boundary between two texturally contrasting materials, particularly a fine-over-coarse contact; under such a scenario, progressive textural-fining of the overlying material leads to increasingly greater dissimilarity in hydraulic tensions between the two materials.

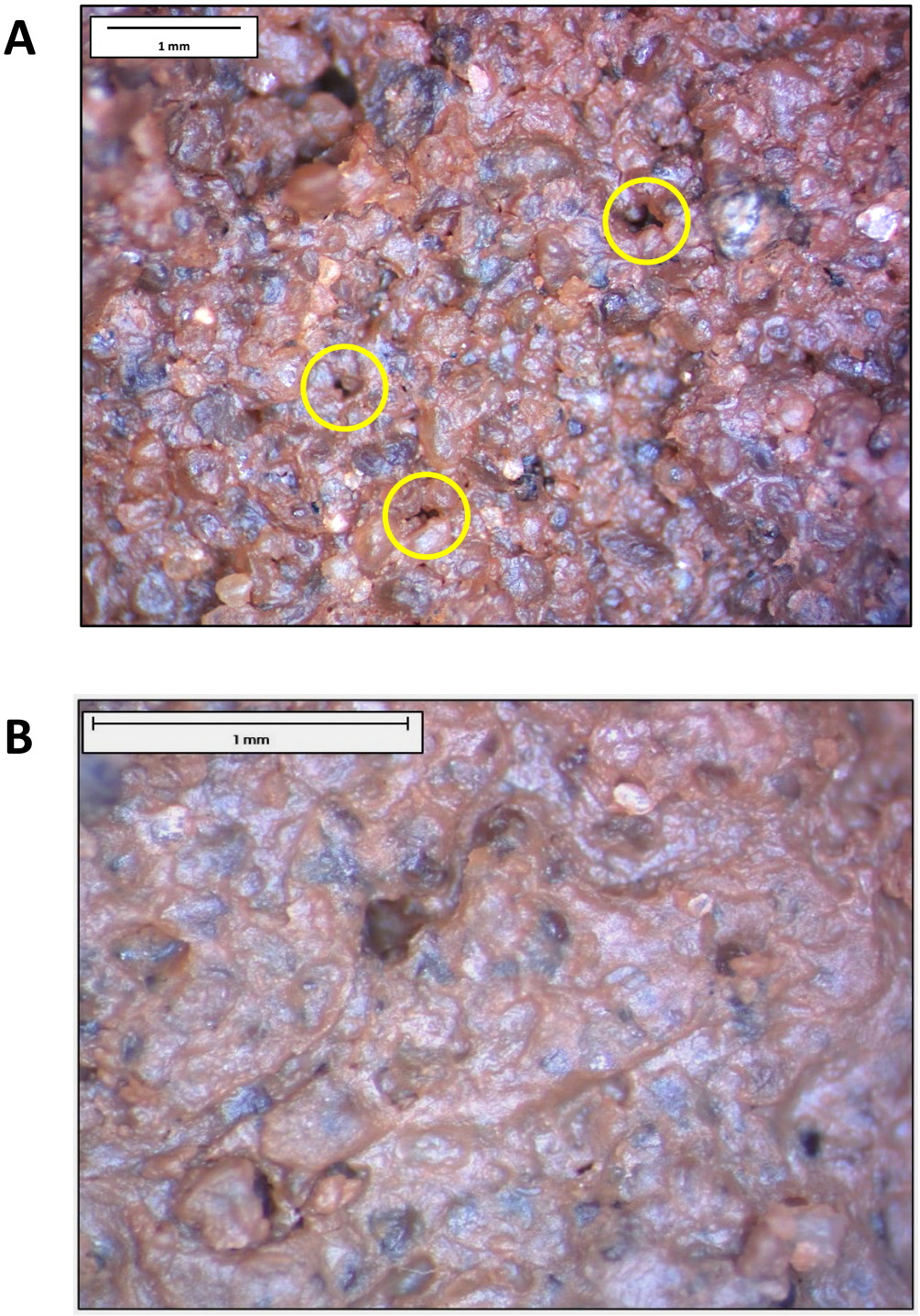

Figure 5.1 Photomicrographs of Group I (non-degraded) peds. A) illuvial clays coating and bridging primary grains and lining active macropore flowpaths (highlighted by yellow circles) in ped center; B) clay film (argillan) on ped faces. Ped orientations were not recorded.

Regardless of the condition(s) that favor deposition of translocated clays in a preferred zone, in well-drained soils their incorporation into the soil matrix generally occurs during desiccation (or drying) of the wetting front (Sumner, 1999; Chesworth, 2008; Schaetzl and Thompson, 2015). In essence, as the wetting front stalls, capillary withdrawal of water *into* dry peds leads to deposition of clay *onto* ped surfaces. Thus, in addition to textural fining, morphological indicators, particularly laminated coatings of clay (i.e., argillans) on grain surfaces, within pores, and along ped faces, are generally considered a primary criterion for identification of clay translocation and deposition in a preferred zone (Chesworth, 2008; Bockheim and Hartemink, 2013; Soil Survey Staff, 2014; Schaetzl and Thompson, 2015). In peds collected from the Bt1 horizon (Group I) of the ATL pedons, illuvial coatings were observed bridging primary grains and lining pores and ped faces (Figure 5.1). Mean particle size data for these coatings (taken from ped faces – "argillan sample", as described in Chapter 2) confirm that they have a clay texture and are mainly composed (≈72%) of clay (< 8 μm), and of that, ≈28% is in the fine clay subfraction (< 2 μm) (Figure 5.2). Virtually all (≈95%) of the remaining portion of the illuvial coatings are composed of fine silt (8-25 μm), approximately half of which occurs within the 8-12 μm range. Mixed (clay and silt) illuvial coatings have been referred to in thin section studies simply as "impure clay coatings" (Bullock and Thompson, 1985; Douglas, 1990; Payton, 1993b; Stoops, 2003), however, for the purpose of clarity, I will refer to these coatings through the remainder of this thesis as *"silty-argillans"*.

It is important to note that the translocation of pedogenic clay may occur mechanically and/or chemically. In mechanical clay translocation (i.e., lessivage), discrete clay particles migrate to lower levels within the soil profile with their original crystalline structure intact (Bockheim and Hartemink, 2013). Conversely, in chemical translocation, aka decomposition and neoformation,

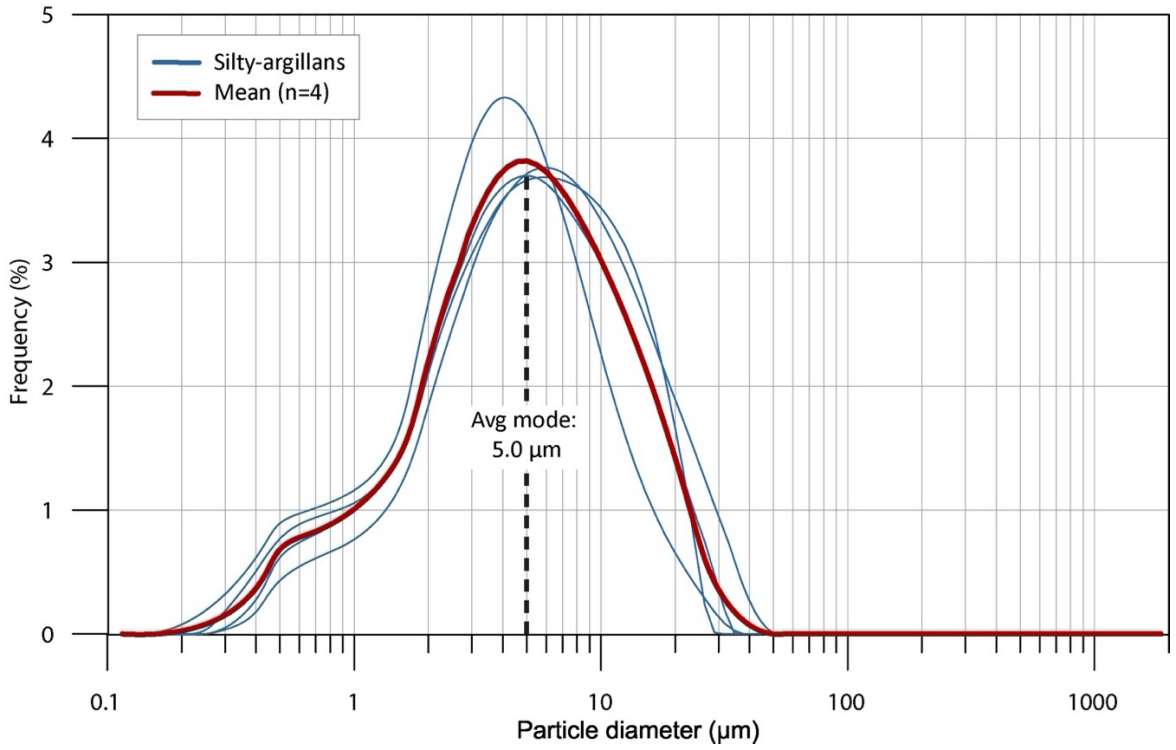

Figure 5.2 Continuous particle-size curves for Bt1 horizon (Group I) illuvial coatings.

the original crystalline structures of the particles are decomposed by chemical weathering processes and the associated weathering products migrate to lower levels within the soil profile, where they are neoformed into new, more stable (secondary) clay minerals. It is generally assumed that neither process alone is responsible for the formation of clay-enriched subsurface horizons (Birkeland, 1999; Phillips, 2004; Bockheim and Hartemink, 2013; Soil Survey Staff, 2014). The degree to which a particular pedogenic process or multiple processes operate, however, tends to vary between soils. In some soils, clay eluviation-illuviation processes dominate, whereas in others they may be overshadowed by in-situ weathering of coarser particles into clay-size material (Quenard et al., 2011; Soil Survey Staff, 2014). Given the relative youth and pH status of the ATL pedons, it is reasonable to assume that the primary mechanism responsible for the observed textural

differentiation is mechanical translocation. Although chemical translocation of clays has likely been operative to some degree, this mechanism is assumedly subordinate to mechanical translocation given that chemical dissolution of most silicate minerals tends to be minimal at pH values > 5.0.

The presence of silty-argillans in the Bt1 horizon provides a critical supporting line of evidence that clay and silt translocation is occurring contemporaneously in the ATL pedons. Although the mechanism(s) responsible for clay translocation in humid environment soils are reasonably well understood (as discussed previously), those responsible for silt translocation have largely eluded soil scientists. It has been generally hypothesized that silt particles can act as plasma (i.e., a mobile constituent) in coarse-textured soils under favorable conditions (Birkeland 1999; Sumner 1999; Schaetzl and Thompson, 2015), however, such a mechanism has traditionally proven difficult to explain empirically. Indeed, accumulations of silt in subsurface illuvial zones have been observed in coarse-textured bisequal soils forming in the upper Great Lakes region (Schaetzl, 1996; Bockheim, 2003; Schaetzl and Weisenborn, 2005), suggesting that pervection (silt translocation) is an ongoing pedogenic process in the region. However, evidence from those studies to support the occurrence of such phenomenon (when provided) were largely qualitative (e.g., thin-section analysis). Data from this study, gathered through the application of modern high-resolution analytical technologies (i.e., laser diffraction particle size analysis), provide valuable quantitative evidence that translocation of silt can and does occur in some coarse-textured soils.

Translocation of fine silt in the ATL pedons occurs according to the same three primary components as that of clay: i) mobilization, ii) transportation, and iii) deposition. It seems plausible that mobilization of discrete fine silt particles occurs primarily following removal of soil binding agents, particularly clays and associated “free” iron oxides. As clays and “free” iron oxides are

gradually stripped from the matrix, exposed fine silt particles may be subjected to physical detachment by percolating water. Additionally, it is possible that a portion of the fine silt subfraction is composed of clay-type minerals (e.g., illite, chlorite, etc.), as has been observed in in both soils and sediments (Malcom and Kennedy, 1970; Peinemann et al., 2000; Su and Suarez, 2004). Such particles may act similarly to clay particles in the soil solution; if so, their mobilization may be favored by chemical dispersion (as discussed previously). Additional mineralogic data on the silt fraction, however, would be necessary to confirm this hypothesis. Regardless of the particular mode of mobilization, most of the natural void spaces and pores in the soil matrix, considering that the pedons are composed of > 50% sands larger than 500 μm (i.e., medium sand and coarser) (Table 4.2), would likely allow for passage of fine silt particles during percolation events, especially those in the 8-12 μm range. Deposition and accumulation of fine silts in a preferred zone in the subsoil is most likely associated with hanging of water at a textural discontinuity and/or filtration due to gradual textural fining. The filtration effect is assumedly of greater importance for fine silt than clay however, however, given the inherently larger diameter of the particles. Subsequent incorporation of translocated fine silt particles into the soil matrix occurs during desiccation, as confirmed by the presence of fine silts in illuvial coatings (i.e., silty-argillans) in the Bt1 horizon (Figure 5.2).

5.2 Condition 2: Degradation of the Illuvial Zone

The development of a glossic horizon, by definition, results from the degradation of an initially developed illuvial zone (as described in section 5.1) (Soil Survey Staff, 2014). Therefore, subsequent examination of the processes by which the illuvial zone degrades is necessarily required in order to adequately evaluate the pedogenic evolution of the glossic (E/B) horizon in

the ATL pedons. Discussion in this section will focus primarily on comparison of the remaining glossic horizon "degradational" groups (as defined in Chapter 3) to the intact (non-degraded) zone of illuvial accumulation (i.e., the Bt1 horizon – Group I).

5.2.1 Weakly Degraded Zone

The eluvial portion (E part) of weakly degraded (Group II) peds represent the initial stage of degradation of the illuvial zone. As described previously (Chapter 3), eluvial materials of Group II peds occur as thin (≤ 2 mm) light colored (7.5YR 6/3) skeletal grains, usually surrounding intact illuvial (Bt) materials at ped margins (Figure 3.4). Particle-size data for the eluvial materials indicate that they have a sandy loam texture and are composed of 12.2% and 16.2% clay and silt, respectively (Table 5.1; Figure 5.3). These values represent a net loss of ≈21% clay and ≈4% silt

Table 5.1 Select particle-size data for the glossic horizon degradational groups.

Group	**sand** 2-0.05 mm	**silt** 50-8 µm	**clay** < 8 µm	**csi** 50-35 µm	**msi** 35-25 µm	**fsi** 25-8 µm	**cc** 8-2 µm	**fc** < 2 µm	**fc/cc** ratio
I (Bt)	67.7	16.9	15.4	3.5	3.3	10.1	11.8	3.6	0.31
II (E part)	71.6	16.2	12.2	3.3	3.2	9.7	10.3	1.9	0.18
II (B part)	69.8	15.6	14.6	3.4	3.3	8.9	11.0	3.6	0.33
III (E part)	74.7	14.3	10.0	3.2	2.8	8.3	8.5	1.5	0.18
III (B part)	67.2	16.8	16.0	3.5	3.3	10.0	11.6	4.4	0.38
IV (E part)	79.1	12.5	8.3	2.9	2.5	7.1	7.1	1.2	0.17
IV (B part)	55.5	24.3	20.2	3.8	4.5	16.0	16.7	3.5	0.21
V (E')	82.6	10.0	7.4	2.3	2.1	5.5	6.3	1.1	0.17

Notes to Table 5.1:
csi - coarse silt
msi - medium silt
fsi - fine silt
cc = coarse clay
fc = fine clay

Table 5.2 Ion exchange and extractable cation data for the glossic horizon degradational groups.

Group	**CEC** (me/100g)	**Base Sat** (%)	**Ca** (me/100g)	**Mg** (me/100g)	**K** (me/100g)	**Na** (me/100g)
I (Bt)	9.4	100	7.33	2.16	0.23	0.05
II (E part)	1.8	100	1.73	0.41	0.08	0.07
II (B Part)	ND	ND	ND	ND	ND	ND
III (E part)	1.8	100	1.43	0.38	0.07	0.10
III (B part)	12.8	86	8.21	2.27	0.38	0.13
IV (E part)	ND	ND	ND	ND	ND	ND
IV (B part)	8.4	74	4.32	1.56	0.26	0.09
V (E')	1.0	82	0.55	0.18	0.06	0.03

Notes to Table 5.2:
Ca – Calcium
Mg – Magnesium
K – Potassium
Na – Sodium
ND – No data

Table 5.3 Select geochemical data for the glossic horizon degradational groups.

Group	**Ca** (ppm)	**Fe** (ppm)
I (Bt)	8997	31076
II (E part)	8199	12943
II (B part)	8571	24955
III (E part)	7579	12701
III (B part)	8469	27347
IV (E part)	7083	12443
IV (B part)	8234	23092
V (E')	6723	12330

Notes to Table 5.23:
Ca – Calcium
Fe - Iron

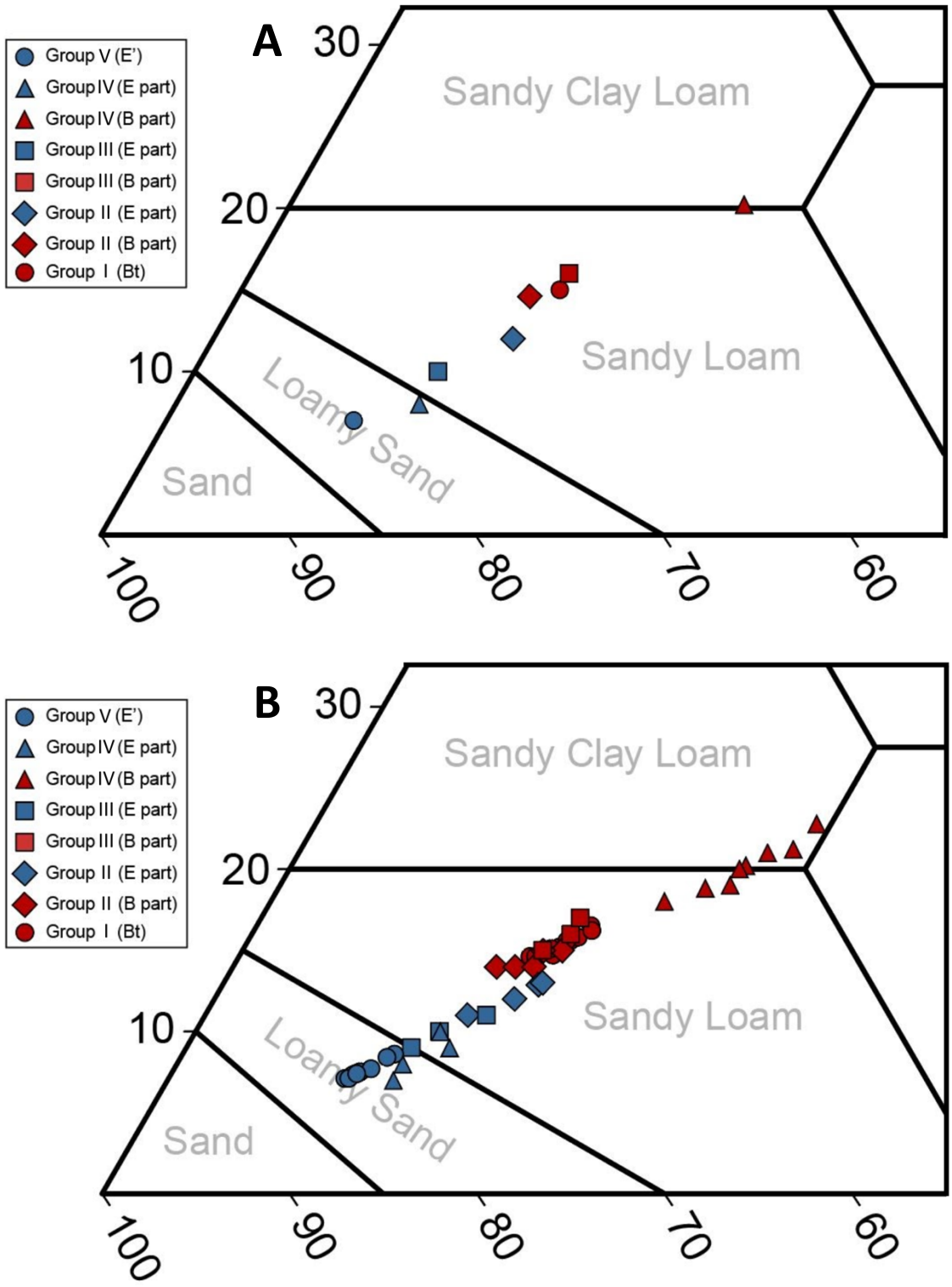

Figure 5.3 Particle-size data for the glossic (E/B) horizon degradational groups plotted on the lower left portion of a standard NRCS textural triangle. A) mean particle-size data for each group; B) particle-size data for all samples.

relative to non-degraded (Group I) peds (Figure 5.4). The majority (≈53%) of the observed clay loss from the eluvial materials has occurred in the fine clay subfraction (< 2 µm), suggesting that fine clays are preferentially removed during the earliest stages of degradation. The preferential loss of fine clay is further reflected by a decrease in the fine-to-coarse clay ratio (0.18 vs. 0.31). The majority (≈57%) of the observed silt loss, albeit relatively negligible overall (0.7%), has occurred in the fine silt subfraction (8-25 µm). The textural coarsening associated with the onset of Bt horizon degradation is assumedly responsible for the large decrease in CEC (1.8 vs. 9.4) (Table 5.2). Taken together, particle-size and CEC data indicate that clays remaining in the eluvial

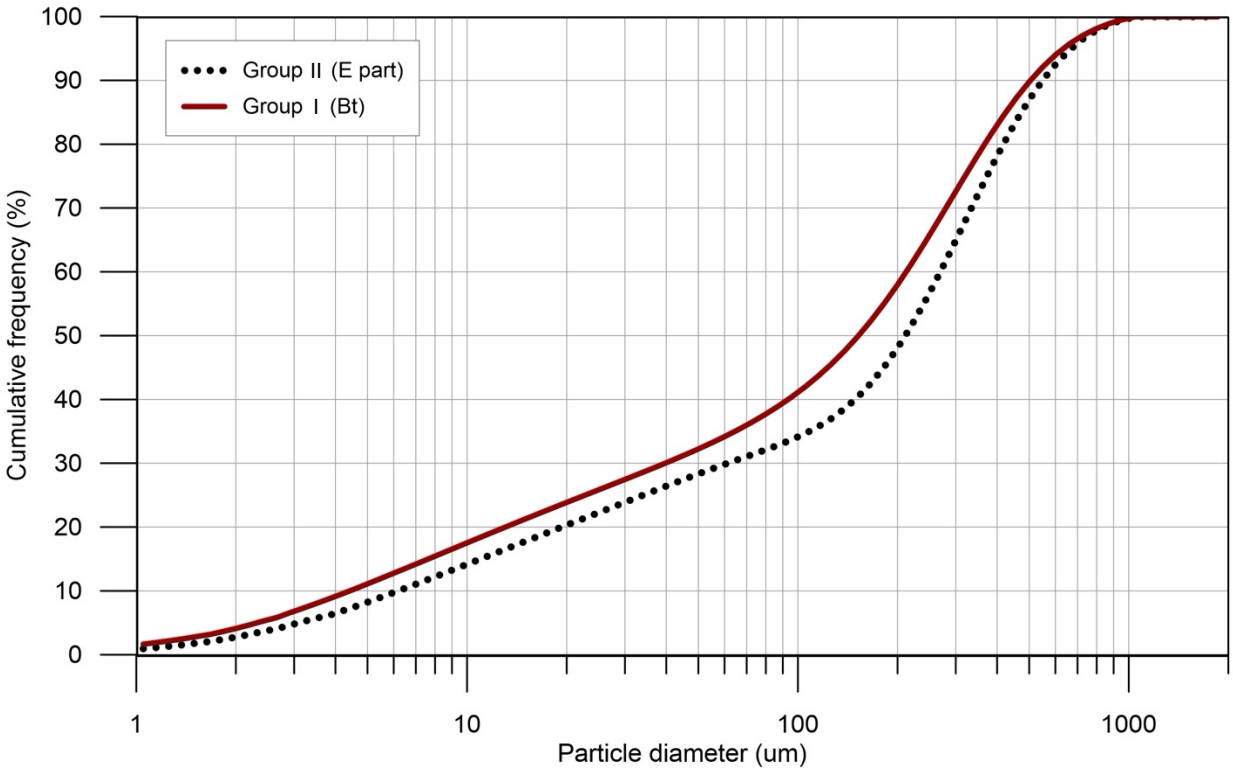

Figure 5.4 Cumulative particle-size distribution curve for the eluvial portion (E part) of Group II (weakly degraded) peds, relative to non-degraded (Group I peds). Chart produced according to particle size data reported in Table 5.1.

materials are primarily coarse, likely 1:1 (low activity) clays. Additional clay mineralogy data, however, would be necessary to confirm this hypothesis. Despite the clay loss and associated decrease in CEC, the exchange complex remains saturated entirely (100%) by basic cations (Figure 5.5), mainly Ca^{2+}.

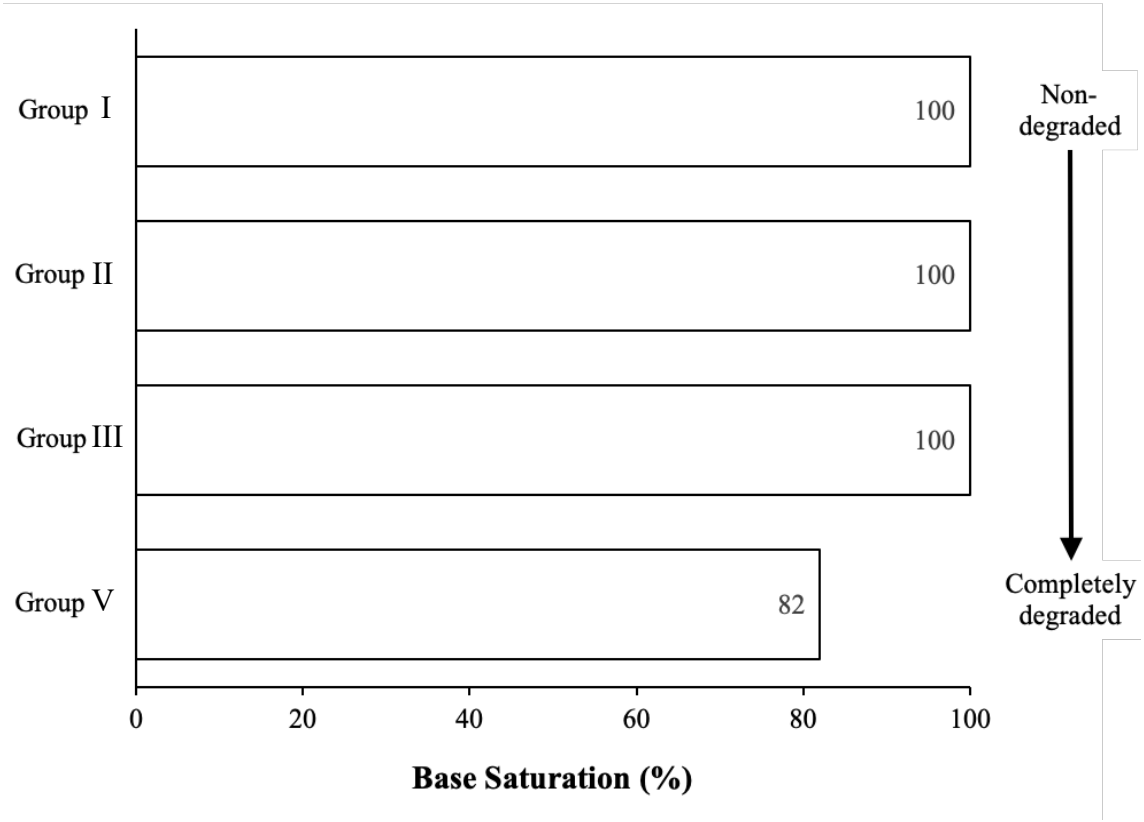

Figure 5.5 Base saturation for eluvial materials in the glossic horizon, relative to non-degraded (Group I peds). Chart produced according to exchangeable cationdata reported in Table 5.2.

Although it is possible that the present saturation value does not correspond with the conditions during which clay removal occurred, geochemical data indicate that the total calcium content of the eluvial materials in Group II peds has decreased by only ≈9% (8199 ppm vs. 8997 ppm) (Table 5.3). Therefore, it is likely that an adequate quantity of "free" Ca^{2+} still remains to satisfy the reduced exchange complex, especially considering that the remaining clays are likely

of 1:1 type (i.e., lower net negative charge). In other words, as the capacity to retain cations has decreased, so has the need for cations to satisfy the charge. Base saturation values of 100% can be achieved even under acidifying conditions, so as long as the availability of exchangeable cations remains greater than the retention capacity. It is important to note that geochemical data also revealed a considerable net loss of ≈59% total iron relative to non-degraded (Group I) peds (Table 5.3; Figure 5.6), suggesting that its removal (probably as "free" iron oxides) is likely of greater importance to the remobilization of pedogenic materials, particularly clay, than desaturation of the exchange complex during the earliest stages of degradation. Jamagne et al. (1984) and Payton (1993b) reported similar findings for degrading clay-enriched zones in France and England, respectively.

Destabilization and mobilization of iron oxides in soil, including those associated with illuvial coatings, generally occurs under reducing conditions, whereby stable ferric iron (Fe^{3+}) compounds are converted to more soluble ferrous iron (Fe^{2+}) forms (Carroll, 1957; Gotoh and Patrick, 1974). According to Jamagne et al. (1984) and Payton (1993b), reduction of Fe^{3+} in iron oxides, as it is related to degradation, is initiated as a result of a decrease in hydraulic conductivity at the upper boundary of the illuvial zone. As was discussed in section 5.1, wetting fronts may occasionally stop at or near the point of contact between the two texturally contrasting materials, leading to temporary localized saturation and subsequent limitation of oxygen (O_2) (i.e., anoxic conditions) at various micro sites. Under anoxic conditions, biotic reduction of Fe^{3+} in iron oxides is important for both microbial and plant root respiration (Roden, 2012; Schaetzl and Thompson, 2015). Generally, the biotic reduction of ferric iron occurs as "iron-reducing" bacteria, acting as a reductant, donate electrons to react with iron oxides and H^+ ions in the soil solution, thereby producing "free" Fe^{2+} and dissolved O_2. It is important to note, however, that the reduction of Fe^{3+}

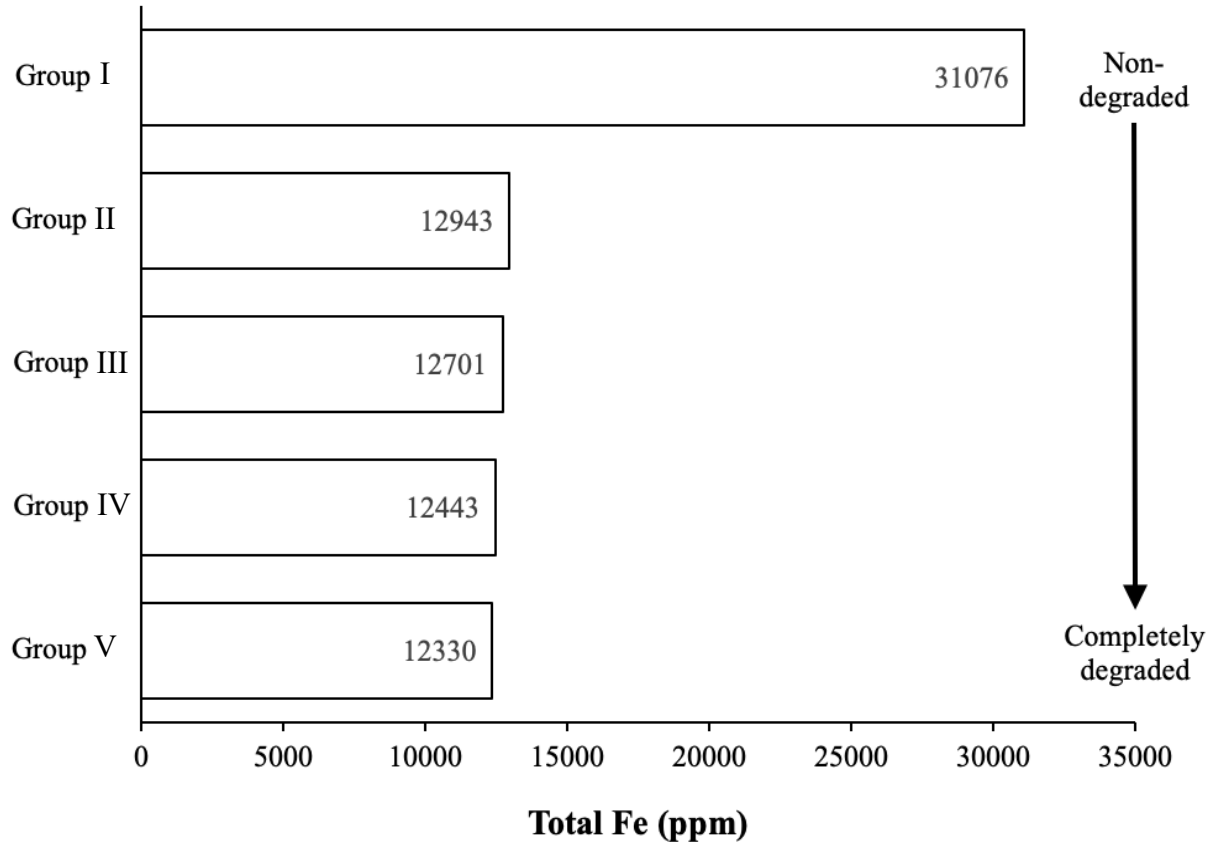

Figure 5.6 Total Fe content for eluvial materials in the glossic horizon, relative to non-degraded (Group I peds). Chart produced according to geochemical data reported in Table 5.3.

in iron oxides is negligible in calcareous soils, including under saturated conditions, due to its reaction with bicarbonate anions produced during the dissolution of calcium carbonate (Loeppert, 1986; Mengel, 1994). Therefore, a sufficient decrease in the overall acid neutralizing capacity of the soil is required for reduction of Fe^{3+} in iron oxides to occur. When associated with illuvial coatings, the reduction and loss of iron oxides results in the "bleaching" (i.e., lightening of color) of the coating (Federoff, 1972; Jamagne et al., 1984; Payton, 1993b) – this likely explains the exceedingly light (7.5YR 6/3) colors of the clays and fine silts that remain in the degraded (eluvial) coatings on Group IV peds. The resulting bleached, Fe-poor pedogenic materials, having lost their

primary binding agents (fine clays and Fe oxides), are then susceptible to micro-erosion and mobilization during subsequent percolation events (Jamagne et al., 1984; Payton, 1993b).

The illuvial portion (B part) of weakly degraded (Group II) peds represents the remaining intact portion of the illuvial zone at the initial stage of degradation. Particle-size data for the illuvial materials indicate that these soil components have a sandy loam texture and are composed of 14.6% and 15.6% clay and silt, respectively (Table 5.1; Figure 5.3). These values are slightly lower than in non-degraded (Group I) peds. The observed differences can be accounted for entirely in the coarse clay and fine silt subfractions. Assuming that the two zones are closely related, the slightly finer textures in the Group I peds indicate stronger illuvial development, probably due to illuvial contributions from zones of degradation nearby (but mainly above). Geochemical data indicate lower total iron contents in the B part of Group II peds (24955 ppm vs. 31076 ppm) (Table 5.3), suggesting that some of the iron lost during degradation (via reduction and eluviation) has also likely been gained in the underlying non-degraded zone where the pH (7.1) is adequate for reprecipitation of Fe^{2+} as Fe^{3+} from the soil solution. It is possible, however, that the seemingly "intact" illuvial materials have themselves begun to degrade, resulting in coarser textures and lower Fe contents, but show no visible evidence of such. Geochemical data also indicate that the total calcium content of the B part of Group II peds is slightly lower than that of Group I peds (8571 ppm vs. 8997 ppm, respectively) (Table 5.3). This difference, however, although relatively negligible overall (≈5%), is likely a result of enhanced decarbonation in the illuvial portion of the weakly degraded zone, rather than a gain of calcium in the non-degraded zone. The vertical distribution of total calcium contents in both pedons, which indicate that decarbonation is indeed active and ongoing throughout the entire solum (as discussed in section 5.1.1), generally support this assumption.

Important differences also occur relative to the E part of Group II peds. Aside from the obviously higher clay contents, particularly fine clays, the B part of Group II peds contain slightly less fine silt (8.9% vs. 9.7%). These data not only provide a supporting line of evidence that fine clay is preferentially removed during the earliest stages of degradation, but also that the removal may be associated primarily with silty-argillans that were previously deposited on ped faces. It seems plausible that removal of such coatings would be a necessary precursor to the degradation of the ped interior.

5.2.2 Moderately Degraded Zone

The eluvial portion (E part) of moderately degraded (Group III) peds represents the intermediate stage of degradation of the illuvial zone. As described previously (Chapter 3), eluvial materials of Group III peds occur primarily as thick (≤ 5 mm) light colored (7.5YR 6/3) skeletal grains surrounding generally intact illuvial (Bt) materials (Figure 3.4). Generally, the boundary between the eluvial materials and the underlying intact matrix materials tends to be diffuse and irregular, indicating further and uneven encroachment of degradation processes into ped interiors (Figure 5.7). Eluvial materials were also occasionally observed along macropore flow paths and active root channels within Group III peds, suggesting that the process of degradation may also occur from the ped interior-outward, at preferred sites (Figure 5.8). Particle size data for the eluvial materials of Group III indicate that they have a sandy loam texture and are composed of 10.0% and 14.3% clay and silt, respectively (Table 5.1; Figure 5.3). These values represent a net loss of ≈35% clay and ≈15% silt relative to non-degraded (Group I) peds (Figure 5.9). The majority (≈61%) of the clay loss from the eluvial materials has, however, now occurred in the coarse clay subfraction (2-8 μm). Considering data for Group II eluvial materials, this suggests that removal

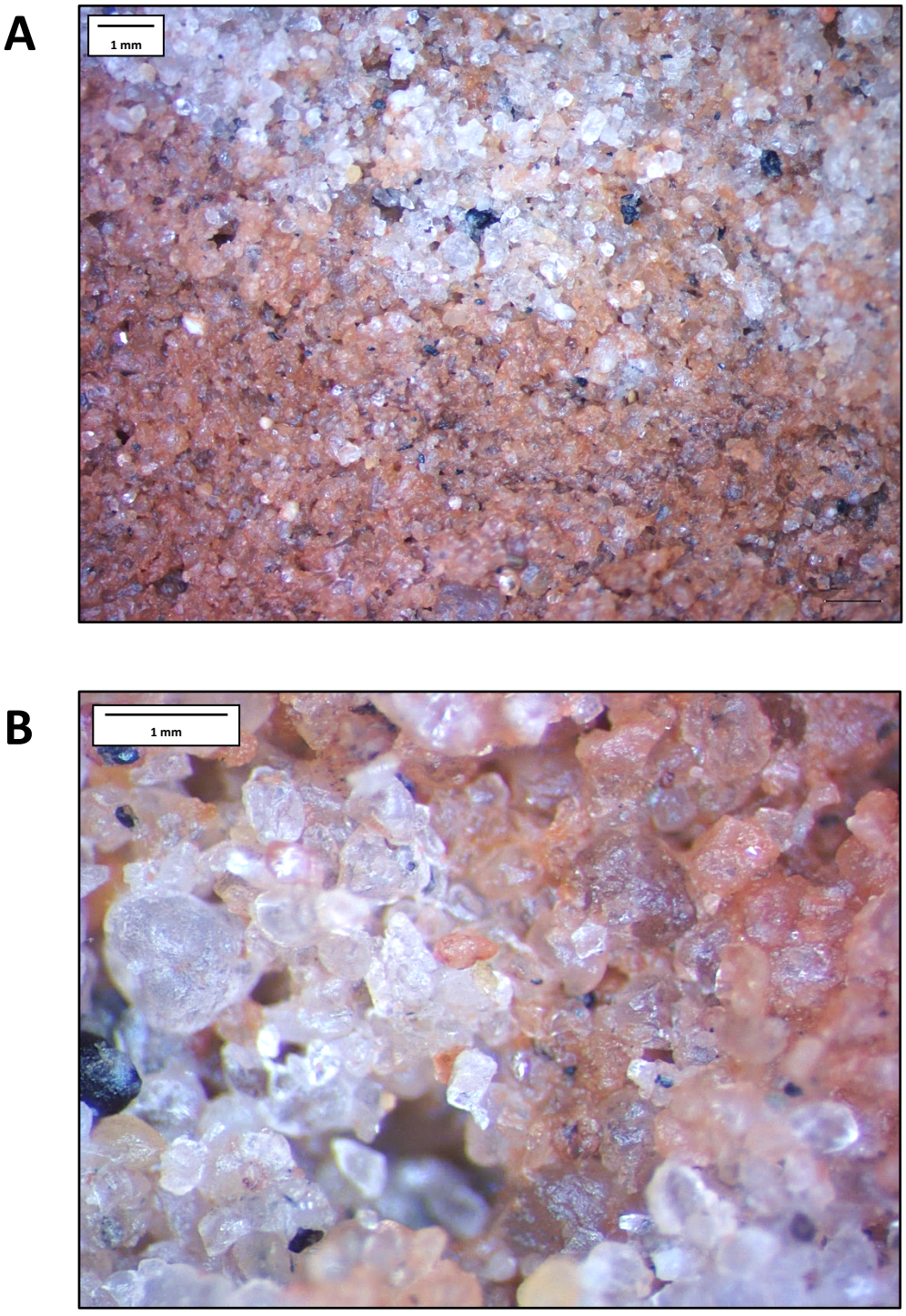

Figure 5.7 Photomicrographs of Group III (moderately degraded) peds. A) typical degrading eluvial-illuvial boundary in ped center showing uneven encroachment of degradation; B) closer view of a typical degrading eluvial-illuvial boundary in ped center showing stripped skeletal grains adjacent to coated skeletal grains. Ped orientations were not recorded.

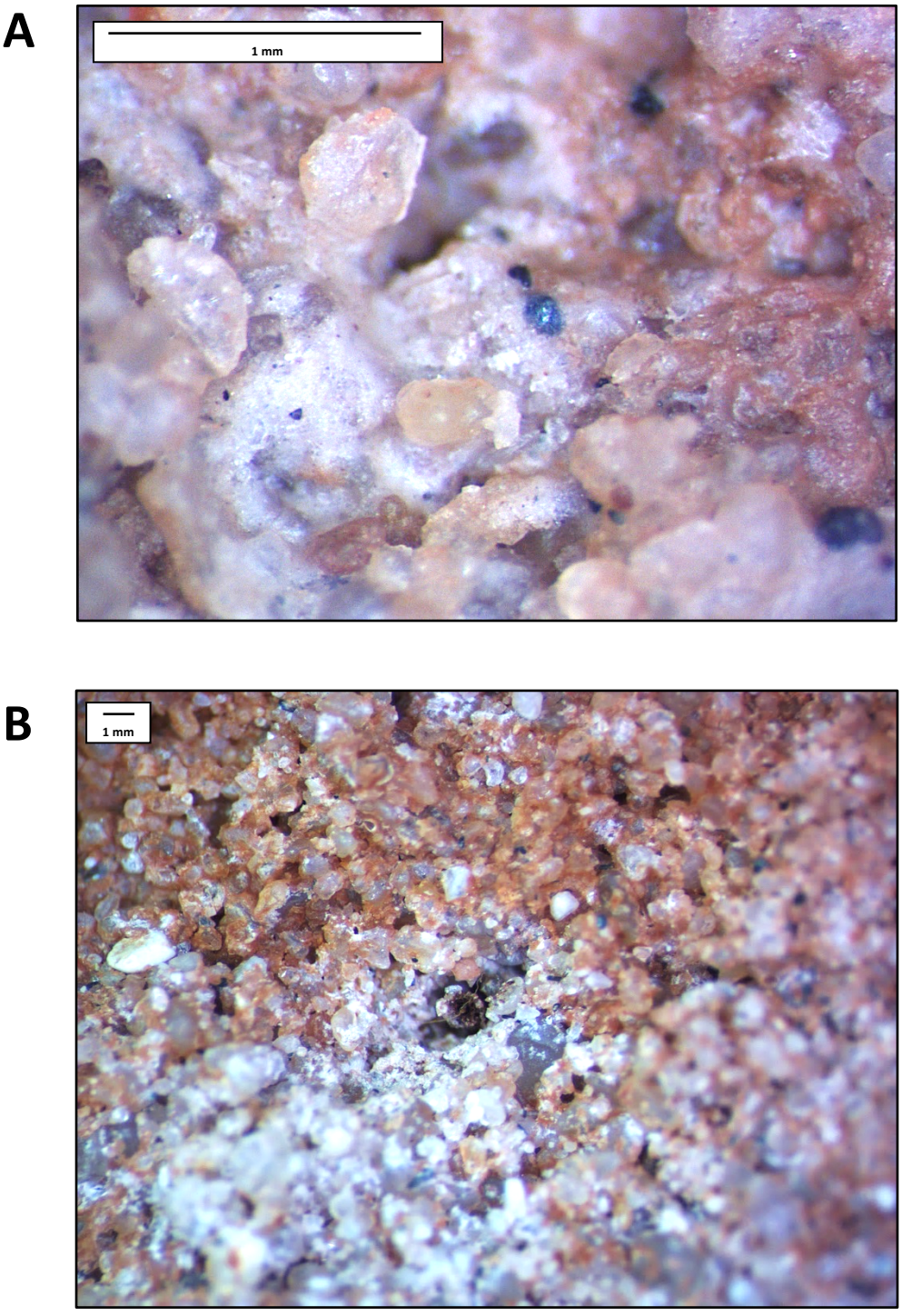

Figure 5.8 Photomicrographs of Group III (moderately degraded) peds. A) degrading eluvial-illuvial boundary along a macropore flowpath in ped center; B) degrading eluvial-illuvial boundary along an active root channel in ped center. Ped orientations were not recorded.

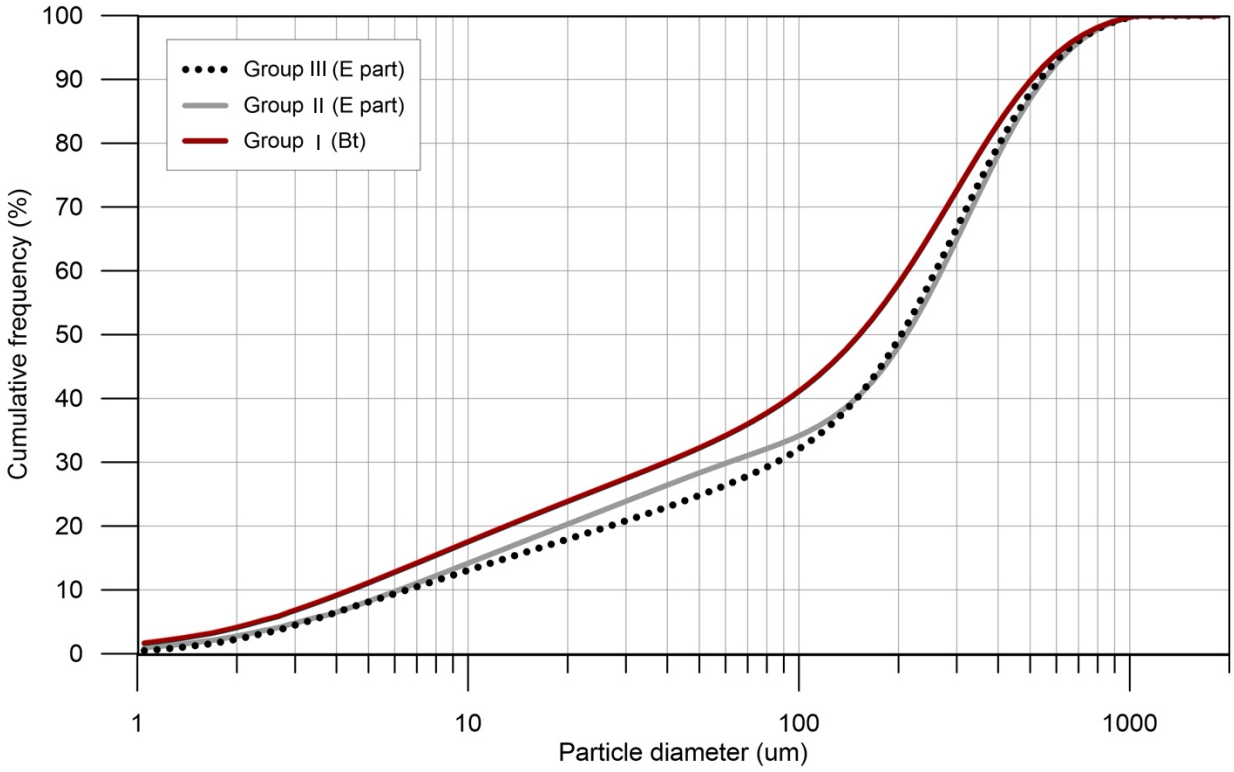

Figure 5.9 Cumulative particle-size distribution curve for the eluvial portion (E part) of Group III (moderately degraded) peds, relative to non-degraded (Group I peds) and the eluvial portion (E part) of Group II (weakly degraded) peds. Chart produced according to particle size data reported in Table 5.1.

of coarse clays becomes more prominent following adequate removal of fine clays and associated "free" Fe-oxides during the earliest stages of degradation. Similarly, removal of silts, albeit subordinate to the removal of coarse clay, also becomes more prominent during the intermediate stage of degradation; again, the majority (≈69%) of the observed silt loss has occurred in the fine silt subfraction (8-25 μm).

Despite further textural coarsening of eluvial materials in Group III peds associated with ongoing degradation, however, the CEC value remains constant (1.8), and only a very slight decrease in the total exchangeable cation content is observed (Table 5.2). Thus, the exchange

complex continues to remain saturated entirely (100%) with basic cations (Figure 5.5), mainly Ca^{2+}. Geochemical analysis indicates that the total calcium content of the eluvial materials has decreased by ≈16% (7579 ppm vs. 8997 ppm) (Table 5.3). Although a greater loss of calcium has occurred relative to the eluvial materials in the Group II peds (i.e., since the initial stage of degradation), suggesting that acidification also becomes of greater importance at the intermediate stage of degradation, it is likely that an adequate quantity of "free" Ca^{2+} still remains to satisfy the exchange complex. Considering that less clay remains in the eluvial materials in the Group III peds, of which are likely of 1:1 (low activity) type (as described previously), seemingly less "free" Ca^{2+} would be necessary to saturate the remaining exchange sites. It is plausible, however, that high base saturation values may still be observed despite acidification if ample amounts of "free" Ca^{2+} are reintroduced to the local clay-soil solution system, e.g., through dissolution of a nearby coarse fragment or grain of carbonate lithology. Geochemical data also indicate that only a minor decrease (≈2%) in total iron content has occurred relative to the eluvial materials on Group II peds (Table 5.3; Figure 5.6), which strongly suggests that Fe eluviation is no longer an important component of the degradational process. Thus, other forms of clay and fine silt removal, most likely physical dislodgement (i.e., slaking), have likely become of greater importance.

The illuvial portion (B part) of moderately degraded (Group III) peds represents the remaining intact portion of the initial illuvial zone at the intermediate stage of degradation. Particle-size data for the illuvial materials indicate that they have a sandy loam texture and are composed of 16.0% and 16.8% clay and silt, respectively (Table 5.1; Figure 5.3). These values are generally comparable to those in non-degraded (Group I) peds, with the exception of a slightly higher (0.8%) content of fine clay in the B part of Group III peds). Relative to the B part of Group II peds, however, these values are noticeably higher; the observed differences can be accounted

for in the fine clay, coarse clay, and fine silt subfractions (i.e., all of the constituents assumed to be mobile). This suite of data implies that pedogenic materials have been gained from the surrounding degradational zone. The increase in clay content, particularly in the fine clay subfraction, is assumedly responsible for the highest observed CEC value in the soil, in this suite of samples (12.8) (Table 5.2; Table C.4). Despite an associated increase in basic cations on the exchange complex, however, the base saturation value (86%) indicates that a portion of the exchange complex is also occupied by acidic cations (Figure 5.4). The apparent increase in exchangeable acidity has occurred despite a relatively negligible loss of total calcium (≈6%) (Table 5.3). Thus, it is likely that the acidic cations on the exchange complex are aluminum (Al^{3+}), considering that any H^{+} cations would be preferentially replaced by "free" Ca^{2+} in the soil solution under alkaline conditions, given its higher sorption selectivity (as discussed in Chapter 4). The presence of exchangeable Al^{3+} would provide a supporting line of evidence that the observed increase in fine clays in the B part of Group III peds is also likely due to remobilization from the surrounding zone of degradation (i.e., where conditions are more acidic). Indeed, it is unlikely that Al^{3+} would become available for exchange under the alkaline conditions of the non-degraded ped interior. Further geochemical analysis of the clay fraction, however, would be required to confirm this hypothesis.

Similar to what was observed in the B part of Group II peds, geochemical data indicate a noticeably lower total iron content, relative to Group I peds (27347 ppm vs. 31076 ppm) (Table 5.3; Figure 5.5), providing an additional supporting line of evidence that some of the iron lost during degradation has likely been gained in the underlying non-degraded (Group I) zone. However, the total iron content in the B part of Group III peds is higher than was observed in the B part of Group II peds, which also suggests localized remobilization of pedogenic materials to

the ped interior during degradation.

5.2.3 Strongly Degraded Zone

The eluvial portion (E part) of strongly degraded (Group IV) peds represents the advanced stage of degradation of the illuvial zone. As described previously (Chapter 3), eluvial materials of Group IV peds occur primarily as light colored (7.5YR 6/3) skeletal grains surrounding small remnant aggregates of intact illuvial (Bt) materials (Figure 3.4). Particle size data for the eluvial materials indicate that they have a loamy sand texture and are composed of 8.3% and 12.5% clay and silt, respectively (Table 5.1; Figure 5.3). These values represent a net loss of ≈46% clay and ≈26% silt relative to non-degraded (Group I) peds (Figure 5.10). Similar to what was observed for Group III peds, the majority (≈66%) of the observed clay loss from the eluvial materials has occurred in the coarse clay subfraction (2-8 μm). As well, the majority (≈68%) of the observed silt loss has occurred in the fine silt subfraction (8-25 μm). Although CEC and exchangeable cation data were not collected for eluvial materials of Group IV peds, it is likely, based on the observed textural coarsening, that these values have likely decreased, relative to the eluvial materials of Groups II and III. Geochemical analysis indicates that the total calcium content of the eluvial materials has decreased by ≈21% (7083 ppm vs. 8997 ppm) (Table 5.3). Geochemical data also indicate that only a minor decrease (≈4%) in total iron content has occurred relative to the eluvial materials on Group II peds (i.e., since the initial stage of degradation) (Table 5.3; Figure 5.6), suggesting that slaking remains primarily responsible for further particle remobilization from the degrading zone.

The illuvial portion (B part) of strongly degraded (Group IV) peds represents the remaining intact portion of the initial illuvial zone at the advanced stage of degradation. As described

previously (Chapter 3), the illuvial portion of Group IV peds occurs as small (≤ 1 cm in diameter) aggregates in ped interiors (Figure 3.4). Particle size data for the remnant illuvial aggregates indicate that they have a sandy clay loam texture and – surprisingly - contain noticeably more clay (24.3%) and fine silt (20.2%) than was observed in peds of any other group, including non-

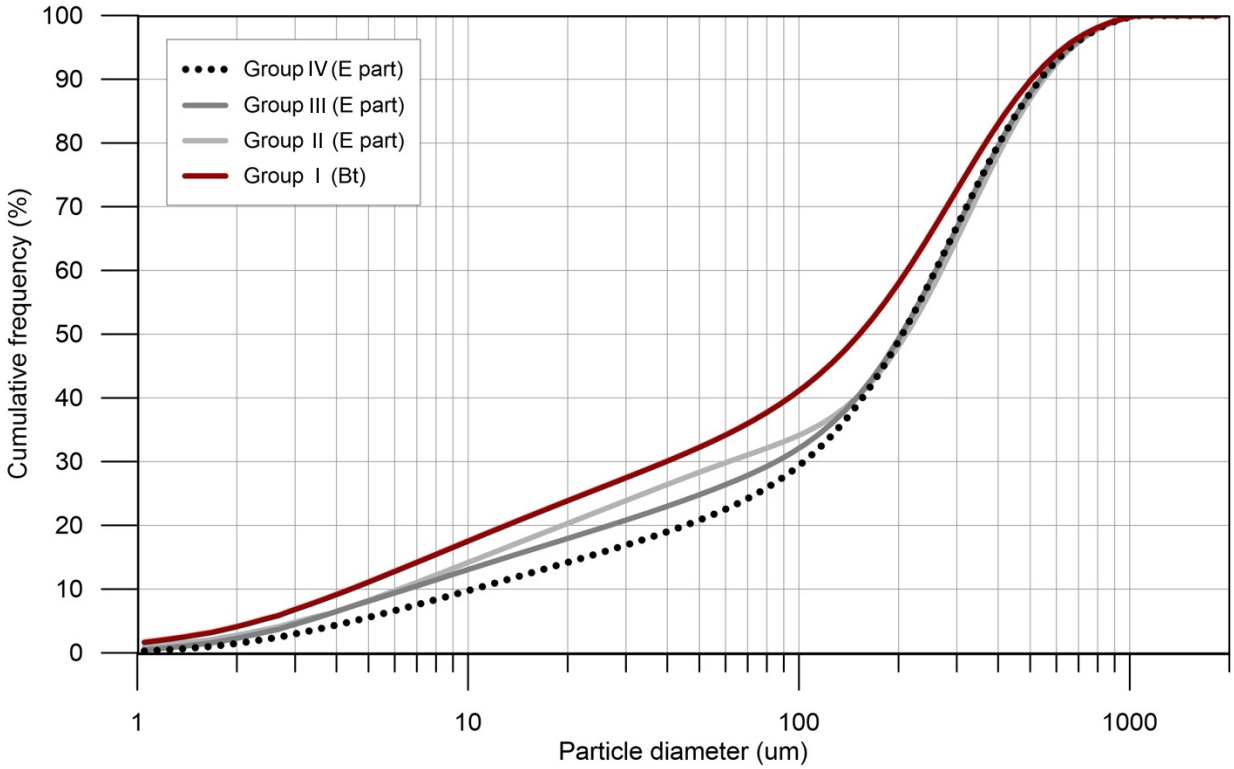

Figure 5.10 Cumulative particle-size distribution curve for the eluvial portion (E part) of Group IV (strongly degraded) peds, relative to non-degraded (Group I peds) and the eluvial portion (E part) of Group II (weakly degraded) and Group III (moderately degraded) peds. Chart produced according to particle size data reported in Table 5.1.

degraded (Group I) peds (Table 5.1; Figure 5.3). The clay fraction is largely dominated (≈83%) by the coarse clay subfraction (2-8 μm); the fine clay subfraction is of similar concentration to that observed for Group I peds (3.5%). As observed in other illuvial portions of the glossic zone, however, the silt fraction is again dominated (≈80%) by the fine silt subfraction (8-25 μm). It is

worth noting that a slight increase in the concentration of medium silt (25-35 μm), albeit relatively minimal (1.2%), is also observed. Although illuvial development has apparently been stronger in these microzones than observed in either Group I peds or the B (illuvial) part of Group III peds, the associated CEC (8.4) is lower, suggesting that a higher concentration of coarse, 1:1 (low activity) clays is present. The associated base saturation value is also lower (74%) (Figure 5.4), despite an only ≈8% loss of total calcium (Table 5.3). Thus, the increase in illuvial materials is likely due to localized remobilization from the surrounding zone of degradation (similar to the B part of Group III peds). As described previously, saturation of the exchange complex by H^+ ions is not likely to occur under the presence of abundant "free" Ca^{2+}, and thus, the acidic cations on the exchange complex are probably Al^{3+}. Because Al^{3+} is generally unavailable for exchange under alkaline conditions, it must be introduced into the illuvial zone on clays from an outside source where conditions are more acidic. Taken together, these data imply that such aggregates are not simply interior ped locations furthest from encroaching degradation, as has been suggested by previous authors (Bullock et al., 1974), but rather, are microzones where previous illuviation processes have been particularly strong. Conceptually, however, it is unclear if such microzones represent the illuvial "end-member" for all peds of the glossic zone or if they are simply localized phenomenon where specific conditions have favored their development and persistence. Nevertheless, when and where such microzones do occur (as observed in Group IV peds), it seems plausible that they would be the most resistant portion of the ped to encroaching degradation.

5.2.4 Completely Degraded Zone

Completely degraded (Group V) peds represent the final stage of degradation of the illuvial zone. As described previously (Chapter 3), Group V peds occur wholly as light colored (7.5YR

6/3) sandy and silty skeletal grains (Figure 3.4; Figure 5.11) in the glossic zone, and therefore, contain no apparent physical evidence of the former illuvial zone. It is worth noting, however, that isolated, remnant flakes of clay on the surfaces of skeletal grains were occasionally observed under the microscope (Figure 5.11). In essence, Group V peds represent the ultimate point to which the illuvial zone is expected to degrade. Thus, if (and when) a laterally contiguous zone (or layer) of such material occurs, the zone would be designated as an E' horizon (i.e., it would no longer be considered a component of the glossic horizon).

Particle-size data for Group V peds indicate that they have a loamy sand texture and contain 7.4% and 10.0% clay and silt, respectively (Table 5.1; Figure 5.3). These values represent a net loss of ≈52% clay and ≈41% silt relative to non-degraded (Group I) peds (Figure 5.12). Relative to eluvial materials in Group IV peds, this indicates that the magnitude of fine silt removal ultimately supersedes that of clay at the final stages of degradation. The textural coarsening associated with ongoing degradation is assumedly responsible for the very low CEC (1.0 vs. 9.4) - the lowest observed CEC value in the soil (Table 5.2; Table C.4). Despite the clay loss and associated decrease in CEC, however, the exchange complex continues to remain saturated primarily (86%) by basic cations (Figure 5.5), mainly Ca^{2+}. Geochemical data indicate that the total calcium content of Group V peds has decreased by ≈30% relative to Group I peds (Table 5.3), which suggests that the observed exchangeable acidity is certainly related to desaturation of the exchange complex due to acidification. It is worth mentioning that the total calcium content of Group V peds is nearing (< 400 ppm) values observed in the upper sequum (E-Bs1-Bs2) horizons, where base saturation values drop below 50%. Additionally, geochemical data also indicate that only a minor decrease (≈5%) in iron content has occurred relative to the eluvial coatings on Group II peds (i.e., since the initial stage of degradation) (Table 5.3; Figure 5.6). Taken together, these

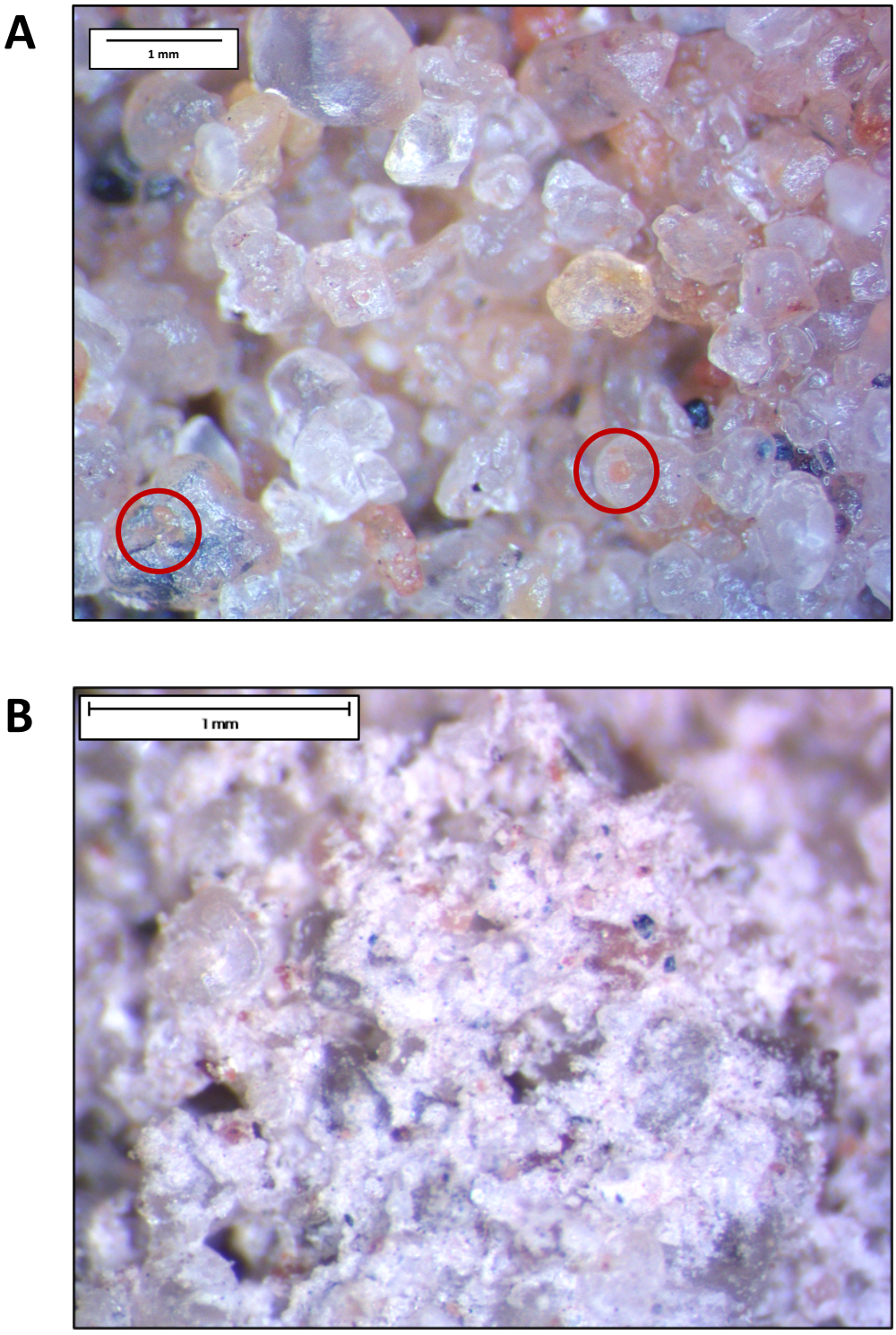

Figure 5.11 Photomicrographs of Group V (completely degraded) peds. A) primary grains stripped of illuvial coatings in ped center (remnant flakes of clay highlighted by red circles); B) primary grains stripped of illuvial coatings on ped face (after drying). Ped orientations were not recorded.

data indicate that slaking, and to some degree, desaturation, are primarily responsible for further particle remobilization from the degrading zone at the final stages of degradation.

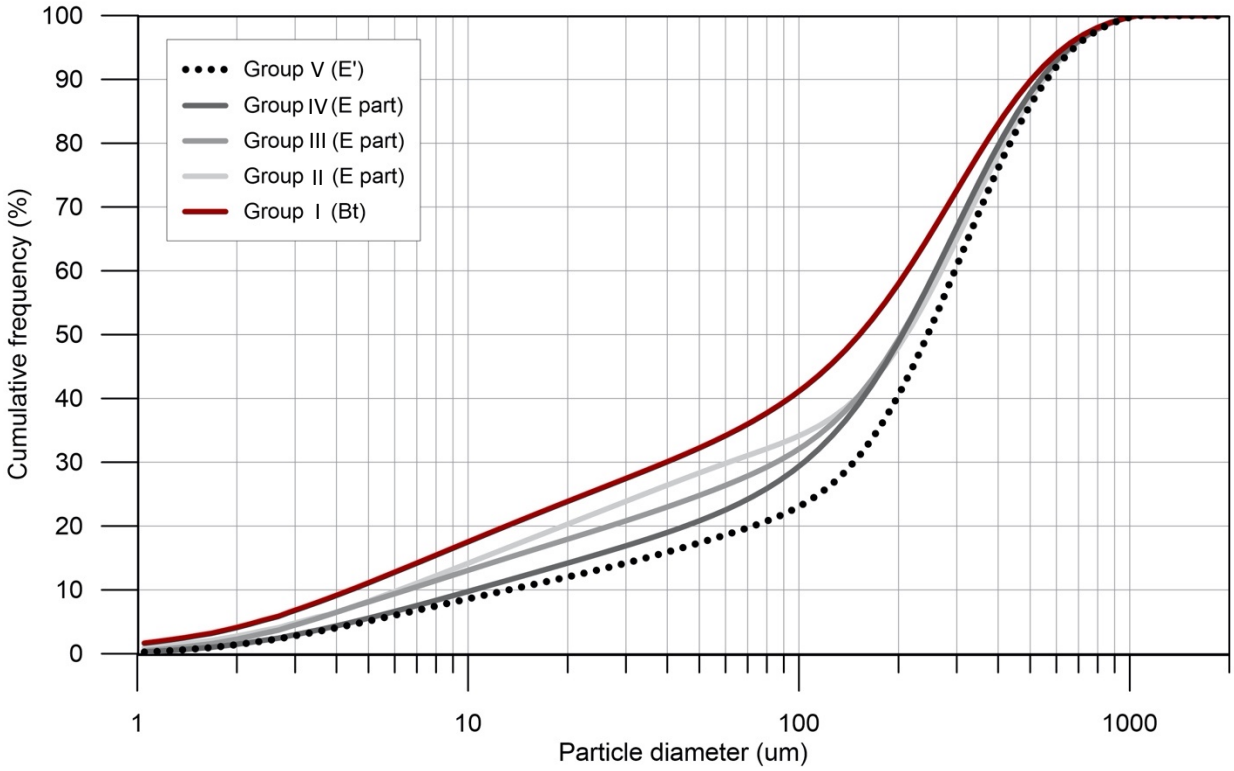

Figure 5.12 Cumulative particle-size distribution curve for Group V (completely degraded) peds, relative to non-degraded (Group I peds) and the eluvial portion (E part) of Group II (weakly degraded), Group III (moderately degraded), and Group IV (strongly degraded) peds. Chart produced according to particle size data reported in Table 5.1.

5.2.5 Summary

In summary, degradation of the illuvial zone and subsequent formation of the glossic horizon in the ATL pedons occurs primarily as a result of the gradual removal of clays and fine silts from the zone. Although clay and fine silt removal occurs contemporaneously throughout the degradational process, the magnitude of removal of these components at progressive stages of degradation follows a distinct sequence: fine clay > coarse clay > fine silt (Figure 5.13).

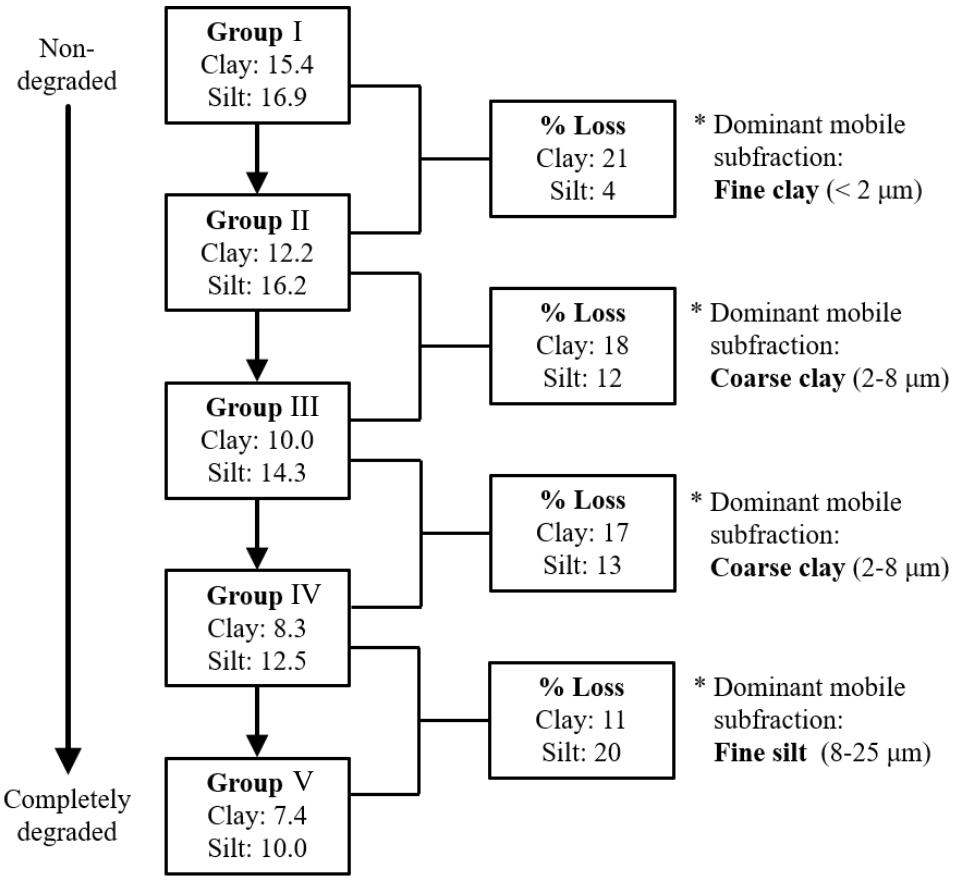

Figure 5.13 Degradational sequence observed in eluvial materials (E part of peds) of the glossic zone, relative to non-degraded (Group I) peds. Chart produced according to particle-size data reported in Table 5.1.

The onset of degradation and initial development of eluvial rinds on ped margins is initiated by the (1) loss of iron (probably as "free" iron oxides), presumably due to reducing conditions under temporary localized anoxic conditions as percolating water is held-up at the texturally contrasting boundary between the eluvial-illuvial zones, and (2) the contemporaneous removal of associated fine clays. At the subsequent (intermediate) stage of degradation, eluvial rinds become thicker and coarser in texture as the removal of bleached, Fe-poor, low activity, coarse clays and

to a lesser extent, fine silts, is initiated. Other mechanisms of removal (as opposed to Fe-eluviation), such as slaking and/or desaturation, apparently become of greater importance at this stage. As degradation progresses into the advanced stage, coarse clays and still to a lesser extent, fine silts, continue to be lost, as eluvial rinds become the dominant component of the ped matrix. At this stage, the only remaining visual evidence of the former Bt horizon are small remnant microzones where initial illuvial development may have been particularly strong. Eventually, even these microzones succumb to encroaching degradation, resulting in little to no apparent physical evidence of the former illuvial zone. The pedogenic materials lost during the degradational process are ultimately remobilized deeper into the solum where they are deposited as fresh, compound cutans (i.e., silty-argillans) in the subjacent Bt horizon.

5.3 Models of Glossic Horizon Genesis

In this section, several conceptual models of glossic horizon genesis from the literature are introduced. Although I focus the discussion primarily on models developed for soils forming in glacigenic sediments of similar age in the upper Great Lakes region, I also present a select number of relevant models from other (i.e., non-regional) locales that may help to explain additional soil characteristics and processes observed in the ATL pedons that are not addressed by local (regional) models. Findings from this study (discussed in section 5.2) are then evaluated in light of these models to help explain glossic horizon genesis in Michigan. Upon evaluation of the models, I propose a new, integrating model for glossic horizon genesis in some Michigan soil. As stated previously, I present the model as a sequence of stages in order to capture processes that occur sequentially over time – each predicated on the occurrence of the previous.

5.3.1 Upper Great Lakes Region Models

5.3.1.1 Model 1: Cline (1949)

Cline (1949) described a pedogenic model for soil development across a sequence of soils intergrading from Alfisols to Spodosols in New York. This model has generally been accepted as the primary theoretical foundation for genesis of soils of this climatic regime (cool summers, snowy winters), which includes the upper Great Lakes region. Similar to what has since been observed and reported on in Michigan, Cline found that Alfisols were confined primarily to calcareous parent materials in the central and southern part of the state. Here, the slightly warmer and drier climatic conditions have generally favored the long-standing dominance of strong-base-cycling vegetation. Under these conditions, the gradual development of weak acidity in near-surface horizons promotes the subsurface accumulation of clay and development of E-Bt horizon sequa. Conversely, he found that Spodosols were confined primarily to acidic parent materials in the northern part of the state. This area has cooler and wetter climatic conditions, generally favoring weak and/or non-base-cycling vegetation. Under these conditions, the rapid development of strong acidity in near-surface horizons promotes thicker litter layers, which decay to produce soluble organic (fulvic) acids. These acids eventually accumulate in the subsurface and carry with them iron and aluminum sesquioxides, thereby promoting the development of E-Bs horizon sequences. However, where calcareous parent materials occur in the northern portion of the state, Cline noted that the soils had bisequal morphologies, exhibiting characteristics of both Alfisols and Spodosols. The occurrence of bisequal soils led him to conclude that the pedogenic transformation of Alfisols to Spodosols can occur in parent materials with inherently high base status, as long as they develop under a long-term acid leaching regime. This scenario fits nicely with the soil-forming factors at the ATL study site.

According to Cline, the development and evolution of soils with bisequal morphology in calcareous parent materials of New York is strongly influenced by the state of the calcium cycle. In the early stages of soil development on calcareous parent materials, the soil-development pathway is toward Alfisols, given the calcareous parent material and the biocycling of bases by vegetation. The biocycling largely buffers acid inputs from the litter. In the end, a clay-enriched zone (i.e., Bt horizon) forms. In theory, a threshold is eventually reached when depletion of bases outpaces the ability of these mechanisms to offset losses by acid leaching, thus inhibiting the calcium cycle. During the ensuing period of acidification, the eluvial zone (i.e., E horizon) is expected to increase in thickness and develop downward, into the underlying Bt horizon. The encroachment of acidic conditions within the upper profile causes the Bt horizon to undergo "degradation", whereby clays are destroyed and/or translocated deeper into the profile, where more alkaline conditions favor their deposition. This assumption was supported by the presence of "pale materials", comparable to that of the E horizon, coating the outsides of peds in the upper portion of the Bt horizon. Today, this distinct eluvial-illuvial transition zone would be described as a glossic (E/B or B/E) horizon. As the E horizon becomes increasingly acidic and clay impoverished, a second threshold is eventually reached, as the overstory vegetation becomes less base-cycling in nature, and thus, the litter turns more acidic. The accumulation of organic matter and sesquioxides is initiated, forming a Bs horizon in the upper portion of the E horizon, as the development of bisequal morphology begins.

5.3.1.2 Model 2: Ranney and Beatty (1969)

Some 20 years after Cline's (1949) classic paper, Ranney and Beatty (1969) published a paper on the pedogenic processes associated with glossic horizon formation in acidic ($pH < 5.0$),

silty, Alfisols in northwestern Wisconsin. The primary objective of the study to was evaluate the mechanisms responsible for clay translocation, as well as the formation of albic (degraded) materials associated with degradation of the clay-enriched zone. To accomplished this, the authors examined and compared the differences in particle size and clay mineralogy between the 1) E and Bt horizons and 2) degraded (glossic) and adjacent Bt materials in the glossic horizon. Thin-section analysis was also conducted to examine the micromorphology of both degraded and intact portions of the glossic horizon.

Ranney and Beatty's particle size data indicated that the formation of the clay-enriched zone was accomplished via translocation and accumulation of clay; increases in fine/coarse clay ratios between the E and Bt horizons suggested preferential movement of the fine clay subfraction. The mobilization and deposition of fine clay in the zone of accumulation was attributed primarily to lessivage, as indicated by mineralogical similarities of the fine clay fraction between the E and Bt horizons, and preferential removal of more resistant minerals (i.e., vermiculite, montmorillonite, chlorite, and kaolinite) in the coarse clay fraction between the E and Bt horizons. The authors suggested that 1) differences in the mineralogy of the fine clay fraction and 2) preferential removal of more weatherable minerals - those less resistant to weathering - in the coarse clay fraction should be expected if chemical translocation (i.e., dissolution in the eluvial zone followed by neoformation of clay minerals in the illuvial zone) was responsible for the increase in clay content in the Bt horizon. Macro- and micro-morphological evidence for clay translocation was also observed in the form of dark brown, laminated clay coatings on ped surfaces and in pores in the Bt horizon. Although not directly discussed by the authors, similarities in reported silt concentrations between the E and Bt horizons suggest that pervection (i.e., silt translocation) was not active in the formation of the illuvial zone.

The authors noted the presence of "gray silt coats" that lacked continuously oriented clays on ped faces, in pores, and as tongues surrounding intact illuvial materials in the upper portion of the Bt horizon. They took this morphological evidence to indicate degradation of the clay-enriched zone and subsequent formation of the glossic features. Small, isolated "fragments" of remnant (relict) Bt materials were commonly observed in degraded (glossic) materials in thin-section, suggesting that the degrading zones had once been zones of clay illuviation. This conclusion was supported by a 6-12% loss of total clay in the gray, degraded materials, relative to adjacent (intact) Bt horizon materials. Proportionally more fine clay had been lost from the degraded materials, however, as indicated by lower fine/coarse clay ratios. Similar to what was observed for the E and Bt horizons, mineralogical similarities in the fine clay fraction and preferential removal of more resistant minerals - those less susceptible to weathering - were observed between degraded and adjacent Bt horizon materials. It is worth noting that mineralogical similarities were also observed between degraded and overlying E horizon materials, including in the coarse clay subfraction, indicating that the two eluvial zones were genetically similar. Thus, the authors concluded that degradation of the clay-enriched zone was also accomplished primarily via lessivage as a result of the advancement of the E horizon down, into the Bt horizon.

5.3.1.3 Model 3: Bullock et al. (1974)

With the intention of expanding on Cline's (1949) model, Bullock et al. (1974) evaluated the pedogenic processes associated with glossic horizon formation in silty, calcareous (pH > 7.0) Alfisols in New York. Similar to Ranney and Beatty (1969), the primary objective of the study was to evaluate the mechanisms responsible for clay translocation and the formation of albic (degraded) materials within the degrading, clay-enriched zone. To accomplish this, the authors

examined and compared the differences in particle size and clay mineralogy data between the 1) E and Bt horizons and 2) degraded (exterior) and remnant Bt (interior) ped materials along a sequence of degradation in the glossic horizon. Thin-section analysis was also conducted to examine the micromorphology of both degraded and intact portions of the glossic horizon.

According to Bullock et al., particle size data indicated that the formation of the clay-enriched zone was accomplished as a result of pedogenic translocation and accumulation of clay, particularly fine clay. The mobilization and deposition of fine clay in the zone of accumulation was attributed primarily to lessivage, as indicated by relatively uniform K_2O contents in the coarse clay subfraction of the E and Bt horizons (which was dominated by micaceous minerals). The authors suggested that significant differences in the K_2O content of the coarse clay subfraction should be expected if chemical translocation (dissolution and re-synthesis) had been responsible for the increase in clay content in the Bt horizon. Macro- and micro-morphological evidence for clay translocation was also observed in the form of dark brown, laminated, clay coatings on ped surfaces and in pores in the Bt horizon. The authors attributed the dark brown color of the coatings to adsorption of iron oxides (although no particular mechanism for Fe accumulation was discussed). It is worth noting that a "gravelly" textural discontinuity was also observed below the zone of maximum clay accumulation in one of the studied soils.

The authors noted the presence of "sugary coatings" that lacked continuously oriented clay on ped faces, in pores (and root channels), and as tongues surrounding intact illuvial materials in the upper portion of the Bt horizon. They took this morphological evidence to indicate degradation of the clay-enriched zone and subsequent formation of the glossic features. Small, isolated "flakes" of remnant Bt material were commonly observed in degraded (glossic) materials in thin-section, suggesting that the degrading zones had once been zones of clay illuviation. This conclusion was

supported by lower amounts of total clay than any other part of the soil, and that, proportionally, more fine clay had been lost from the degraded materials than any other subfraction. As a result, the degraded zones have very low fine/coarse clay ratios. The degraded coatings were thicker on peds in the upper portion of the degrading zone, indicating that the associated clay loss was proceeding from the ped surfaces inward and downward.

According to Bullock et al., the fine clay lost from the degraded zone had accumulated preferentially as fresh (secondary) cutans in lower (illuvial) Bt horizons. Particle size data indicated that these cutans were composed of between 42-75% total clay; no further mention was given as to the remaining textural composition of these illuvial cutans, however. Indeed, these values indicate that other particle fractions had likely been remobilized in addition to clay. Nevertheless, just as was observed between the E and Bt horizons, similar contents of K_2O and amorphous materials were observed in the coarse clay subfraction between ped exterior and interior materials in the zone of degradation. Again, the authors suggested that significant differences in the contents of K_2O and amorphous material should be expected if chemical decomposition and neoformation had been responsible for the translocation of clay. Thus, similar to Ranney and Beatty (1969), Bullock et al. concluded that degradation of the clay-enriched zone was accomplished primarily via clay loss by lessivage.

5.3.1.4 Summary

Cline's (1949) pedogenic model provided an important conceptual foundation for the occurrence of degraded features in soils with a subsurface accumulation of clay in the upper Great Lakes region. Subsequent work by Ranney and Beatty (1969) and Bullock et al. (1974) expanded on this model, providing physical evidence to better explain the processes responsible for the

formation of such features in fine-textured soils. Based on their findings, degradation was attributed primarily to clay loss from the zone via mechanical remobilization (i.e., lessivage), associated with the gradual downward advancement of the eluvial horizon. Largely lacking from these studies, however, was quantitative explanation for the mechanism by which degradation and associated clay loss is initiated during this degradational process. Subsequent discussion will focus on applicable models previously reported in other regions that may help to explain such phenomenon for the soils under study here.

5.3.2 Other Models of Relevance

5.3.2.1 Model 4: Jamagne et al. (1983)

Jamagne et al. (1983) evaluated the pedogenic processes associated with clay translocation in mildly acidic (pH < 5.6-6.5), silty Alfisols in northern France. The primary objectives of the study to were evaluate the mechanisms responsible for the 1) formation of clay-enriched zones in non-degraded soils and 2) initiation of degradation of the clay-enriched zone in degraded soils that were assumed to be in a later stage of soil evolution. To accomplish the second objective (the focus of discussion here), the authors examined and compared the differences in the chemical and mineralogical composition of the clay fraction between the degraded and adjacent Bt materials in the glossic horizon.

According to Jamagne et al., the presence of bleached "degradation" spots and tongues that lacked continuously oriented clay in the upper portion of the Bt horizon of the glossic soils was taken as evidence for degradation of the clay-enriched zone (and subsequent formation of the glossic horizon). The authors assumed that the illuvial zone had initially formed as a result of co-migration of clay (via lessivage) and iron oxides under well-drained (oxidizing) conditions. CEC

and exchangeable cation data also indicated that the degraded materials had lower base saturation levels, relative to the adjacent Bt materials, although values remained high (60%). The authors suggested that desaturation of the exchange complex alone, therefore, could not explain the onset of degradational processes. Relative to the adjacent Bt materials, the degraded materials contained significantly less "free" iron oxides (5.7% vs. 8.6%). Thus, initiation of clay translocation and subsequent degradation was attributed to the Fe-eluviation from the zone. According to the authors, temporary, localized saturation conditions, formed due to dissimilarity in hydraulic tensions at the texturally contrasting boundary between the E-Bt horizons, had likely facilitated reduction and loss of Fe associated with surface complexed iron oxides. As a result of Fe-eluviation, the remaining "bleached" clays were assumedly destabilized, remobilized out of the zone (although no particular mechanism was discussed), and ultimately redeposited as fresh (secondary) cutans lower in the illuvial zone. Similar to previous authors (Ranney and Beatty, 1969; Bullock et al., 1974), Jamagne et al. concluded that remobilization of clays out of the zone of degradation was accomplished primarily via lessivage, as indicated by mineralogical similarities of clay between degraded and adjacent Bt materials.

5.3.2.2 Model 5: Payton (1993)

In a three-paper series, Payton (1992; 1993a; 1993b) evaluated the pedogenic processes associated with fragipan evolution in acidic (pH < 4.5-6.0), two-storied (loamy-over-gravelly sand) Alfisols in northeastern England. The primary objective of the study was to evaluate the mechanisms responsible for progressive and regressive fragipan development. The final paper in the series (the focus of discussion here) examined the relationship between fragipan degradation and development of glossic features, which tend to form in the upper part of fragipans (Payton

1993b; Lindbo et al., 2000; Weisenborn and Schaetzl, 2005). To accomplish this, Payton examined and compared the differences in the micromorphology (viz. thin-section and SEM analyses) between degraded and intact Btx materials in the degrading zone. Energy dispersive X-ray analysis (EDXRA) was also conducted to examine the chemical composition of both degraded and intact portions of the degrading zone.

According to Payton, the presence of "skeletal surface residues" lacking continuously oriented clay on ped faces, on pore walls, alongside root channels, and as tongues in the upper portion of the Btx horizon was taken as evidence for degradation of the illuvial fragipan zone (and subsequent formation of glossic features). He assumed that the illuvial fragipan horizons had initially formed as a result of co-migration of clay (via lessivage) and iron oxides under well-drained (oxidizing) conditions. Small, isolated "islands" of remnant Bt material were commonly observed in degraded (glossic) materials in thin-section, suggesting that the degrading zones above the fragipan had once been zones of clay illuviation. Further chemical (EDXRA) data revealed that degraded materials contained noticeably less (2% vs. 10%) total iron than adjacent Btx materials. Thus, Payton described a similar process to the one invoked by Jamagne et al. (1983) for the onset of degradation, whereby remobilization of clay and other fragipan materials from the upper boundary of the Btx horizon occurred in response to temporary, localized saturation conditions. The difference now is that these soils have a fragipan, not just a Bt horizon. These conditions facilitated reduction and eluviation of clay associated iron oxides, followed by the destabilization of illuvial coatings. As had previous authors, Payton also suggested that the remobilization of clays out of the zone of degradation was accomplished primarily via lessivage, as indicated by similarities in the K contents of clays (assumed to be associated with illite) within both degraded and adjacent Btx materials. Payton concluded that remobilization of clay out of the

fragipan was accomplished primarily via particle dislodgement by turbulent flow of percolating water (i.e., slaking). This hypothesis was supported by the apparently contemporaneous translocation of fine silt during the degradational process, as indicated by the presence of compound, secondary, illuvial coatings containing both clay and fine silt.

5.3.2.3 Summary

Unlike previous models developed for soils in the upper Great Lakes region (discussed in section 5.3.1), Jamagne et al. (1983) in France and Payton (1993b) in England focused primarily on evaluating the *mechanism* responsible for the initiation of degradation in soils with a subsurface zone of illuvial accumulation. Based on their findings, the onset of degradation was attributed primarily to the chemical reduction and subsequent eluviation of clay-bound Fe from illuvial coatings, following temporary localized saturation conditions that had developed as a result of a decrease in hydraulic conductivity between the texturally contrasting eluvial-illuvial zones. As a consequence of Fe-oxide removal from the coatings, the remaining "bleached" illuvial materials became destabilized, thereby facilitating their remobilization (via micro-erosion) during subsequent percolation events and deposition as secondary – occasionally compound – coatings in the illuvial zone. Although developed from and for soils in Europe, these models describe pedogenic processes that have seemingly significant implications for soils forming under similar conditions in the upper Great Lakes region, including those in this study. Indeed, Weisenborn and Schaetzl (2005) invoked similar processes to infer the cause of illuvial fragipan degradation in some northern Michigan (Upper and Lower Peninsula) soils; such a mechanism has not been observed or suggested for the development of glossic features in soils of this region without a fragipan, however.

5.3.3 New Model of Glossic Horizon Genesis in Michigan

Prior to discussion of the model I have developed for glossic horizon genesis in soils similar those at the study site, it is important to reiterate some key points. First, the foremost goal in developing this model is to provide a more accurate and data-informed explanation for glossic horizon genesis in coarse-loamy soils in Michigan. The need for such a model, as discussed at previous points throughout this thesis, is two-fold: (1) glossic horizon genesis has never been intensively studied in Michigan, and (2) previous, regionally applicable models, nearly all of which date back more than five decades, have not examined glossic horizon genesis in coarse-loamy parent materials. In essence, current theory regarding the development of glossic soils in Michigan with similar characteristics to those in this study is based largely on dated observations from soils forming under different conditions in other regional locales.

In order to more adequately explain glossic horizon genesis in Michigan, the model integrates findings from this study with applicable components of models previously reported in the literature from (1) the upper Great Lakes region, and (2) other locales that help to explain some soil characteristics and processes not addressed by local (regional) models. Used together, these various empirical interpretations provide important insight into (1) the general prerequisite conditions influencing glossic profile development, (2) mechanisms for the formation of the illuvial zone, (3) a mechanism for initiation of degradation of the illuvial zone, and (4) mechanisms for the evolution of glossic expression. The end result is a unifying model that illustrates the most likely scenario for glossic horizon genesis in calcareous coarse-loamy, upland soils in Michigan. Although developed from and for such soils, the model may have, theoretically, wider regional applicability.

5.3.3.1 Prerequisite Conditions

Jenny's (1941) functional-factorial theory posits that the development and properties of soils depends on five primary soil-forming factors: climate, organisms (vegetation), relief (topography), parent material, and time. In essence, a particular combination of these factors, acting as external controls on soil forming (pedogenic) processes, at any given location results in the formation of a discrete body of soil with a specific morphology. Working within this paradigm, several prerequisite conditions, related to both the *active* (climate and organisms) and *passive*[1] (relief and parent material) soil-forming factors, can be identified that likely favor the development of glossic features in Michigan soils. Discussion of these prerequisite conditions provides an important foundation for the model.

For the purpose of simplicity, I have grouped these prerequisite conditions into two general categories: (1) environmental and site conditions and (2) parent materials conditions (listed below). Generally, environmental and site conditions influence the supply and/or regulation of energy entering the soil system, whereas parent material conditions influence the initial state of the soil system to be modified by the various energy inputs.

Environmental and site conditions:

1) Adequate seasonal precipitation inputs (rainfall and/or snowmelt) to facilitate deep infiltration into the mineral soil, at least occasionally;
2) Vegetation that produces primarily acidic litter to facilitate decarbonation and acidification, both of which are necessary for translocation of most pedogenic materials to occur in calcareous soils; and

[1] Although "time" is also considered a *passive* soil forming factor, in and of itself, it does not have a direct control on pedogenesis; rather, it is a control on the duration of which the other factors are considered to be operative. Thus, time was not considered a perquisite condition in this discussion.

3) Well-drained landscape position (i.e., lack of a persistently high water table) to allow for relatively unimpeded vertical water percolation and associated translocation of pedogenic materials to sufficient depth, under oxidizing conditions.

Parent material conditions:

1) An adequate quantity of basic cations (in "free" and/or fixed form) in the parent material to facilitate the deposition of suspended clay minerals in a preferred and continuous zone;
2) An adequate quantity of fine material (i.e., clays and fine silts) in the parent material to facilitate development of a discrete zone of illuvial accumulation;
3) An adequate quantity of iron (in "free" and/or fixed form) in the parent material to facilitate surface complexion with clay minerals; and
4) An adequate quantity of coarser sands (i.e., medium sand and larger) in the parent material to facilitate development of pores and voids in the matrix that allow for both turbulent water flow and translocation of coarser pedogenic materials (i.e., fine silt).

5.3.3.2 Stage I: Development of the Illuvial Zone

Following deposition of the parent material and subsequent activation of pedogenesis, early processes such as melanization, decarbonation, bioturbation, and acidification ensue (Figure 5.14). In coarse-textured parent materials, especially under the presence of vegetation that produces primarily acidic litter, the inherent acid neutralizing capacity of the upper solum declines rapidly (Cline, 1949; Schaetzl, 1996). Under increasingly acidic conditions, lessivage (Ranney and Beatty,

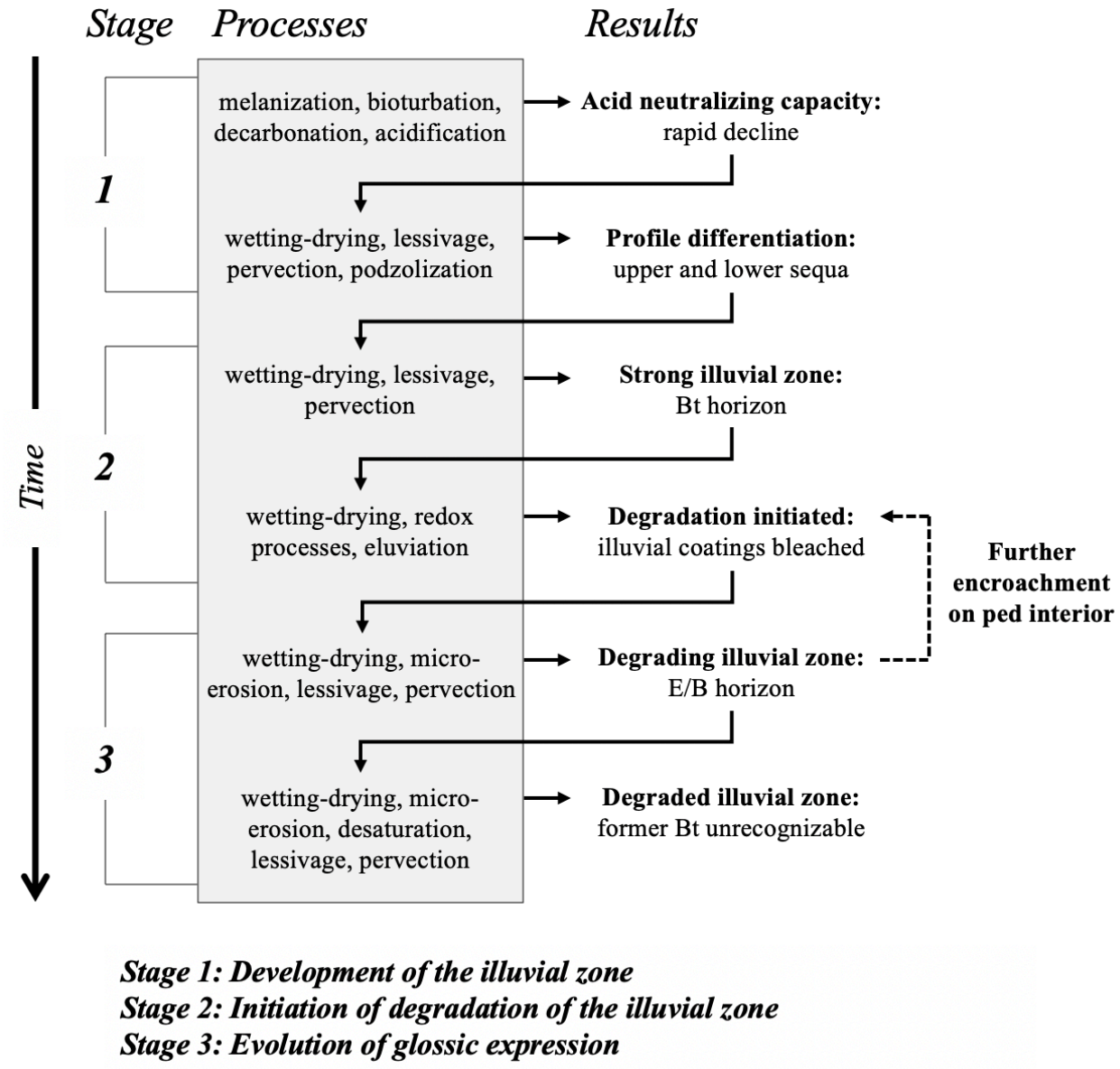

Figure 5.14 Schematic diagram for the presented model of glossic horizon genesis in calcareous coarse-loamy soils of northern Lower Michigan.

1969; Bullock et al., 1974; Schaetzl, 1996), and to a lesser extent, pervection (i.e., silt translocation), are eventually initiated. Likely occurring contemporaneously, "free" iron (Fe) cations, in various forms, derived from the weathering of primary minerals in the parent materials or from decay of litter, are complexed by clay minerals, particularly those in the fine clay fraction. These compounds would be initially immobile because they are forming in a well-aerated soil environment. Textural differentiation in the solum begins around this time, as the mechanical co-migration of clays and fine silts results in the formation distinct eluvial-illuvial (E-Bt) zones (Figure 5.14). Initial deposition of illuvial materials and the formation of a Bt horizon under oxidizing conditions is likely facilitated by an increase in basic cation content (primarily Ca^{2+}) at depth, which generally favors coagulation of discrete particles in the soil solution. The deposition of illuvial materials in the Bt horizon manifests as reddish, compound (i.e., clay- and fine-silt-enriched) cutans that bridge primary grains, line pores, and coat ped faces. Soon thereafter, podzolization is initiated in the upper solum (via fulvic-add formation followed by chelation and cheluviation), leading to development of bisequal horizonation (Schaetzl, 1996; Bockheim, 2003; Weisenborn and Schaetzl, 2005).

As time progresses, continued wetting-drying cycles and associated pedogenic processes (i.e., decarbonization, acidification, and lessivage) facilitate the gradual downward advancement and thickening of the illuvial zone into fresh parent material. The solum thickens and the textural and pH differentiation between the upper and lower sequa becomes increasingly apparent and marked (Figure 5.14). The presence of a fine-over-coarse textural break at depth may pause and/or delay the downward advancement of the illuvial zone, however. Differences in hydraulic tensions force the wetting front to be "hang" at the interface between the two texturally contrasting materials, leading to preferential deposition and accumulation of pedogenic materials during

subsequent desiccation (Bartelli and Odell, 1960; Khakural et al., 1993; Schaetzl, 1996; Schaetzl, 1998). Progressive textural-fining in the upper (finer) material generates a temporary positive feedback loop that fosters increasingly greater dissimilarity in hydraulic tensions between the two materials, and thus, enhanced deposition in the zone of illuviation.

5.3.3.3 Stage II: Initiation of Degradation of the Illuvial Zone

As the illuvial expression of the Bt horizon increases, the porosity of the zone is gradually diminished. As a result, the Bt horizon becomes increasingly effective as an internal drainage impediment, eventually acting as an aquitard during seasonally wet periods (Figure 5.14), likely most notably during spring snowmelt (Schaetzl and Isard, 1991; Schaetzl et al., 2015). A threshold is ultimately reached when the duration of temporary, localized episaturation at and/or near the upper boundary of the Bt horizon is long enough to incite chemical reduction of iron oxides due to anoxia (i.e., lack of oxygen). At this point, reduction of "free" iron oxides, many of which may be physically or chemically bound (i.e., complexed) to illuvial clays, is favored (Jamagne et al., 1983; Payton, 1993b). Under reducing conditions, Fe in various forms becomes mobile and soluble, leaving it potentially susceptible to eluviation, resulting in the bleaching and subsequent destabilization of associated illuvial coatings (Figure 5.14). The destabilized particles remaining in the illuvial coatings (i.e., clay and fine silt) become vulnerable to remobilization during subsequent percolation events, thereby inciting the initiation of degradation of the Bt horizon and associated formation of glossic features. Thus, in the degrading portion of the Bt horizon, processes associated with the development of glossic features gradually become dominant over those associated with further illuvial development.

5.3.3.4 Stage III: Evolution of Glossic Expression

Either occurring contemporaneously with, or immediately following, eluviation of Fe oxides, fine clays are preferentially remobilized from the degrading zone. Thus, glossic features manifest first (morphologically) as thin "bleached" eluvial rinds, largely depleted of Fe and fine clay, on ped margins. With each subsequent percolation event, fresh, discrete zones of degradation gradually encroach deeper into the Bt horizon and farther into peds along the most permeable conduits (e.g., between peds and along macropore flowpaths and root channels) (Bullock et al., 1974). In coarse-textured parent materials, glossic features may lack distinct form and orientation (i.e., tongues), as is typically observed in finer-textured soils (Ranney and Beatty, 1969; Bullock et al., 1974). Instead, in coarse-loamy soils like the ATL pedons, clay and Fe oxides can be mobilized from areas in the Bt horizon that may not initially appear as ped faces or large pores, due to the inherently dense network of flowpaths and conduits. Thus, degradation appears more "random" than in finer-textured soils, where the initial stages of degradation are focused along ped faces.

As pedogenic development in the degraded zone gradually progresses into the intermediate stage, eluvial rinds on peds become thicker and coarser in texture as micro-erosion and remobilization of "bleached", destabilized, pedogenic materials, mainly coarse, low activity (as indicated by low CEC values) clays and to a lesser extent, fine silts, is initiated. Remobilization of the destabilized particles is likely accomplished primarily via dislodgement by turbulent flow of percolating water (i.e., slaking) (Payton, 1993b). Although acidification is simultaneously ongoing, as indicated by slight losses in total calcium (Table 5.3), base saturation values of 100% suggest that loss of calcium from the degrading zone likely has little influence on particle remobilization at this stage. This is assumedly due to the decrease in total charge of the degrading

materials related to further textural coarsening. Some of the pedogenic materials lost from degrading zones may illuviate to the remaining intact (remnant) portion (B part) of associated ped interiors, thereby further facilitating the occurrence of localized saturation conditions and Fe-redox processes at the boundary between degrading and intact materials during subsequent percolation events. With time, differentiation (i.e., glossic expression) in the degrading eluvial-illuvial transition zone becomes well enough expressed that a glossic horizon is formed.

As degradation progresses into the advanced stages, the increasingly coarse-textured eluvial rinds, due to further loss of coarse clay and fine silt, eventually become the dominant component of the ped matrix. Particle remobilization from degrading zones at this stage likely remains accomplished primarily via slaking, although acidification may become of greater importance due to the further loss of calcium from the zone (Table 5.3). Additional base saturation data is needed to confirm this hypothesis, however. The only remaining visual evidence of the former Bt horizon at this stage is small remnant (intact) microzones where illuvial development has been particularly strong due to the remobilization of pedogenic materials further into the ped interior. These microzones (where present) contain more clay and fine silt than any other location in the profile, and thus, are seemingly the most resistant portion of the ped to encroaching degradation and likely persist the longest. However, even these microzones are eventually remobilized as degradational processes continue to further into the ped matrix. Further loss of calcium from the zone and an increase in exchangeable acidity indicates that acidification, although seemingly remaining subordinate to slaking, becomes of greater importance at the final stages of degradation (Table 5.2; Table 5.3). Once the former Bt horizon becomes completely degraded, it no longer retains any of its former illuvial character (Figure 5.14). With time, the completely degraded “zone” becomes thicker and more contiguous, until ultimately, it is no longer

considered a component of the glossic horizon and is designated as an E or E' horizon, according to the broader profile morphology.

The pedogenic materials ultimately lost during the degradational process are translocated downward, where they are deposited as fresh, compound cutans (i.e., silty argillans) in the subjacent Bt horizon (Jamagne et al., 1983; Payton, 1993b). Under this degradational scenario, the soil might be seen as maintaining its original, predominant pedogenic pathway, whereby the eluvial zone gradually advances downward and thickens, just as the illuvial zone advances downward and thickens (Cline, 1949; Ranney and Beatty, 1969; Bullock et al., 1974). In soils where a textural or lithologic change (subtle or obvious) occurs below the Bt1 horizon, however, such as those in this study, the eluvial zone may gradually thicken at the expense of the underlying illuvial zone. In essence, the discontinuity may act as an impediment to the vertical advancement pedogenic processes, thereby restricting soil development (partially or completely) to overlying horizons. Thus, the Bt horizon, while simultaneously acquiring materials from the associated advancing eluvial zone and thereby becoming more strongly expressed, may gradually decrease in thickness.

CHAPTER 6

SUMMARY

Coarse-loamy soils with glossic horizons have not been extensively studied in the upper Great Lakes region, and thus, questions remain regarding their genesis. As a first step toward resolving this problem, I examined glossic horizon development in two calcareous coarse-loamy, bisequal soils in northeastern Lower Michigan. The specific objectives of this thesis research were to: (1) identify and characterize two coarse-loamy textured soils, each of which contains a glossic diagnostic horizon; (2) use data collected from these soils to infer glossic horizon genesis; and (3) evaluate findings in light of applicable conceptual models of glossic horizon genesis that have been previously reported in the literature in order to develop a new model – one that integrates existing models and findings from this study.

The two soils chosen for study are located in central Montmorency County and mapped within the Millersburg series (Coarse-loamy, mixed, active, frigid Haplic Glossudalfs). The soils (1) have a cool, humid continental climatic regime (Köppen Dfb), (2) have formed primarily under pine dominated, mixed coniferous-deciduous forest, (3) are located on a relatively stable well-drained, upland position of a glacigenic (dissected till plain) landform, and (4) have formed in calcareous, coarse-loamy till of Port Huron age (≈15,500 cal yr B.P). Both soils have typical bisequal horizonation for coarse-loamy textured soils in the area, with weakly expressed spodic-like (E-Bs) horizon sequences overlying alfic (E/B-Bt) horizon sequences that show evidence of a transitional zone of degradation (i.e., glossic horizon) in their upper portion. The glossic (E/B) horizon is largely dominated by irregular, discontinuous eluvial (albic) bodies that envelop illuvial materials in the upper portion of the once intact and much thicker Bt horizon.

The soils were described and sampled in the field according to standard methods. In addition to bulk genetic horizon samples, special samples were also taken from within the glossic horizon in order to capture the sequence by which discrete soil units (peds) evolve throughout the degradational process. Special samples were classified and separated into five distinct groups along the degradational sequence, ranging from non-degraded to completely degraded. Subsequent laboratory examination was conducted to characterize the physical and chemical properties of both the bulk genetic horizon and special samples. Physical characterization consisted of particle-size analysis (PSA) and bulk density determinations; chemical characterization consisted of soil reaction (pH), organic carbon (SOC), geochemistry, and cation exchange capacity (CEC) and extractable bases determinations. General morphological characterization was also conducted on intact peds from select groups within the degrading zone using low-magnification binocular microscopy.

Overall, the soils are dominated by sand, particularly medium and fine sands, with lesser components of silt and clay. Generally, textures in the upper sequum (E-Bs1-Bs2) horizons range from sand (E horizon) to loamy sand (Bs horizons), whereas textures in the lower sequum (E/B-Bt1-Bt2-BCt) horizons are sandy loam. Finer-textures in the lower sequum, particularly in the Bt1 horizon, are associated with the translocation and accumulation of clay and silt, particularly fine silt. Bulk density values generally reflect the vertical distribution of fine materials and distance from the soil surface, with higher values occurring in the lower sequum, with the exception of the Bt2 “stone zone” horizon, which has a noticeably low bulk density due to containing a high concentration of coarse fragments. This textural break, albeit subtle, has likely helped to facilitate enhanced expression in the Bt1 horizon by occasionally causing water to “hang” at its upper boundary and deposit illuvial materials.

Soil reaction (pH) values are also generally reflective of depth with in the sola, with acidic values occurring in the upper sequum horizons and neutral to alkaline values occurring in the lower sequum horizons. Overall, the observed trends in pH are associated primarily with calcium content, which decrease predictably with proximity to the soil surface. Increases in both Fe and SOC occur in the illuvial zones of both sequa, most notably in the Bs1 and Bt1 horizons (i.e., locations of maximum illuvial accumulation), relative to their associated eluvial zone. The increase in Fe is more prominent in the Bt1 horizon, however, due to it being translocated contemporaneously with clays during the initial development of the zone. Conversely, the increase in SOC is more prominent in the Bs1 horizon due to active podzolization in the upper sequum. Given the higher concentration of negatively charged particles (i.e., clays and/or organic matter) associated with illuvial accumulation, CEC and exchangeable cation values are also highest in the Bt1 and Bs1 horizons. These values are notably higher in the Bt1 horizon, however, given the greater content and accumulation of clay in this horizon.

The glossic (E/B) horizon, occurring at the interface of the upper and lower sequa, generally exhibits a range of characteristics that are intermediate between the two opposing zones. Generally, the intact (remnant) illuvial (Bt) parts of the glossic horizon retain a similar reddish brown color, sandy loam texture, and neutral pH to that of the associated Bt1 horizon. On the other hand, the eluvial (E) parts of the glossic horizon, which become increasingly coarse (via remobilization of clay and fine silt) and depleted of iron and calcium (via reduction and acidification, respectively) at successive stages of degradation, develop a light color, loamy sand texture, and moderately acid pH that is more comparable to that of the overlying Bs2 (formerly an E horizon). Although the illuvial parts of the glossic horizon also retain a similar content of SOC to that of the Bt1 horizon, the eluvial parts have the overall lowest observed content of SOC in the

sola. The gradual textural coarsening and acidification associated with progressive degradation is further reflected by decreasing CEC and exchangeable cation values.

An evaluation of several previously reported models related to the development of glossic features reveals that a combination of models best explains the many observed properties in the glossic horizons of the two soils. The Fe-reduction mechanism for the initiation of degradation proposed by Jamagne et al. (1983) and Payton (1993b) and the mechanical remobilization mechanism for subsequent evolution of glossic expression proposed by Ranney and Beatty (1969) and Bullock et al. (1974) were integrated with my findings to provide the foundation for a modern and data informed explanation of glossic horizon genesis in calcareous, coarse-loamy soils in Michigan.

The model involves the acidification of a calcareous parent material, followed by mechanical translocation of clay (and associated Fe-oxides) and fine silt to a preferred (illuvial) zone under oxidizing conditions. The illuvial zone, a Bt horizon, eventually functioning as an aquitard during seasonally wet periods, facilitates temporary localized saturation and change in redox status near its upper boundary. Subsequently, clay-bound Fe compounds are reduced and eluviated from the zone, resulting in the destabilization, degradation, and remobilization of illuvial cutans to form glossic features. The expression of glossic features evolve gradually as a result of micro-erosion and eluviation of clays and fine silts from preferred locations within the degrading zone, the magnitude of which follows a distinct sequence at progressive stages of the degradational process: (1) fine clay and Fe, (2) coarse clay, and finally, (3) fine silt. With time, the glossic character of the degrading zone becomes increasingly pronounced, until ultimately, little to no evidence of the former Bt horizon remains. At this point, Bt horizon morphology has progressed through glossic to an albic horizon. Although developed from and for soils in Michigan, the model

may have, theoretically, wider regional applicability.

In conclusion, this research is the first to provide detailed examination of the processes associated with glossic horizon genesis in Michigan soils. More broadly, it is the first to provide detailed examination of glossic horizon genesis in the upper Great Lakes region in nearly five decades, and furthermore, the first ever in calcareous, coarse-loamy parent materials. Although the primary objective of this work was to develop a modern and data informed model for glossic horizon genesis in the region, in hopes that it may make a valuable contribution to the existing literature, of equal importance was to shed light on a small number of the many potential avenues for future research, in hopes that it may encourage further exploration of these unique pedogenic features in Michigan and the upper Great Lakes region.

APPENDICES

APPENDIX A

PEDON DESCRIPTIONS

Contents:

OFFICIAL SOIL SERIES DESCRIPTION (OSD)

MILLERSBURG SERIES

The Millersburg series consists of very deep, well drained soils formed in sandy and loamy till on ground moraines, disintegration moraines, and drumlins. Slope ranges from 0 to 35%. Mean annual precipitation is about 762 mm, and the mean annual temperature is about 5.6 degrees C.

TAXONOMIC CLASS:
Coarse-loamy, mixed, active, frigid Haplic Glossudalfs

TYPICAL PEDON: Millersburg loamy sand, on a south-facing, convex, 5% slope under mixed hardwoods and conifers at an elevation of 274 meters above mean sea level. (Colors are for moist soil unless otherwise stated.)

A 0 to 5 cm; black (7.5YR 2.5/1) loamy sand, black (7.5YR 2.5/1) dry; moderate medium granular structure; very friable; common fine and very fine and few medium roots; about 1% gravel; extremely acid; abrupt smooth boundary. [5 to 10 cm thick]

E 5 to 13 cm; brown (7.5YR 5/2) sand; pinkish gray (7.5YR 7/2) dry; weak fine subangular blocky structure; very friable; many fine and very fine, and few medium and coarse roots; about 1% gravel; very strongly acid; clear wavy boundary. [5 to 13 cm thick]

Bw 13 to 25 cm; strong brown (7.5YR 4/6) loamy sand; moderate medium subangular blocky structure; very friable; common fine and very fine and few medium and coarse roots; about 2% gravel; strongly acid; clear wavy boundary. [10 to 23 cm thick]

E/B 25 to 46 cm; pale brown (10YR 6/3) sand (E), pinkish gray (7.5YR 7/2) dry; occupies 65% of the horizon surrounding reddish brown (5YR 4/4) sandy loam (Bt); moderate medium subangular blocky structure parting to moderate very fine subangular blocky; very friable; common fine and very fine roots; clay bridging between sand grains; about 4% gravel; very strongly acid; clear irregular boundary. [15 to 38 cm thick]

B/E 46 to 66 cm; reddish brown (5YR 4/4) sandy loam (Bt); occupies about 75% of the horizon surrounded by pinkish gray (7.5YR 7/2) loamy sand (E); moderate medium and coarse subangular blocky structure; Bt part is firm and E part is friable; many fine roots; clay bridging between sand grains; about 4% gravel; slightly acid; clear wavy boundary. [10 to 30 cm thick]

Bt 66 to 86 cm; yellowish red (5YR 4/6) sandy loam; moderate medium and coarse subangular blocky structure; friable; common fine roots; clay bridging between sand grains; about 1% cobbles and 1% gravel; slightly acid; clear broken boundary. [18 to 28 cm thick]

BC 86 to 109 cm; light reddish brown (5YR 6/3) sandy loam; moderate thick platy structure inherent from deposition; friable; few fine roots; clay films around gravel and clay bridging between sand grains; about 1% gravel; strongly effervescent; slightly alkaline; clear wavy boundary. [0 to 25 cm thick]

C 109 to 203 cm; light yellowish brown (10YR 6/4) loamy sand; single grain; loose; few yellowish brown (10YR 5/4) sand lenses about 5 cm (2 inches) long and 19 mm thick; few fine roots; about 12% gravel; violently effervescent; moderately alkaline.

TYPE LOCATION: Montmorency County, Michigan; 569 m north and 101 m west of the southeast corner of sec. 2, T. 32 N., R. 2 E., west central part Montmorency Township; USGS Lake Geneva, Michigan 7.5 minute topographic quadrangle; lat. 45 degrees 11 minutes 24 seconds N. and long. 84 degrees 8 minutes 44 seconds W., NAD 27.

RANGE IN CHARACTERISTICS:
Depth to carbonates: 76 to 152 cm
Thickness of the sand or loamy sand mantle: 28 to 50 cm
Depth to the glossic horizon: 25 to 51 cm
Sandy mantle above the glossic horizon (A, E and Bw horizons): contains 2 to 12% clay and more than 50% sand coarser than very fine sand
Series control section: 0 to 5% cobbles and 0 to 14% gravel; average 1 to 15% total rock fragments
Argillic horizon: averages between 8 to 18% clay; individual subhorizons may range up to 22% clay

GEOGRAPHIC SETTING: The Millersburg soils are on ground moraines, disintegration moraines, and drumlins of Wisconsinan age. Slope gradients are dominantly 2 to 35% but range from 0 to 35%. Millersburg soils formed in sandy and loamy till. Mean annual precipitation ranges from 711 to 914 mm. Mean annual temperature ranges from 4.4 to 6.7 degrees C. Frost-free period ranges from 80 to 110 days.

DRAINAGE AND SATURATED HYDRAULIC CONDUCTIVITY: Well drained. Potential for surface runoff is negligible to high, depending on slope gradient. Saturated hydraulic conductivity is moderately high. Permeability is moderate.

DISTRIBUTION AND EXTENT: MLRAs 94A and 96 in the northern Lower Peninsula of Michigan. The series is of moderate extent.

SERIES ESTABLISHED: Montmorency County. Michigan, 1992.

REMARKS: Diagnostic horizons and features recognized in this pedon are:
Ochric epipedon: from the surface to a depth of 13 cm (A and E horizons).
Albic horizon: from a depth of 5 to 13 cm (E horizon).
Glossic horizon: from a depth of 25 to 66 cm (E/B and B/E horizons).
Argillic horizon: from a depth of 46 to 86 cm (Bt part of B/E horizon and Bt horizon).

KLACKING SERIES

The Klacking series consists of very deep, well drained soils formed in sandy and loamy deposits on outwash plains, kames, kame moraines, and moraines. Slope ranges from 0 to 70%. Mean annual precipitation is about 762 mm, and mean annual temperature is about 6.6 degrees C.

TAXONOMIC CLASS: Loamy, mixed, semiactive, frigid Arenic Glossudalfs

TYPICAL PEDON: Klacking sand, on a 13% slope in a wooded area. (Colors are for moist soil unless otherwise stated.)

A 0 to 5 cm; black (10YR 2/1) sand; dark grayish brown (10YR 4/2) dry; weak fine granular structure; very friable; many fine and common medium roots; strongly acid; abrupt smooth boundary. [3 to 10 cm thick]

Bw1 5 to 31 cm; yellowish brown (10YR 5/8) sand; weak fine granular structure; very friable; many fine and medium and common coarse roots; about 7% gravel; strongly acid; clear wavy boundary.

Bw2 31 to 61 cm dark yellowish brown (10YR 4/6) sand; weak fine granular structure; very friable; many fine and common medium roots; about 9% gravel; slightly acid; clear wavy boundary.

Bw3 61 to 86 cm yellowish brown (10YR 5/6) sand; weak fine granular structure; very friable; common medium and few fine roots; about 11% gravel; slightly acid; clear irregular boundary. [Combined thickness of the Bw horizon is 38 to 81 cm (15 to 32 inches).]

E&Bt 86 to 112 cm; yellowish brown (10YR 5/4) sand (E) and lamellae of strong brown (7.5YR 4/6) loamy sand (Bt); weak fine subangular blocky structure; very friable; few fine and medium roots; about 9% gravel; slightly acid; abrupt irregular boundary. [18 to 76 cm thick]

B/E 112 to 203 cm; 60 % strong brown (7.5YR 4/6) sandy loam (Bt) surrounded by light yellowish brown (10YR 6/4) sand (E); moderate medium subangular blocky structure; friable; few fine and medium roots; about 6% gravel; neutral.

TYPE LOCATION: Ogemaw County, Michigan; about 3 miles north of Lupton; 2,400 feet north and 1,500 feet east of the southwest corner of sec. 7, T. 24 N., R. 4 E., Goodar Township; USGS South Branch topographic quadrangle; lat. 44 degrees 29 minutes 12 seconds N. and long. 84 degrees 00 minutes 03 seconds W.

RANGE IN CHARACTERISTICS:
Thickness of the solum: 89 to greater than 203 cm
Rock fragment content: 0 to 15% throughout

GEOGRAPHIC SETTING: Klacking soils are on outwash plains, kames, kame moraines, and moraines. Slope ranges from 0 to 70%. The Klacking soils formed in sandy and loamy deposits. Mean annual precipitation ranges from 711 to 813 cm. Mean annual temperature ranges from 6.1 to 8.3 degrees C.

DRAINAGE AND SATURATED HYDRAULIC CONDUCTIVITY: Well drained. The potential for surface runoff is low or medium. Saturated hydraulic conductivity is high or moderately high.

DISTRIBUTION AND EXTENT: MLRAs 94A, 94C, and 98 in the northern part of lower Michigan. This series is of large extent.

SERIES ESTABLISHED: Ogemaw County, Michigan 1987.

REMARKS: Diagnostic horizons and features recognized in this pedon are:
Ochric epipedon: from the surface to a depth of 5 cm (A horizon).
Argillic horizon: from a depth of 86 to 203 cm (Bt part of E and Bt horizon and B/E horizon).
Glossic horizon: from a depth of 112 to 203 cm (B/E horizon).

GRAYCALM SERIES

The Graycalm series consists of very deep, somewhat excessively drained soils formed in sandy glaciofluvial deposits on moraines, kames, stream terraces, outwash plains, and glacial drainage channels. Slope ranges from 0 to 70%. Mean annual precipitation is about 760 mm, and mean annual temperature is about 6.7 degrees C.

TAXONOMIC CLASS: Isotic, frigid Lamellic Udipsamments

TYPICAL PEDON: Graycalm sand, on a 1% slope on an outwash plain in a forested area at an elevation of about 340 meters above mean sea level. (Colors are for moist soil unless otherwise stated.)

A 0 to 8 cm; very dark brown (10YR 2/2) sand, very dark grayish brown (10YR 3/2) dry; moderate medium granular structure; very friable; many fine roots; very strongly acid; clear wavy boundary. [2 to 13 cm thick]

Bw1 8 to 15 cm; brown (7.5YR 4/4) sand; weak fine granular structure; very friable; common fine roots; strongly acid; clear irregular boundary. [8 to 30 cm thick]

Bw2 15 to 33 cm; strong brown (7.5YR 5/6) sand; weak fine granular structure; very friable; few fine roots; moderately acid; gradual wavy boundary. [0 to 30 cm thick]

Bw3 33 to 56 cm; yellowish brown (10YR 5/6) sand; single grain; loose; few fine roots; slightly acid; gradual wavy boundary. [0 to 25 cm thick]

E 56 to 89 cm; light yellowish brown (10YR 6/4) sand; single grain; loose; very few fine roots; slightly acid; abrupt broken boundary. [0 to 64 cm thick]

E&Bt 89 to 152 cm; light yellowish brown (10YR 6/4) sand (E); single grain; loose; lamellae of brown (7.5YR 5/4) and reddish brown (5YR 5/4) loamy sand (Bt); weak very fine to medium subangular blocky structure; friable; lamellae are 6 mm to 5 cm in thickness with a total accumulation of 13 cm; about 5% gravel; slightly acid.

TYPE LOCATION: Clare County, Michigan; about 2310 feet west and 700 feet north of the southeast corner of sec. 6, T. 20 N., R. 4 W., Frost Township; USGS Cooperton, Michigan topographic quadrangle; lat. 44 degrees 8 minutes 55 seconds N. and long. 84 degrees 50 minutes 17 seconds W., NAD 27.

RANGE IN CHARACTERISTICS:
Depth to the first lamella: 64 to 122 cm
Depth to carbonates: 127 to greater than 203 cm
Content of rock fragments: 0 to 14% gravel and 0 to 3% cobbles throughout the profile
Series control section, 0 to 152 cm: averages 20 to 50 percent fine sand and very fine sand
Mean annual soil temperature: 4.4 to 8.3 degrees C

Other features: Typical pedon has an average sand distribution of about 55% medium sand, 26% fine sand, 16% coarse sand, 2% very coarse sand, and 1% very fine sand

GEOGRAPHIC SETTING: Graycalm soils are on moraines, kames, stream terraces, outwash plains, and glacial drainage channels of Wisconsinan age. Slope ranges from 0 to 70%. Graycalm soils formed in sandy glaciofluvial deposits. Mean annual precipitation ranges from 686 to 813 mm. Mean annual temperature ranges from 3.3 to 8.3 degrees C. Frost-free period is 90 to 150 days. Elevation is 183 to 396 meters above mean sea level.

DRAINAGE AND SATURATED HYDRAULIC CONDUCTIVITY: Somewhat excessively drained. Potential for surface runoff is negligible to low depending on slope. Saturated hydraulic conductivity is high.

DISTRIBUTION AND EXTENT: MLRAs 57, 88, 90A, 90B, 93A, 94A, 94C, 96, and 98 in the central and northern part of Lower Michigan, north-central part of Minnesota, and northern Wisconsin. The type location is in MLRA 94A. The series is of large extent.

SERIES ESTABLISHED: Clare County, Michigan, 1977.

REMARKS: Diagnostic horizons and features recognized in this pedon are:
Ochric epipedon: from the surface to a depth of 8 cm (A horizon).
Lamellic feature: cumulative thickness of lamellae in the E and Bt horizon is 13 cm; within 203 cm, total lamellae thickness is less than 15 cm.

SOIL PFOFILE DESCRIPTION SHEET

Figure A.1. Form used to record soil profile data in the field.

Site name _____ Sample bag ID or abbreviation _____

Location _____

Date _____ Slope at pit (%) _____ Drainage Class _____ Aspect _____

Vegetation at site _____

Slope element _____ Landform type _____

Parent material (stratigraphy if appropriate) _____

Quadrangle _____ Erosion? _____

Water table (cm) _____ Evidence of bioturbation? _____

HOR	Depth	Color (m)	Structure			Consistence		Texture	Boundary		Coarse	Other
			grade	size	shape	H2O	feel		dist	topo	(%)	
											gr co	
											gr co	
											gr co	
											gr co	
											gr co	
											gr co	
											gr co	
											gr co	
											gr co	

PEDON DESCRIPTIONS

ATL Pedons

Taxonomic subgroup: Haplic Glossudalfs
Date: June 2019
Described and sampled by: Christopher Baish and Randall Schaetzl

Table A.1. Geographic setting description of the ATL-1 pedon.

Site name: ATL	**Soil survey:** Montmorency County, Michigan (Purkey, 2013)
Location: Atlanta State Forest – Briley Township, Michigan	
Landform: Dissected till upland; Atlanta Channel Uplands (Burgis, 1977), Northern Lower Peninsula Tunneled Uplands (Schaetzl et al., 2013)	
Parent material: Glacial till	**Aspect:** North
Slope element: Backslope (concave)	**Slope (%):** 4%
Drainage class: Well-drained	**Water table (cm):** None detected
Bioturbation: None detected	**Erosion:** None detected
Vegetation: quaking aspen (*Populus tremuloides*), northern red oak (*Quercus rubra*), red maple (*Acer rubrum*), black cherry (*Prunus serotina*), white pine (*Pinus strobus*), paper birch (*Betula papyrifera*)	
Effervescence: BC horizon, weakly effervescent; C horizon, strongly effervescent	

USGS 7.5-minute topographic quadrangle: Atlanta, Michigan; Montmorency County; 2017
Location: SE 1/4, SE 1/4, Section 13, T31N, R2E, Briley Township, Montmorency County, Michigan
Geographic coordinates: 45°04'29.8"N 84°08'00.1"W
Elevation (asl): 312 m
Directions to pedon: from the City of Atlanta, head north on M-33 for ≈4 km, then turn right onto Scenic Route 1 and head east for ≈3 km, then turn left onto Stevens Spring Road and head north for ≈4 km; the pit is about 100 m east of Stevens Spring Road and is accessible via a former logging road
Property owner (as of 2020): the study site is part of the Atlanta State Forest, owned by the State of Michigan and managed by the Michigan Department of Natural Resources (DNR)

ATL-1 description

Oi 0-1 cm (<1 inch); slightly decomposed forest litter (mixture of hardwood leaves, pine needles and sticks)

Oa 1-7 cm (1-3 inches); black (7.5YR 2.5/1); highly decomposed plant material; very strongly acid; abrupt smooth boundary.

E 7-14 cm (2 to 5 inches); pinkish gray (7.5YR 6/2) sand, brown (7.5YR 5/2) moist; weak fine subangular blocky structure; very friable; about 5 percent gravel; strongly acid; clear wavy boundary.

Bs1 14-25 cm (5 to 10 inches); brown (7.5YR 5/4) loamy sand, strong brown (7.5YR 4/6) moist; weak fine and medium subangular blocky structure; very friable; about 5 percent gravel; strongly acid; clear wavy boundary.

Bs2 25-42 cm (10 to 13 inches); light brown (7.5YR 6/4) loamy sand, strong brown (7.5YR 5/6) moist; weak fine and medium subangular blocky structure; very friable; about 5 percent gravel; moderately acid; gradual wavy boundary.

E/B 42-58 cm (13 to 23 inches); pinkish gray (7.5YR 7/2) loamy sand (E), light brown (7.5YR 6/3) moist; occupies 75 percent of the horizon surrounding reddish brown (5YR 5/4) sandy loam (Bt), reddish brown (5YR 4/4) moist; moderate fine and medium subangular blocky structure; friable; clay bridging between sand grains; about 5 percent gravel; clear wavy boundary.

Bt1 58-72 cm (23 to 28 inches); reddish brown (5YR 5/4) sandy loam, reddish brown (5YR 4/4) moist; moderate fine and medium subangular blocky structure; friable; clay bridging between sand grains; about 5 percent gravel; neutral; clear broken boundary.

Bt2 72-95 cm (28 to 37 inches); yellowish red (5YR 5/6) sandy loam, yellowish red (5YR 4/6) moist; moderate fine and medium subangular blocky structure; friable; clay bridging between sand grains; about 20 percent cobbles and 35 percent gravel; slightly alkaline; gradual wavy boundary.

BCt 95-123 cm (37 to 48 inches); light reddish brown (5YR 6/3) sandy loam; brown (7.5YR 5/4) moist; moderate fine and medium subangular blocky structure; friable; clay bridging between sand grains; about 5 percent cobbles and 10 percent gravel; moderately alkaline; strongly effervescent; gradual broken boundary.

C 123-165+ cm (48 to 65+ inches); light gray (10YR 7/2) loamy sand; brown (10YR 5/3) moist; moderate medium platy structure; friable; about 5 percent cobbles and 10 percent gravel; strongly alkaline; violently effervescent.

ATL-2 description

Oi 0-1 cm (<1 inch); slightly decomposed forest litter (mixture of hardwood leaves, pine needles and sticks)

Oa 1-7 cm (1-3 inches); black (7.5YR 2.5/1); highly decomposed plant material; very strongly acid; abrupt smooth boundary.

E 7-14 cm (2 to 5 inches); pinkish gray (7.5YR 6/2) sand, brown (7.5YR 5/2) moist; weak fine subangular blocky structure; very friable; about 5 percent gravel; strongly acid; clear wavy boundary.

Bs1 14-24 cm (5 to 9 inches); brown (7.5YR 5/4) loamy sand, strong brown (7.5YR 4/6) moist; weak fine and medium subangular blocky structure; very friable; about 5 percent gravel; strongly acid; clear wavy boundary.

Bs2 24-56 cm (9 to 22 inches); light brown (7.5YR 6/4) loamy sand, strong brown (7.5YR 5/6) moist; weak fine and medium subangular blocky structure; very friable; about 5 percent gravel; moderately acid; gradual wavy boundary.

E/B 56-74 cm (22 to 29 inches); pinkish gray (7.5YR 7/2) loamy sand (E), light brown (7.5YR 6/3) moist; occupies 75 percent of the horizon surrounding reddish brown (5YR 5/4) sandy loam (Bt), reddish brown (5YR 4/4) moist; moderate fine and medium subangular blocky structure; friable; clay bridging between sand grains; about 5 percent gravel; clear wavy boundary.

Bt1 74-81 cm (29 to 32 inches); reddish brown (5YR 5/4) sandy loam, reddish brown (5YR 4/4) moist; moderate fine and medium subangular blocky structure; friable; clay bridging between sand grains; about 5 percent gravel; neutral; clear broken boundary.

Bt2 81-98 cm (32 to 39 inches); reddish brown (5YR 5/4) sandy loam, reddish brown (5YR 4/4) moist; moderate fine and medium subangular blocky structure; friable; clay bridging between sand grains; about 15 percent cobbles and 25 percent gravel; slightly alkaline; gradual wavy boundary.

BCt 98-123 cm (39 to 48 inches); reddish brown (5YR 5/3) sandy loam; brown (7.5YR 4/4) moist; moderate fine and medium subangular blocky structure; friable; clay bridging between sand grains; about 5 percent cobbles and 10 percent gravel; moderately alkaline; strongly effervescent; gradual irregular boundary.

C 123-140+ cm (48 to 55+ inches); light gray (10YR 7/2) loamy sand; brown (10YR 5/3) moist; moderate medium platy structure; friable; about 5 percent cobbles and 10 percent gravel; strongly alkaline; violently effervescent.

Table A.2. Diagnostic soil characteristics and horizons in the ATL-1 and ATL-2 pedons.

		ATL-1	ATL-2
Diagnostic soil characteristics			
Albic Materials		E; E part of E/B	E; E part of E/B
Diagnostic horizons			
Surface	Ochric epipedon	Oi; Oa; E	Oi; Oa; E
Subsurface	Albic	E	E
	Argillic	E/B; Bt1; Bt2; BCt	E/B; Bt1; Bt2; BCt
	Glossic	E/B	E/B

Notes to Table A.2:
Diagnostic soil characteristics and horizons are defined according to particular morphological, physical, and/or chemical criteria, as described in *Soil Taxonomy* (Soil Survey Staff, 2014).

APPENDIX B

LABORATORY DATA: PHYSICAL

Contents:

Table B.1. Particle-size conversion chart for Malvern data.

Particle size	USDA	Malvern
fine clay	0 - 1 um	0 - 1 um
coarse clay	1 - 2 um	1 - 8 um
fine silt	2 - 20 um	8 - 25 um
coarse silt	20 - 50 um	25 - 50 um
very fine sand	50 - 125 um	50 - 125 um
fine sand	125 - 250 um	125 - 250 um
medium sand	250 - 500 um	250 - 500 um
coarse sand	500 - 1000 um	500 - 1000 um
very coarse sand	1000 - 2000 um	1000 - 2000 um

Table B.2. Data from the modified Uniformity Value (UV) and Comparative Particle Size Distribution (CPSD) indices designed to show lithologic discontinuities, based on clay- and fine silt-free particle size data.

HOR	UV [a]	CPSD [b]
ATL-1 Pedon		
E-Bs1	0.06	94
Bs1-Bs2	-0.10	92
Bs2-E/B	-0.11	97
E/B-Bt1	0.17	88
Bt1-Bt2	-0.04	91
Bt2-BCt	0.01	88
BCt-C	0.13	95
ATL-2 Pedon		
E-Bs1	-0.01	97
Bs1-Bs2	-0.09	96
Bs2-E/B	0.01	94
E/B-Bt1	-0.09	90
Bt1-Bt2	-0.04	90
Bt2-BCt	0.00	92
BCt-C	0.25	97

Notes to Table C.3:
UV [a] – Modified UV index using the medium sand subfraction (Cremeens and Mokma, 1986)
CPSD [b] – Cumulative Particle Size Distribution (CPSD) index (Langhor et al., 1976)

Table B.3. Bulk density data for the ATL-1 pedon.

HOR	Oven-dry soil mass (g)	Rock fragment mass (g)	Soil bulk density (g/cm^3)	Mean soil bulk density (g/cm^3)	Mean rock fragment content (mass %)
ATL-1 Pedon					
E-Bs1[1]	442.87	30.48	1.22	1.29	5
E-Bs1 [2]	481.05	13.05	1.36		
Bs2 [1]	530.61	20.62	1.49	1.40	8
Bs2 [2]	487.44	57.42	1.31		
E/B [1]	521.71	17.75	1.47	1.47	3
E/B [2]	523.43	18.52	1.48		
Bt1 [1]	527.38	10.22	1.50	1.47	3
Bt1 [2]	512.89	19.04	1.44		
2Bt2 [1]	396.05	165.51	0.80	0.68	50
2Bt2 [2]	355.58	207.78	0.55		
3BCt [1]	548.70	25.83	1.54	1.53	4
3BCt [2]	537.02	18.58	1.52		
3C [1]	545.27	45.50	1.51	1.55	9
3C [2]	583.50	60.53	1.60		

Notes to Table B.3:
[1] = Sample 1
[2] = Sample 2

APPENDIX C

LABORATORY DATA: CHEMICAL

Contents:

Table C.1. Soil pH data for the ATL-1 and ATL-2 pedons.

HOR	1:1 pH	Reaction Class
ATL-1 Pedon		
Oa	4.9	Very strongly acid
E	5.2	Strongly acid
Bs1	5.5	Strongly acid
Bs2	5.8	Moderately acid
E/B	6.3	Slightly acid
E part	6.0	Moderately acid
B part	7.1	Neutral
Bt1	7.2	Neutral
Bt2	7.8	Slightly alkaline
BCt	8.1	Moderately alkaline
C	8.6	Strongly alkaline
ATL-2 Pedon		
Oa	4.7	Very strongly acid
E	4.5	Very strongly acid
Bs1	5.3	Strongly acid
Bs2	5.5	Strongly acid
E/B	5.9	Moderately acid
Bt1	7.1	Neutral
Bt2	7.5	Slightly alkaline
BCt	7.9	Moderately alkaline
C	8.6	Strongly alkaline

Notes to Table C.1:
pH reaction classes as defined by the USDA (Soil Survey Staff, 2017)

Table C.2. Soil organic carbon data for the ATL-1 and ATL-2 pedons.

HOR	Organic matter (g kg $^{-1}$)	Organic carbon [1] (g kg $^{-1}$)	Organic carbon [2] (g kg $^{-1}$)	Organic matter (%)	Organic carbon [3] (%)	Organic carbon [4] (%)
ATL-1 Pedon						
E	11.3	6.5	5.6	1.1	0.7	0.6
Bs1	21.5	12.5	10.8	2.2	1.2	1.1
Bs2	11.6	6.7	5.8	1.2	0.7	0.6
E/B	9.6	5.5	4.8	1.0	0.6	0.5
E part	3.1	1.8	1.6	0.3	0.2	0.2
B part	16.5	9.5	8.2	1.6	1.0	0.8
Bt1	18.4	10.7	9.2	1.8	1.1	0.9
Bt2	9.0	5.2	4.5	0.9	0.5	0.4
BCt	7.2	4.2	3.6	0.7	0.4	0.4
C	5.5	3.2	2.8	0.6	0.3	0.3
ATL-2 Pedon						
E	9.9	5.8	5.0	1.0	0.6	0.5
Bs1	22.9	13.3	11.5	2.3	1.3	1.1
Bs2	13.2	7.7	6.6	1.3	0.8	0.7
E/B	5.1	3.0	2.6	0.5	0.3	0.3
Bt1	15.0	8.7	7.5	1.5	0.9	0.7
Bt2	11.7	6.8	5.9	1.2	0.7	0.6
BCt	8.6	5.0	4.3	0.9	0.5	0.4
C	6.0	3.5	3.0	0.6	0.3	0.3

Notes to Table C.2:
[1] = SOC (g kg $^{-1}$) assuming SOM is 58% carbon (van Bemmelen, 1890)
[2] = SOC (g kg $^{-1}$) assuming SOM is 50% carbon (Pribyl, 2010)
[3] = SOC (%) assuming SOM is 58% carbon (van Bemmelen, 1890)
[4] = SOC (%) assuming SOM is 50% carbon (Pribyl, 2010)

Table C.3. Geochemical data for the ATL-1 and ATL-2 pedons.

HOR	Ca (ppm)	Ti (ppm)	Fe (ppm)	Rb (ppm)	Sr (ppm)	Zr (ppm)	Ba (ppm)
ATL-1 Pedon							
E	6166	3001	11844	65	282	658	443
Bs1	6292	2770	21602	69	272	484	555
Bs2	6362	2956	20664	66	274	503	513
E/B	7179	2353	22867	87	254	569	854
Bt1	7533	2784	35417	100	257	555	910
Bt2	16768	2805	31265	78	264	430	660
BCt	37150	1849	17854	71	267	386	577
C	72362	1812	14302	67	264	404	558
ATL-2 Pedon							
E	6052	2948	7502	66	280	724	461
Bs1	6048	2523	18252	65	277	553	526
Bs2	6384	2671	14076	67	273	531	615
E/B	6926	2413	16170	77	258	583	727
Bt1	9310	2516	31625	95	249	581	895
Bt2	22941	2833	29079	80	264	416	638
BCt	25779	1847	18597	73	270	363	607
C	55235	1693	13998	66	270	388	550

Notes to Table C.3:
Ca – Calcium
Fe – Iron
Sr – Strontium
Ba - Barium
Ti - Titanium
Rb – Rubidium
Zr – Zirconium

Table C.4. Ion exchange and extractable cations data for the ATL-1 pedon.

HOR	CEC (me/100g)	Base Sat (%)	Ca (me/100g)	Mg (me/100g)	K (me/100g)	Na (me/100g)
ATL-1 Pedon						
E	2.0	45	0.6	0.2	0.0	0.1
Bs1	5.3	30	1.2	0.3	0.1	0.0
Bs2	2.2	36	0.6	0.1	0.1	0.0
E/B	4.5	87	2.9	0.8	0.2	0.0
Bt1	9.4	100	7.3	2.2	0.2	0.0
Bt2	4.8	100	6.6	1.3	0.1	0.0
BCt	3.7	100	17.6	1.1	0.1	0.0
C	2.5	100	18.5	0.9	0.1	0.0

Notes to Table C.4:
Ca – Calcium Mg – Magnesium
K – Potassium Na – Sodium

APPENDIX D

TAXONOMIC CLASSIFICATION

Contents:

SOIL CONTROL SECTION

Table D.1. Control section of the ATL-1 pedon.

HOR	Depth (cm)	Thickness (cm)	Control Section (%)
E/B	42-58	16	32
Bt1	58-72	14	28
Bt2	72-92	20	40

Notes to Table D.1:
The control section represents the upper 50 cm of the argillic horizon, as defined in *Soil Taxonomy* (Soil Survey Staff, 2014, pg. 319).

Table D.2. Particle-size class data for the ATL-1 pedon.

HOR	% Sand > 100 µm	Clay (%)	Coarse Frags (est. vol. %)
E/B	67.6	12.3	5
Bt1	50.6	17.9	5
Bt2	66.6	10.4	55

Table D.3. Cation-exchange activity class data for the ATL-1 pedon.

HOR	CEC (me/100g)	Clay (%)	CEC/Clay Ratio
E/B	4.5	12.3	0.37
Bt1	9.4	17.9	0.53
Bt2	4.8	10.4	0.46
WA	**6.0**	**13.1**	**0.45**

Notes to Table D.3:
WA = weighted average

POD INDEX

After Schaetzl and Mokma (1989):

POD Index = $\Sigma \Delta V * 2^{\Delta H}$

V = color value (moist) difference between the E and B horizon
H = the number of Munsell pages different in color hue:
- 1 (if no hue change)
- 2 (one hue page difference)
- 4 (two hue pages difference)
- 8 (three hue pages difference)

Table D.4. POD Index data for the ATL-1 and ATL-2 pedons.

HOR	V	H
ATL-1 Pedon		
E-Bs1	1	1
E-Bs2	0	1
ATL-2 Pedon		
E-Bs1	1	1
E-Bs2	0	1

Notes to Table D.1:
The POD Index was calculated using color data are reported in Table 4.1.

Calculations
Pedon 1:
$\Sigma (1 * 2^1) + (0 * 2^1)$
POD Index = 2

Pedon 2:
$\Sigma (1 * 2^1) + (0 * 2^1)$
POD Index = 2

REFERENCES

REFERENCES

Ahr, S.W., Nordt, L.C. and S.G. Driese. 2012. Assessing lithologic discontinuities and parent material uniformity within the Texas sandy mantle and implications for archaeological burial and preservation potential in upland settings. *Quaternary Research,* 78:60-71.

Ahr, S.W., Nordt, L.C. and R.J. Schaetzl. 2017. Lithologic Discontinuities in Soils. In: The International Encyclopedia of Geography. Wiley and Sons, New York (USA).

Allen, B.L. and E.P. Whiteside. 1954. The characteristics of some soils on tills of Cary and Mankato age in Michigan. *Soil Science Society of America Proceedings,* 18:203-206.

Anda, M., Chittleborough, D.J., and R.W. Fitzpatrick. 2009. Assessing parent material uniformity of a red and black soil complex in the landscapes. *Catena* 78:142–153.

Anderson, B. J. 2005. The historical development of the tension zone concept in the Great Lakes Region of North America. *The Michigan Botanist*, 44:127-138.

Applegarth, M.T. and D.E. Dahms. 2001. Soil catenas of calcareous tills, Whiskey Basin, Wyoming, USA. *Catena*, 42:17-38.

Arbogast, A.F., and T.P. Jameson. 1998. Age estimates of inland dunes in East Central Lower Michigan using soils data. *Physical Geography*, 19:485–501.

Arnaud, R.S. and E.P. Whiteside. 1963. Physical breakdown in relation to soil development. *Journal of Soil Science*, 14:267-281.

Barbour, M. G. and W.D. Billings. 2000. North American Terrestrial Vegetation. 2nd ed. Cambridge University Press, Cambridge (UK). 724 pp.

Barrett, L.R. and R.J. Schaetzl. 1993. Soil Development and Spatial Variability on Geomorphic Surfaces of Different Age. *Physical Geography* 14:39-55.

Bartelli, L.J. and R.T. Odell. 1960. Field Studies of a Clay-Enriched Horizon in the Lowest Part of the Solum of Some Brunizem and Gray-Brown Podzolic Soils in Illinois. *Soil Science Society of America Journal*, 24:388-390.

Beaver, A.J., 1966. Characteristics and genesis of some bisequal soils in eastern Wisconsin. Unpublished doctoral dissertation, University of Wisconsin. 212 pp.

Berrow, M.L., Wilson, M.J. and Reaves, G.A., 1978. Origin of extractable titanium and vanadium in the A horizons of Scottish podzols. *Geoderma*, 21:89-103.

Birkeland, P.W. 1999. Soils and geomorphology. 3rd ed. Oxford University Press, Oxford (UK). 448 pp.

Blewett, W.L., Winter, H.A., and R.L. Rieck. 1993. New Age Control on the Port Huron Moraine in Northern Michigan. *Physical Geography,* 14:131-138.

Blewett, W.L. and H.A. Winters. 1995. The importance of glaciofluvial features within Michigan's Port Huron moraine. *Annals of the Association of American Geographers*, 85:306-319.

Bockheim, J.G. 1997. Soils in a hemlock-hardwood ecosystem mosaic in the Southern Lake Superior Uplands. *Canadian Journal of Forest Research*, 27:1147-1153.

Bockheim, J.G. 2003. Genesis of bisequal soils on acidic drift in the upper Great Lakes region, USA. *Soil Science Society of America Journal*, 67:612-619.

Bockheim, J.G. and A.E. Hartemink. 2013. Distribution and classification of soils with clay-enriched horizons in the USA. *Geoderma*, 209: 153-160.

Bockheim, J.G. 2016. Classification and distribution of soils with albic horizons in the USA: A preliminary analysis. *Geoderma*, 262: 85-93.

Buggle, B., Glaser, B., Hambach, U., Gerasimenko, N. and S. Marković. 2011. An evaluation of geochemical weathering indices in loess–paleosol studies. *Quaternary International*, 240:12-21.

Bullock, P., Milford, M.H. and M.G. Cline. 1974. Degradation of Argillic Horizons in Udalf Soils of New York State. *Soil Science Society of America Journal*, 38:621-628.

Bullock, P. and Thompson, M.L., 1985. Micromorphology of alfisols. In: Soil micromorphology and soil classification. Soil Science Society of America, Madison (USA). pp.17-47.

Burgis, W.A. 1977. Late-Wisconsinan History of Northeastern Lower Michigan. Unpublished doctoral dissertation, University of Michigan. 396 pp.

Carroll, D. 1958. Role of clay minerals in the transportation of iron. *Geochimica et Cosmochimica Acta*, 14:1-28.

Chadwick, O.A. and J. Chorover. 2001. The chemistry of pedogenic thresholds. *Geoderma*, 100:321-353

Chesworth, W. 2008. Encyclopedia of Soil Science. Springer, Dordrecht (NL). 902 pp.

Chorom, M. and P. Rengasamy. 1995. Dispersion and zeta potential of pure clays as related to net particle charge under varying pH, electrolyte concentration and cation type. *European Journal of Soil Science*, 46:657-665.

Cline, M.G.,1949. Profile studies of normal soils of New York: I. Soil profile sequences involving brown forest, gray-brown podzolic, and brown podzolic soils. *Soil Science*, 68:259-272.

Comer, P.J., D.A. Albert, H.A. Wells, B.L. Hart, J B. Raab, D.L. Price, D.M. Kashian, R.A. Corner, and D.W. Schuen. 1995. Michigan's native landscape, as interpreted from the General Land Office surveys 1816-1856. Rept. to the US EPA Water Division and the Wildlife Division, MI Dept. of Natural Resources, Michigan Natural Features Inventory, Lansing (USA). 78 pp.

Cremeens, D.L., and D.L. Mokma. 1986. Argillic horizon expression and classification in the soils of two Michigan hydrosequences. *Soil Science Society of America Journal*, 50:1002-1007.

Dąbkowska-Naskręt, H. and H. Jaworska, H. 2001. Titanium in Alfisols formed from glacial deposits of different ages in Poland. *Quaternary International*, 78:61-67.

Daly, B.K. 1982. Identification of podzols and podzolised soils in New Zealand by relative absorbance of oxalate extracts of A and B horizons. *Geoderma*, 28:29-38.

Davies, B.E. 1974. Loss-on-ignition as an estimate of soil organic matter. *Soil Science Society of America Proceedings*, 38:150–151.

Denton, S.R. 1985. Ecological climatic regions and tree distributions in Michigan. Unpublished doctoral dissertation, University of Michigan. 390 pp.

De Vries, W. and A. Breeuwsma. 1987. The relation between soil acidification and element cycling. *Water, Air, and Soil Pollution*, 35: 293-310.

Duchaufour, P.H. and B. Souchier. 1978. Roles of iron and clay in Genesis of acid soils under a humid, temperate climate. *Geoderma*, 20:15-26.

Douglas, L.A. 1990. Soil micromorphology: A basic and applied science. Elsevier, Amsterdam (NL). 715 pp.

Eberl, D.D. 1984. Clay mineral formation and transformation in rocks and soils. *Philosophical Transactions of the Royal Society of London. Series A, Mathematical and Physical Sciences*, 311:241-257.

Eichenlaub, V.L., 1970. Lake effect snowfall to the lee of the Great Lakes: Its role in Michigan. *Bulletin of the American Meteorological Society*, 51:403-413.

Eichenlaub, V.L., Harman, J.R., Numberger, F.V., and H.J. Stolle. 1990. The climatic atlas of Michigan. University of Notre Dame Press. 165 pp.

Eylem, C., Erten, H.N., and H. Göktürk. 1990. Sorption-desorption behavior of barium on clays. *Journal of environmental radioactivity*, 11:183-200.

Farrand, W.R. 1995. The Pleistocene Glacial Record in the area of Alpena, Montmorency and Presque Isle Counties, Michigan. In Karst Geology of the Northeast Lower Peninsula, Michigan, ed. T.J. Black, Michigan Basin Geological Society, Department of Geol. Sciences, Michigan State University. pp. 35–41.

Federoff, N. 1972. Clay illuviation. Proceedings of the 3rd International Working Meeting of Soil Micromorphology, Wroclaw, Poland.

Forman, S.L. and G.H. Miller. 1984. Time-dependent soil morphologies and pedogenic processes on raised beaches, Bröggerhalvöya, Spitsbergen, Svalbard Archipelago. *Arctic and Alpine Research*, 16:381-394.

Frei, E. and M.G. Cline. 1949. Profile studies of normal soils of New York: II. Micromorphological studies of the Gray-brown podzolic—Brown podzolic soil sequence. *Soil Science*, 68:333-344.

Fujinuma, R., Bockheim, J. and N. Balster. 2005. Base-cation cycling by individual tree species in old-growth forests of Upper Michigan, USA. *Biogeochemistry*, 74:357-376.

Gardner, D.R. and E.P. Whiteside. 1952. Zonal soils in the transition region between the Podzol and Gray-Brown Podzolic regions in Michigan. *Soil Science Society of America Proceedings*, 16:137-141.

Gotoh, S. and W.H. Patrick Jr. 1974. Transformation of iron in a waterlogged soil as influenced by redox potential and pH. *Soil Science Society of America Journal*, 38:66-71.

Harpstead, M. and R.H. Rust. 1964. A pedological characterization of five profiles in Gray Wooded Soils area of Minnesota. *Soil Science Society of America Journal*, 18:113-118.

Hatipoglu, S., Eylem, C., Göktürk, H. and H.N. Erten. 1990. Sorption of strontium and barium on clays and soil fractions. *Sciences Géologiques, bulletins et mémoires*, 86:79-86.

Haxby, T., Kintigh, K., and D. Price. 2013. Northern Lower Peninsula Regional State Forest Management Plan. Forest Resources Division and Wildlife Division, Michigan Department of Natural Resources, Lansing (USA).

Henne, P. D., F. S. Hu, and D. T. Cleland. 2007. Lake-effect snow as the dominant control of mesic-forest distribution in Michigan. *Journal of Ecology,* 95:517–29.

Henne, P. D., and F. S. Hu. 2010. Holocene climatic change and the development of the lake-effect snowbelt in Michigan, USA. *Quaternary Science Reviews*, 29:940–51.

Hillel, D. 2003. Introduction to Environmental Soil Physics. Elsevier, Amsterdam (NL). 494 pp.

Hole, F.D. 1975. Some relationships between forest vegetation and podzol B horizons in soils of Menominee tribal lands, Wisconsin, USA. *Soviet soil science*, 7:714-723.

Hunckler, R.V. and R.J. Schaetzl. 1997. Spodosol Development as Affected by Geomorphic Aspect, Baraga County, Michigan. *Soil Science Society of America Journal*, 61:1105-1115.

Hupy, C.M. and C.H. Yansa. 2009. Late Holocene vegetation history of the forest tension zone in central Lower Michigan, USA. *Physical Geography*, 30:205-235.

Isard, S.A. and R.J. Schaetzl. 1995. Estimating Soil Temperatures and Frost in the Lake Effect Snowbelt Region, Michigan, USA. *Cold Regions Science and Technology,* 23:317-332.

Jamagne, M., De Coninck, F., Robert, M. and J. Maucorps. 1984. Mineralogy of clay fractions of some soils on loess in northern France. *Geoderma*, 33:319-342.

Jenny, H., 1994. Factors of soil formation: a system of quantitative pedology. Courier Corporation, Massachusetts (USA). 281 pp.

Johnson, D.L. 1989. Subsurface stone lines, stone zones, artifact-manuport layers, and biomantles produced by bioturbation via pocket gophers (Thomomys bottae). *American Antiquity*, 54:370-389.

Kalnicky, D.J., and R. Singhvi. 2001. Field Portable XRF Analysis of Environmental Samples. *Journal of Hazardous Materials,* 83:93–122.

Kellogg, C.E. 1936. Development and significance of the great soil groups of the United States. USDA Misc. Publ. No. 229. Washington, DC (USA). 39 pp.

Khakural, B.R., Lemme, G.D. and D.L. Mokma. 1993. Till thickness and argillic horizon development in some Michigan Hapludalfs. *Soil Survey Horizons*, 34:6-13.

Kilmer, V. J., and L.T. Alexander. 1949. Methods of Making Mechanical Analysis of Soils. *Soil Science,* 68:15-24.

Konert, M., and J. Vandenberghe. 1997. Comparison of laser grain size analysis with pipette and sieve analysis: A solution for the underestimation of the clay fraction. *Sedimentology*, 44:523–535.

Krist, F.K. and DP. Lusch. 2004. Glacial History of Michigan, U.S.A: A Regional Perspective. *Developments in Quaternary Sciences,* 2:111-117.

Langohr, R., C. O. Scoppa, and A. Van Wambeke. 1976. The use of a comparative particle size distribution index for the numerical classification of soil parent materials: Application to Mollisols of the Argentine Pampa. *Geoderma,* 15:305-312.

Larson, G.J., Lowell, T.V., and N.E. Ostrom. 1994. Evidence for the Two Creeks interstade in the Lake Huron basin. *Canadian Journal of Earth Science,* 31:737-797.

Larson, G.J. and R.J. Schaetzl. 2001. Origin and Evolution of the Great Lakes. *Journal of Great Lakes Research,* 27:518-546.

Lavkulich, L.M. and J.M. Arocena. 2011. Luvisolic soils of Canada: Genesis, distribution, and classification. *Canadian Journal of Soil Science*, 91:781-806.

Lindbo, D.L., Rhoton, F.E., Hudnall, W.H., Smeck, N.E., Bigham, J.M. D.D. and Tyler. 2000. Fragipan degradation and nodule formation in Glossic Fragiudalfs of the Lower Mississippi River Valley. *Soil Science Society of America Journal*, 64:1713-1722.

Locke, W.W. 1986. Fine particle translocation in soils developed on glacial deposits, southern Baffin Island, NWT, Canada. *Arctic and Alpine Research*, 18: 33-43.

Loeppert, R.H. 1986. Reactions of iron and carbonates in calcareous soils. *Journal of Plant Nutrition*, 9:195-214.

Luehmann, M.D., Schaetzl, R.J., Miller, B.A., and M. Bigsby. 2013. Thin, Pedoturbated and Locally Sourced Loess in the Western Upper Peninsula of Michigan. *Aeolian Research,* 8:85-100.

Malcolm, R.L. and V.C. Kennedy. 1970. Variation of cation exchange capacity and rate with particle size in stream sediment. *Journal (Water Pollution Control Federation)*, 42:153-160.

Manjaiah, K.M., Kumar, S., Sachdev, M.S., Sachdev, P. and S.C. Datta. 2010. Study of clay–organic complexes. *Current Science*, pp. 915-921.

Medley, K. M. and J.R. Harman. 1987. Relationships between the vegetation tension zone and soils distribution across central Lower Michigan. *The Michigan Botanist*, 26: 78–87.

Melhorn, W.N. 1954. Valders Glaciation of the Southern Peninsula of Michigan. Unpublished doctoral dissertation, University of Michigan. 356 pp.

Mengel, K. 1994. Iron availability in plant tissues-iron chlorosis on calcareous soils. *Plant and soil*, 165:275-283.

Miller, B.A. and R.J. Schaetzl. 2012. Precision of Soil Particle Size Analysis Using Laser Diffractometry. *Soil Science Society of America Journal,* 76:1719-1727.

Mortland, M.M., 1970. Clay-organic complexes and interactions. *Advances in Agronomy*, 22:75-117.

Muhs, D.R. 1984. Intrinsic thresholds in soil systems. *Physical Geography*, 5:99-110.

Nelson, D.W., and L.E. Sommers. 1996. Total carbon, organic carbon, and organic matter. p. 961–1010. In: Methods of soil analysis. Part 3. Chemical methods. SSSA Book Ser. 5. SSSA, Madison, WI.

Nesbitt, H.W. and G. Markovics. 1980. Chemical processes affecting alkalis and alkaline earths during continental weathering. *Geochimica et Cosmochimica Acta*, 44:1659-1666.

Nygard, I.J., P.R. McMiller, and F.D. Hole. 1952. Characteristics of some Podzolic, Brown Forest, and Chernozem soils of the northern portion of the lake states. *Soil Science Society of America Proceedings,* 16:123-129.

Padley, E.A., Bartelli, L.J. and C.C. Trettin. 1985. Spodic horizon criteria applied to soils of northern Michigan. *Soil Science Society of America Journal*, 49:401-405.

Payton, R.W. 1992. Fragipan formation in argillic brown earths (Fragiudalfs) of the Milfield Plain, north-east England. I. Evidence for a periglacial stage of development. *Journal of Soil Science*, 43:624-644.

Payton, R.W. 1993a. Fragipan formation in argillic brown earths (Fragiudalfs) of the Milfield Plain, north-east England, n. Post Devensian developmental processes and the origin of fragipan consistence. *Journal of Soil Science*, 44:703-723.

Payton, R.W. 1993b. Fragipan formation in argillic brown earths (Fragiudalfs) of the Milfield Plain, north-east England. HI. Micromorphological, SEM and EDXRA studies of fragipan degradation and the development of glossic features. *Journal of Soil Science*, 44:725-729.

Peinemann, N., Amiotti, N.M., Zalba, P. and M.B. Villamil. 2000. Minerales de arcilla en fracciones limo de horizontes superficiales de suelos de diferente mineralogía. *Ciencia del suelo*, 18:69-72.

Perkis, W. E. Carey. 1997. Soil survey of Otsego County, Michigan. USDA, Natural Resources Conservation Service. Washington, D.C.: Government Printing Office.

Pennock, D.J., Zebarth, B.J. and E. De Jong. 1987. Landform classification and soil distribution in hummocky terrain, Saskatchewan, Canada. *Geoderma*, 40:297-315.

Phillips, J.D. 2004. Geogenesis, pedogenesis, and multiple causality in the formation of texture-contrast soils. *Catena*, 58:275-295.

Poppe, L.J., V.F. Paskevich, J.C. Hathaway, and D.S. Blackwood. 2001. A Laboratory Manual for X-Ray Powder Diffraction. United States Geological Survey Open-File Report, 1(041), 1-88.

Poesen, J. and H. Lavee. 1994. Rock fragments in top soils: significance and processes. *Catena*, 23:1-28.

Pribyl, D. W. 2010. A critical review of the conventional SOC to SOM conversion factor. *Geoderma*, 156: 75-83.

Purkey, T. H. Carey. 2013. Soil survey of Montmorency County, Michigan. USDA, Natural Resources Conservation Service. Washington, D.C.: Government Printing Office.

Quénard, L., Samouëlian, A., Laroche, B. and S. Cornu. 2011. Lessivage as a major process of soil formation: A revisitation of existing data. *Geoderma*, 167:135-147.

Rahman, M., Lee, S.H., Ji, H.C., Kabir, A.H., Jones, C.S. and K.W. Lee. 2018. Importance of mineral nutrition for mitigating aluminum toxicity in plants on acidic soils: current status and opportunities. *International journal of molecular sciences*, 19:3073.

Ranney, R.W. and M.T. Beatty. 1969. Clay Translocation and Albic Tongue Formation in Two Glossoboralfs of West-Central Wisconsin. *Soil Science Society of America Journal*, 33:768-775.

Rindfleisch, P.R. and R.J. Schaetzl. 2001. Soils and Geomorphic Evidence for a High Lake Stand in a Michigan Drumlin Field. *Physical Geography,* 22:483-501.

Roden, E.E. 2012 Microbial iron-redox cycling in subsurface environments. *Biochemical Society Transactions*, 40:1249-1256.

Rothstein, D.E., Toosi, E.R., Schaetzl, R.J., and A.S. Grandy. 2018. Translocation of Carbon from Surface Organic Horizons to the Subsoil in Coarse-Textured Spodosols: Implications for Deep Soil C Dynamics. *Soil Science Society of America Journal,* 82:969-982.

Rücknagel, J., Hofmann, B., Paul, R., Christen, O. and K.J. Hülsbergen. 2007. Estimating precompression stress of structured soils on the basis of aggregate density and dry bulk density. *Soil and Tillage Research*, 92:213-220.

Ruotsala, A.P. 1980. Mineralogy of Antrim Shale, Michigan: Report FE-2346-79. DOW Chemical Co., Midland, MI (USA). 85 pp.

Schaetzl, R.J., and D.L. Mokma. 1988. A numerical index of Podzol and Podzolic soil development. *Physical Geography*, 9:232–246.

Schaetzl, R.J. and S.A. Isard. 1991. The Distribution of Spodosol Soils in Southern Michigan: A Climatic Interpretation. *Annals of the Association of American Geographers,* 81:425-442.

Schaetzl, R.J. 1996. Spodosol-Alfisol intergrades: Bisequal soils in NE Michigan, USA. *Geoderma,* 74:23-47.

Schaetzl, R.J., W. E. Frederick, and L. Tornes. 1996. Secondary Carbonates in Three Fine and Fine-Loamy Alfisols in Michigan. *Soil Science Society of America Journal,* 60:1862-1870.

Schaetzl, R.J. 1998. Lithologic Discontinuities in Some Soils on Drumlins: Theory, Detection, and Application. *Soil Science,* 163:570-590.

Schaetzl, R.J., Krist, F., Rindfleisch, P., Liebens, J., and T. Williams. 2000. Post-Glacial Landscape Evolution of Northeastern Lower Michigan, Interpreted from Soils and Sediments. *Annals of the Association of American Geographers,* 90:443-466.

Schaetzl, R.J. 2001. Late Pleistocene Ice Flow Directions and the Age of Glacial Landscapes in Northern Lower Michigan. *Physical Geography,* 22:28-41.

Schaetzl, R.J. 2002. A Spodosol-Entisol Transition in Northern Michigan. *Soil Science Society of America Journal* 66:1272-1284.

Schaetzl, R.J., Enander, H., Luehmann, M.D., Lusch, D.P., Fish, C., Bigsby, M., Steigmeyer, M., Guasco, J., Forgacs, C., and A. Pollyea. 2013. Mapping the Physiography of Michigan Using GIS. *Physical Geography,* 34:1-38.

Schaetzl, R.J., Yansa, C.H., and M.D. Luehmann. 2013. Paleobotanical and Environmental Implications of a Buried Forest Bed in Northern Lower Michigan, USA. *Canadian Journal of Earth Sciences,* 50:483-493.

Schaetzl, R.J. and M.L. Thompson. 2015. Soils: Genesis and Geomorphology. 2nd ed. Cambridge University Press, Cambridge (UK). 778 pp.

Schaetzl, R., M. Luehmann, and D. Rothstein. 2015. Pulses of podzolization: The relative importance of spring snowmelt, summer storms, and fall rains on spodosol development. *Soil Science Society of America Journal*, 79:117–131

Schaetzl, R.J., Rothstein, D., and P. Samonil. 2018. Gradients in Lake-Effect Snowfall and Fire across Northern Lower Michigan Drive Patterns of Soil Development and Carbon Dynamics. *Annals of the American Association of Geographers,* 108:638-657.

Schaetzl, R.J., Baish, C., Colgan, P., Knauff, J., Bilintoh, T., Wanyama, D., Church, M., McKeehan, K., Fulton, A., and A.F. Arbogast. 2020. A Sediment-Mixing Process Model of Till Genesis, using Texture and Clay Mineralogy Data from Saginaw Lobe (Michigan, USA) Tills. *Quaternary Research*, 94: 174-194.

Schoeneberger, P.J., D.A. Wysocki, E.C. Benham, and Soil Survey Staff. 2012. Field Book for Describing and Sampling Soils, Version 3.0. Natural Resources Conservation Service, United States Department of Agriculture, National Soil Survey Center, Lincoln (USA).

Schulte, E.E., and B.G. Hopkins. 1996. Estimation of soil organic matter by weight loss-on-ignition. In: Soil organic matter: Analysis and interpretation. Soil Science Society of America Special Publications, 46. Soil Science Society of America, Madison (USA). pp 21-31.

Schulten, H. R., Leinweber, P. and M. Schnitzer. 1998. Analytical pyrolysis and computer modeling of humic and soil particles. In: Environmental Particles: Structure and Surface Reactions of Soil Particles. Wiley, Chichester (UK). pp. 281-324.

Schumacher, B. A., K. C. Shines, J. V. Burton, and M. L. Papp. 1990. Comparison of Three Methods for Soil Homogenization. *Soil Science Society of America Journal*, 54:1187-1190.

Shainberg, I., and G.J. Levy. 2005. Flocculation and Dispersion. In: Encyclopedia of Soils in the Environment. Elsevier, Amsterdam (NL). pp. 27-34.

Simonson, R.W. 1978. A multiple-process model of soil genesis. In: WC Mahaney (ed). Quaternary Soils. Geo Abstracts, Norwich. pp. 1-25.

Singh, S., Tripathi, D.K., Singh, S., Sharma, S., Dubey, N.K., Chauhan, D.K. and M. Vaculík. 2017. Toxicity of aluminium on various levels of plant cells and organism: a review. *Environmental and Experimental Botany*, 137:77-193.

Smith, K.S.1999. Metal sorption on mineral surfaces: an overview with examples relating to mineral deposits. *The Environmental Geochemistry of Mineral Deposits. Part B: Case Studies and Research Topics*, 6:161-182.

Soil Science Division Staff. 2017. Soil survey manual. C. Ditzler, K. Scheffe, and H.C. Monger (eds.). USDA Handbook 18. Government Printing Office, Washington, D.C. (USA).

Soil Survey Staff, Natural Resources Conservation Service, United States Department of Agriculture. Official Soil Series Descriptions. Available online. Accessed [April, 2019].

Soil Survey Staff, Natural Resources Conservation Service, United States Department of Agriculture. Soil Survey Geographic (SSURGO) Database for [Michigan]. Available online. Accessed [April, 2019].

Soil Survey Staff. 2014. Kellogg Soil Survey Laboratory Methods Manual. Soil Survey Investigations Report No. 42, Version 5.0. R. Burt and Soil Survey Staff. Natural Resources Conservation Service, United States Department of Agriculture.

Sparks, D.L., Page, A.L., Helmke, P.A. and R.H. Loeppert. 2020. Part 3: Chemical Methods. In: Methods of soil analysis (Vol. 14). Wiley and Sons, New York (USA). 1424 pp.

Sposito, G. 2016. The Chemistry of Soils. 3rd ed. Oxford University Press, Oxford (UK). 272 pp.

Stobbe, P.C., 1952. The morphology and genesis of the Gray-Brown Podzolic and related soils of Eastern Canada. *Soil Science Society of America Proceedings,* 16:81-84.

Stockman, U., Cattle, S.R., Minasny, B., and A.B. McBratney. 2016. Utilizing Portable X-ray Fluorescence Spectrometry for In-Field Investigation of Pedogenesis. *Catena*, 139:220-231.

Stoops, G., 2003. Guidelines for analysis and description of soil and regolith thin sections. Soil Science Society of America, Madison (USA). 184 pp.

Su, C. and D.L. Suarez. 2004. Boron release from weathering of illites, serpentine, shales, and illitic/palygorskitic soils. *Soil Science Society of America Journal*, 68:96-105.

Sudom, M.D. and R.J. Arnaud. 1971. Use of quartz, zirconium and titanium as indices in pedological studies. *Canadian Journal of Soil Science*, 51:385-396.

Sumner, M.E. 1999. Handbook of soil science. CRC press, Boca Raton (USA). 2148 pp.

Taboada, T., Cortizas, A.M., Garcia, C., and E.G. Rodeja. 2006. Particle-size fractionation of titanium and zirconium during weathering and pedogenesis of granitic rocks in NW Spain. *Geoderma,* 131:218–236.

Teveldal, S., Jørgensen, P., and A.O. Stuanes. 1990. Long-term weathering of silicates in a sandy soil at Nordmoen, southern Norway. *Clay Minerals*, 25:447-465.

Tsai, C.C. and Z.S. Chen. 2000. Lithologic discontinuities in Ultisols along a toposequence in Taiwan. *Soil science*, 165:587-596.

United Stated Department of Commerce, Economics and Statistics Administration, Bureau of the Census. 2019. 2017 Census of Agriculture. Volume I. Geographic Area Series. Part 51, Michigan, state and county data.

United States Geological Survey. 2018. Gap Analysis Project (GAP), 2018, Protected Areas Database of the United States (PAD-US). Available online. Accessed [month/day/2019].

van Bemmelen, J.M., 1890. Über die Bestimmung des Wassers, des Humus, des Schwefels, der in den colloïdalen Silikaten gebundenen Kieselsäure, des Mangans u. s. w. im Ackerboden. *Die Landwirthschaftlichen VersuchsStationen,* 37:279–290.

Van Vliet-Lanoë, B. 1998. Frost and soils: implications for paleosols, paleoclimates and stratigraphy. *Catena*, 34:157-183.

Veatch, J.O. 1931. Soil maps as a basis for mapping original forest cover. Papers Michigan Academy of Science Arts and Letters, 15:267-273.

Veatch, J.O. and C.E. Millar. 1934. Some characteristics of mature soils in Michigan. *American Soil Survey Bulletin*, 15:42-44.

Veatch, J.O. 1953. Soils and land of Michigan. Michigan State College Press, East Lansing. 241 pp.

Vincent, K.R. and O.A. Chadwick. 1994. Synthesizing bulk density for soils with abundant rock fragments. *Soil Science Society of America Journal*, 58:455-464.

Wang, X., Wang, J., and J. Zhang. 2012. Comparisons of three methods for organic and inorganic carbon in calcareous soils of northwestern China. *PLoS One*, 7:e44334.

Whitney, G.G. 1987. An Ecological History of the Great Lakes Forest of Michigan. *Journal of Ecology*, 75:667-684.

Wilde, S.A. 1946. Forest soils and forest growth. Chronica Botanica Co, Waltham (USA). 250 pp.

Wright, R.J. 1989. Soil aluminum toxicity and plant growth. *Communications in Soil Science and Plant Analysis*, 20:1479-1497.

Wright, A. L., Wang, Y., and K.R. Reddy. 2008. Loss-on-ignition method to assess soil organic carbon in calcareous Everglades wetlands. *Communications in soil science and plant analysis*, 39:3074-3083.

Yansa, C., Fulton III, A., Schaetzl, R.J., Kettle, J., and A.F. Arbogast. 2020. Interpreting Basal Sediments and Plant Fossils in Kettle Lakes: Insights from Silver Lake, Michigan, USA. *Canadian Journal of Earth Sciences*: in press.